

Ms. Ref. No.: AMT-2018-254

Title: Quantification of CO₂ and CH₄ emissions over Sacramento, California based on divergence theorem using aircraft measurements

Dear Dr. Christoph Kiemle,

*Thank you very much for your efforts on behalf of our paper titled “**Quantification of CO₂ and CH₄ emissions over Sacramento, California based on divergence theorem using aircraft measurements**” submitted by Ju-Mee Ryoo, Laura T. Iraci, Tomoaki Tanaka, Josette E. Marrero, Emma L. Yates, Inez Fung, Anna M. Michalak, Jovan Tadic, Warren Gore, T. Paul Bui, Jonathan M. Dean-Day, Cecilia S. Chang.*

We found the reviewers’ comments very helpful, and they played a large role in improving the quality of this paper. Based on the reviewers’ comments, we have reformulated our study in three significant ways (as suggested by both reviewers): we have removed the November 2015 flight from the analysis due to low and variable wind speeds; we have included additional plots to make the measured data more directly available to the reader; and we have reorganized the presentation of the material using the scheme suggested by Reviewer 2 (and guided by the confusion we caused Reviewer 1). Some of the related minor comments became immaterial after these major changes were made, but we have addressed the key critiques and suggestions and incorporated them in the revised manuscript. Enclosed is a point-by-point response to the review comments. We have shaded with gray highlighting the many useful specific comments that were implemented in the revised manuscript.

Thank you very much again for your support and consideration, and we look forward to hearing a positive decision from you.

Sincerely,

Ju-Mee Ryoo and Coauthors

Response letter to Review #1

Responses from the Authors are given in blue italicized text throughout: Thank you for your helpful comments. We addressed them to the best of our understanding and appreciated your guidance on areas where you found our discussion or language unclear. Items such as font size, word choice, and grammar which will be fixed in the revised manuscript are noted with gray highlighting.

This paper presents a methodology that estimates CO₂ and CH₄ fluxes using cylindrical flight patterns combined with kriging and Gauss divergence theorem over Sacramento, California and quantifies the corresponding uncertainty. The study finds that fluxes vary as a function of wind pattern, seasonality, background assumption, flight path, and flux estimation approach by a factor of 1.5 to 8. Total flux estimations using the entire circumference are larger than if just downwind region is used. It is stated in the article that using entire circumference to estimate GHGs fluxes allows for accounting of unknown sources that otherwise could be missed.

General Comments

Although the paper does make a lot of important and useful points regarding estimation of GHGs emissions with an aircraft, there are many places that are unclear and need to be elucidated before I can accept this article for publication.

First, I am not exactly clear on how the used methodology is different from a traditional mass balance. I see the explanation, but I am not convinced that it provides any information that is not obtained from the standard method. I would like to see a comparison. Please perform standard mass balance and compare it to your method.

From the Authors: The basic approach we used for estimating CO₂ and CH₄ fluxes is not different from a traditional mass balance. In the traditional mass balance analysis, the incoming mass should be the same as the outgoing mass passing the X-Y plane of the measurements. So, the air pollutants from the city will be observed on the downwind side, along with the wind passing through the region. Similarly with a cylinder of measurements, the mass coming into the cylinder should be equal to the mass leaving the cylinder to satisfy the mass balance.

When we used the raw wind measurement, however, we found that the mass of air mass was not conserved, which means we may not fully apply the mass balance approach. That is why we used the mass-balanced mean wind at each grid level, and the mean wind will distribute the greenhouse gas inside the cylinder. We assume that the well-mixed condition applies.

Furthermore, one of the advantages of applying the mass balance approach with an oval (enclosed shape) flight path is that an assignment of the background concentration is not required. Because we calculated the mass of the GHG plume that entered and exited the sample volume, the background effectively cancels out. Sometimes (actually almost always) background is not homogeneous, so there can be large uncertainty associated with calculating the background. There are also challenges in isolating the plume. In our approach, such problems did not exist.

Our study is also different from the usual implementation because we used in situ measured winds, not model data. Furthermore, we used the mean calculated from measured wind at each level, not just one

level, as has been the case in many previous studies (Turnbull et al., 2011; Karion et al. 2013, 2015). The difference we adopted here is that 1) we tested the flux estimation using observed airborne high-resolution raw wind at each measurement point and kriged grid and 2) we tested the flux estimation using mean wind (averaged observed raw wind at each layer). The previous “standard mass balance approach” often adopts the wind data from coarse-resolution model output. The uniqueness that our study provides is that we showed how the final flux could be different depending on the wind treatment.

Another issue that I find in this article is that the actual plane data is not carefully presented. First, it is important to present data for all of the 3 cases in an equal manner. There are different plots for different days, and it becomes confusing. For example, finding the exact local time of all the flights is difficult (including just take off time is not enough in this case). This information needs to be easily accessible. I could not locate wind measurements for all of the days. Figure S2 (d) is misleading and leads to a flawed assumption regarding steady state for November 17, 2015 (more on that later). The paper needs to be reorganized and improve its clarity of presentation.

A time series plot of CO₂, CH₄, wind, and altitude for each analysis day is shown below and will be included in the revised Supplemental Information.

In addition, we amended the text in Section 2.1 to focus on the time during which sampling occurred and simplify the way we described the implication of daylight savings time in California (PDT vs. PST). Revised text reads: Sampling occurred 21:10 – 22:00 UTC for the November flight (local standard time is UTC minus 8 h, 13:10 – 14:00 PST) and 20:55 – 21:45 UTC for the June flight. Based on comments from both reviewers, we have removed the November 17, 2015 case. The revised manuscript has changes to figures and the table to reflect this removal.

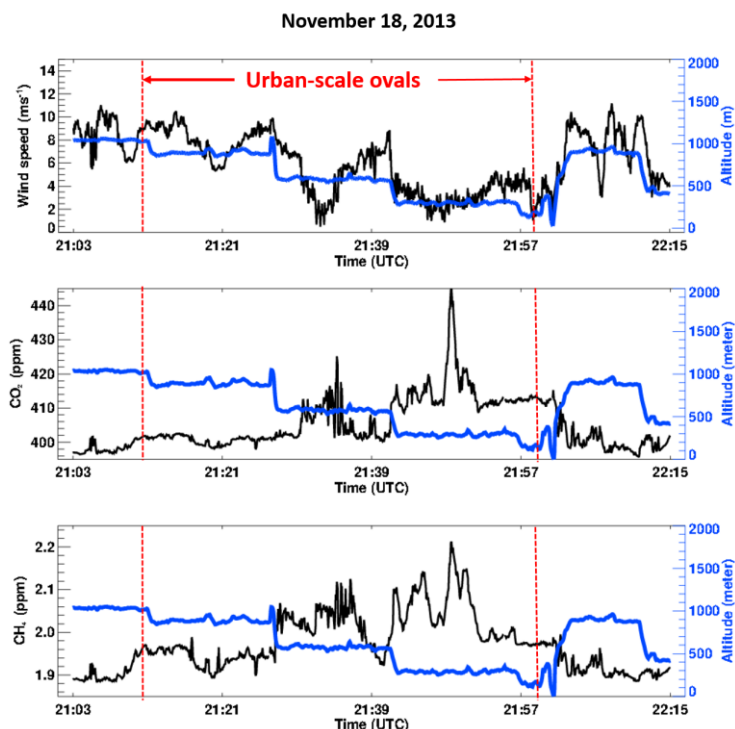


Figure: A time series of (black lines) CO₂, CH₄, horizontal wind speed and (blue lines) altitude of the aircraft for November 18, 2103. The red dashed lines represent a portion of the flight over Sacramento (See Fig. 2a in the revised manuscript).

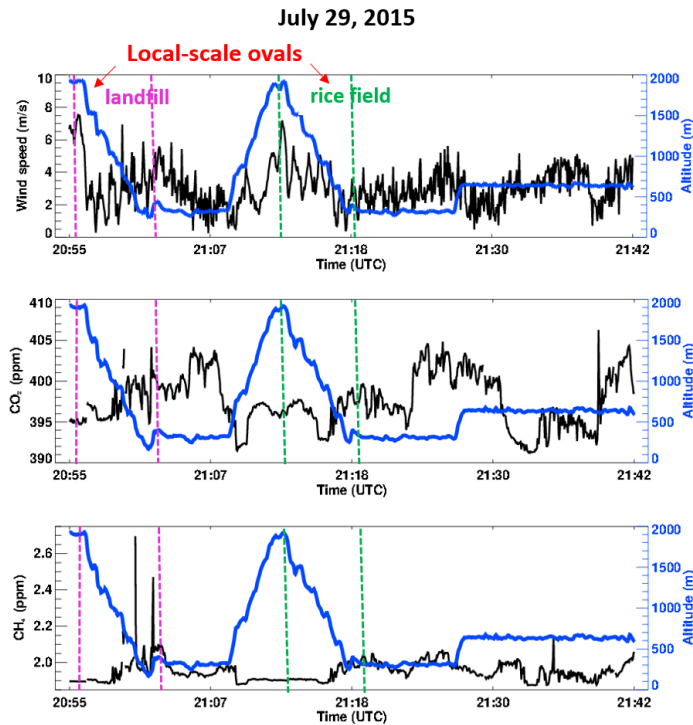


Figure: The same as Fig. above except for July 29, 2015. The magenta dashed lines indicate the portion of the flight over the landfill, and the green dashed lines mark the start and end times of the rice field measurements (see Fig. 2b in the revised manuscript).

The explanation of the background is very confusing. Given the method presented, background should be everything that flows into the cylinder. I am not following the justification for different background assumptions (you would not want to pick a minimum value in this case).

Yes, ideally, the cylindrical flight design removes the need for assigning a background value, as you state. Because we calculated the mass of the GHG that entered and exited the cylinder, we are subtracting all GHG upwind from all GHG downwind. So, the background should cancel out.

We tested this expectation by calculating the flux using various wind and background treatments. In the linear curtain approach, the edges of the flight transect outside the plume or measurements made upwind usually provide the background values. In these cases, the background concentration can be non-homogeneous and difficult to specify, so there is large uncertainty associated with setting the background. Because we want to compare as directly as possible our method to the studies already in the literature, we started by assigning the background as the minimum value in the layer (as a parallel case to the "edges" method). Then as a sensitivity test, we explored how the results would or would not change with a different choice of background (average of the layer values). When the winds were used in a way which required mass-balanced ("mass balance" in Table 1), the choice of background value was shown not to matter (first and second lines of Table 1 and Table 2). The "raw wind" case is discussed in detail in the next item.

We hope the new structure of the manuscript will better communicate this approach.

Also, the concept of raw and mass-balanced mean wind needs to be better explained. Why averaging winds horizontally achieves mass balance? And if the plume is not well mixed, how can you do that? Plume is transported differently at each level. You cannot just assume that all of the levels move at the same rate.

The mass-balanced mean wind is the arithmetic mean of the inflow and outflow raw (measured) wind at each vertical level. Separate calculations were performed to test the sensitivity of the calculated flux to the thickness of the vertical layers. These results were incorporated into an expanded version of Table 1 in the revised manuscript. This table can be seen below. We expanded it in the revised manuscript, separate it into two tables [Table 1 (urban scale), Table 2 (local scale)], and also include a new Table 3 showing a comparison with the Turnbull et al. study and bottom-up inventories. We compared each flux with that from the base case experiment (see the revised manuscript for more detail).

Table 1. Urban scale fluxes over Sacramento on November 18, 2013.

Background	Wind		Urban Scale (large loop)			
			November 18, 2013			
			CO ₂ (Mt yr ⁻¹)	Difference from base case (percent)	CH ₄ (Gg yr ⁻¹)	Difference from base case (percent)
min	Mass-balance	100 m layer avg	25.6±2.6		87.1±8.7	
		Whole column avg	26.6±2.7	3.9%	88.7±8.9	1.8%
avg	Mass-balance	100m layer avg	25.6±2.6	<1%	87.4±8.7	<1%
		Whole column avg	26.6±2.7	3.9%	89.0±8.9	2.1%
min	Raw		3.7±0.4	86%	13.0±1.3	85%
avg	Raw		25.5±2.6	<1%	91.1±9.1	4.6%

Table 2. Local scale fluxes over landfill and rice field over Sacramento on July 29, 2015.

Background	Wind		Local Scale (small loop): July 29, 2015							
			Landfill				Rice Field			
			CO ₂ (10 ⁻¹ Mt yr ⁻¹)	Difference from base case (percent)	CH ₄ (Gg yr ⁻¹)	Difference from base case (percent)	CO ₂ (10 ⁻¹ Mt yr ⁻¹)	Difference from base case (percent)	CH ₄ (Gg yr ⁻¹)	Difference from base case (percent)
min	Mass - balance	100 m layer avg	2.2±0.8		7.1±2.5		2.5±0.4		2.5±0.4	
		Whole column avg	2.2±0.8	<1%	6.9±2.4	2.8%	2.5±0.4	<1%	2.6±0.4	2%
avg	Mass-balance	100 m layer avg	2.2±0.8	<1%	7.1±2.5	<1%	2.5±0.4	<1%	2.5±0.4	<1%
		Whole column avg	2.2±0.8	<1%	6.9±2.4	2.8 %	2.5±0.4	<1%	2.5±0.4	<1%
min	Raw		3.7±1.3	68%	8.9±3.1	25 %	1.7±0.3	30%	1.8±0.3	28%
avg	Raw		2.2±0.8	<1%	7.1±2.5	<1 %	2.6±0.4	2%	2.5±0.4	<1%

Table 3. Flux estimates for the Sacramento urban area from measurements made on November 18, 2013.

		CO ₂ (Mt yr ⁻¹)	CH ₄ (Gg yr ⁻¹)
Whole cylinder-AJAX	(bg = min, 100m layer avg)	25.6 ± 2.6	87.1 ± 8.7
	(bg = avg, 100m layer avg)	25.6 ± 2.6	87.4 ± 8.7
Curtain -AJAX	(bg = min)	17.3 ± 1.7	64.4 ± 6.4
	(bg = avg)	8.9 ± 0.9	24.1 ± 2.4
Turnbull et al. (2011)		13.4 (with uncertainty of ~ 100%)	
Vulcan estimates for Sacramento		11.5	
CEPAM estimate for Sacramento		10.0	

^a Turnbull et al. (2011) data were collected in 2009; the value given here was converted from the mean reported value of 3.5 Mt C yr⁻¹ with a 1.1% yr⁻¹ increase in CO₂ flux to adjust to 2013.

^b Bottom-up inventory estimates of the annual total emissions from Sacramento County from Vulcan (Gurney et al., 2009) and the California Air Resources Board CEPAM database (Turnbull et al., 2011) are included for comparison. The Vulcan inventory is available only for 2002, and the CEPAM database is available for 2004. We applied a 1.1% yr⁻¹ increase in CO₂ flux to adjust to 2013.

Previous studies used a single coarse resolution model ‘mean’ wind throughout all altitudes below the PBLH (Turnbull et al., 2011; Karion et al. 2015), and we agree with you that assuming the winds at all levels move at the same rate is not ideal. Therefore, we used our in situ wind measurements to test the impact of this assumption. We calculated the fluxes using wind averaged on each vertical layer (three separate tests with layer thicknesses of 100, 200, and 500 m) and found the results were actually not very much different from the flux estimate found when we use a single, whole column average.

Specific Comments

Line 170: It says, “The background level is derived from the lowest flight measurement.” When using the kriging method, do you apply kriging to all of the data including the background?

We apologize for the wording in the original manuscript at line 170. Our description of the “constant” method was unnecessarily confusing. The cyan curves in Figure 2 show what we were trying to describe: at all altitudes below the yellow diamond (lowest flight level), the mixing ratio was presumed to be exactly equal to the value measured at the lowest flight level. Please also see the new figure below. The bottom left panel shows more clearly how the values measured along the lowest flight level are assigned to all grid cells below the measurement altitude. The dashed lines represent an approximate lowest flight level.

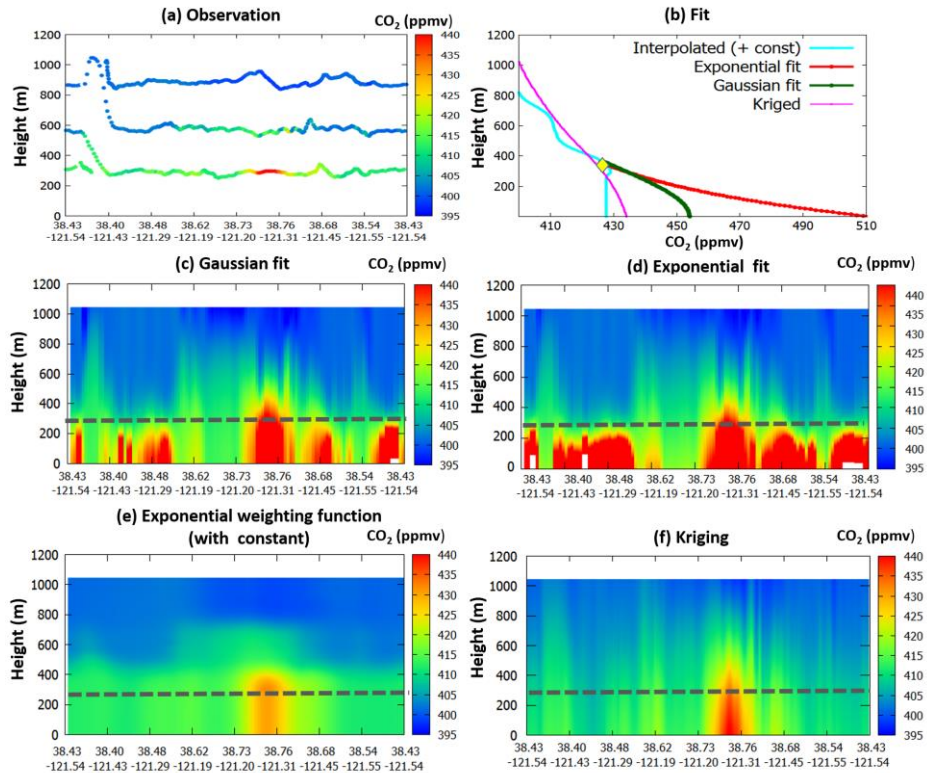


Figure: (a) Observed CO_2 over the Sacramento loop on November 18, 2013. (b) The vertical profiles of calculated CO_2 mixing ratios around 38.75°N , 121.27°W . The yellow diamond indicates the altitude of the lowest flight data. The kriged values (magenta), interpolated values with exponential weighting function and extrapolated values using constant (cyan), gaussian fit (green), and exponential fit (red) are compared. The CO_2 mixing ratio obtained from (c) the gaussian fit, (d) exponential fit, (e) exponential weighting function with constant, (f) kriging method. The empirical fits were generated based on the approach by Gordon et al. (2015). In panels (c) and (d), the white boxes result from no fit due to the lack of the data points. (Fig. 3 in the revised manuscript)

Line 191: How do you know that kriging approach captures better plume features? Kriging method interpolates data, meaning that it basically guesses it. It has no knowledge of the actual plume dispersion mechanism. Figure S4 is misleading as it has different color bar scales for different plots. Please make sure that all of the color bars are the same. In actuality, you don't know how the plume is changing below your lowest measurement point. Anything that you assume below that point is highly uncertain. It could be almost constant for all we know. It depends on the location of the source.

That's why ideally you want to sample the well-mixed layer and not partially mixed layer with an aircraft when estimating flux.

That is exactly why we evaluated several common methods of extrapolation, as shown in Fig. 2 and the new figure above (Fig. 3 in the revised manuscript). As you point out, we do not know which method will better capture the plume features, especially below the lowest flight level. Because kriging uses characteristics of the measured data to make the interpolation, we expect it to be less arbitrary than some of the other methods, and this is what is seen in figure S3. The measured plume shape (panel a) is

captured more faithfully by the kriging method (panel f) than by the exponential weighting function method (panel e), as is the subtle variation of mixing ratio around the oval at a given altitude.

We agree with you that plume behavior below our lowest measurement point is highly uncertain. We don't think one pattern is correct while others are not. We just suggest one estimate might be better based on the other characteristics that we've examined. Your comments on why a well-mixed layer condition is important for estimating flux are also very true.

More attention were paid to the color bar scales in the revised manuscript, and where appropriate they had the same scale, such as panels b, c, and d of Fig. S3. However, if forcing different flight days to use the same scale makes it more difficult to discern features of interest, then we did not force one day's maximum value to set the scale bar for another day's flight. If different scales were necessary for clarity, we noted the change in the relevant figure caption(s).

Section 2.4: See the comment about the raw wind vs. mass-balanced mean wind in the general comments section.

Please see reply above.

Figure 1c: I am confused about the following sentence in the caption, "The shading represents the pressure . . . normal to the cylinder." What shading? I am not sure I see any shading. Please explain what do you mean here. Also, here you say that blue is inflow and red is an outflow. It seems that everything that is in blue should be a background for everything that is in red assuming steady state. Please comment.

We changed the word choice in the revised manuscript. "Shading" was intended to mean "colors" of the cylinder. This is just the sign of the air mass flux [$\text{kg m}^{-2} \text{s}^{-1}$], which is obtained from density multiplied by the wind vector (or pressure divided by the wind vector). Yes, everything in blue represents the inflow air mass, which has negative wind direction, while everything in red represents the outflow air mass, which has a positive wind direction.

Lines 265-270: I do not understand your choice of background. Given your set up you should be using inflow as background. The definitions you describe here are used in regular mass balance because sometimes there is just not enough sampling, but generally, they are flawed. Please explain why you are not using inflow. You need to justify your choices with relevant physical processes.

We agree with you that we do not need to know the background value for estimating flux when adopting the circular pattern of flight. This is clearly demonstrated in our experiments, showing that the flux estimates were not sensitive to the choice of background (minimum or averaged value). We worked harder on the language in the revised manuscript.

Another important point that you do not mention is an uptake of CO_2 by vegetation. That also can affect background and your fluxes quite a bit. I know it is November in two of your cases, but you need to comment on your assumptions. Your case in July could be more problematic with respect to CO_2 , although there you concentrate on CH_4 so it may not matter as much.

We agree that considering an uptake of CO₂ by vegetation could be an important factor on the total flux estimate. When we took a look at CarbonTracker data, we confirmed that there is some contribution of the vegetation of CO₂ to the total fluxes in November (for example, in places like Salt Lake City). However, it is hard to consider the biological impact on CO₂ flux unless we downscale the model data to the small scale we are interested in. This would be better considered in a further study to completely characterize each sector (biological (vegetation or dairy farm) or anthropogenic (industry)). However, we agree with the reviewer that we should mention the potential problem in the interpretation of the flux estimate we obtained in this study and included a comment in the revised manuscript.

Line 306: How come highways and airports are indicative of CH₄ emissions? It is not common for these sources to emit any significant CH₄. Please explain.

Dairy farms and landfills are well known sources of CH₄. However, one of the biggest concerns regarding CH₄ emission is the contribution from unknown sources. We see the slight increase of CH₄ emission over those sites. Broken pipe lines or other facilities at the airport could be possible sources of CH₄, so we called it to attention. But, as you pointed out, this cannot be a deterministic source of CH₄. We modified/rephrased the sentences in the revised manuscript.

I think using kriging when you do not understand your sources is a risky endeavor. It is better to solve for everything without kriging first and then see how kriging may affect your results. But in your situation, you definitely do not want to trust kriging. Using kriging in regular mass balance is also dangerous if you do not have a good understanding of what you are measuring. Unfortunately it is often used without much thought. For example, see Figure 6 in Conley et al. (2017), the paper also uses the divergence methodology that you apply here, but they are careful to note that you want an optimal number of loops around your source before you can get a stabilized estimate of emissions. They estimated an optimal number of loops to be about 15 to 25. That is the case because turbulent conditions tend to increase the magnitude of the random error. I am afraid your sampling here is just too small for a good application of divergence theorem. It is important to acknowledge it. Solve without kriging and see what you can get.

We understand your concerns, and we appreciate the "riskiness". When we calculate fluxes based only on the measured data, without filling in the gaps between flight levels, the total flux estimate will obviously be much smaller than when we account for the entire surface of the cylinder using interpolated data. With an urban-scale cylinder (with a circumference on the order of 100 km), it is impossible to map out the entire surface (~100 km²) with dense measurements. Although kriging cannot be better than actual observations, it can be a good alternative to "mimic" actual data. We disagree with the reviewer's opinion that we solely rely on the kriging without an understanding of the data. We carefully performed the variogram analysis, and carefully chose the kriging parameters (sill, range, and nugget) based on the experimental and theoretical variogram obtained from the actual data we measured.

Figure 2S (b and d): You will have to eliminate November 17, 2015 case from your article. You cannot assume steady state conditions on a day with calm to variable winds near the surface. The wind rose is misleading as you mainly show free tropospheric winds, which should not be used for boundary layer flux calculation. Your boundary layer winds have no consistent direction. The data from a local weather station in Sacramento, CA supports that (and actually if you look carefully at your wind data you will see it too in your Figure). This comes back to the point I made earlier, where you need to show your actual

wind data from every case. You cannot just pick and choose what you show. It is no surprise that your flux estimations did not work well on that day. None of the aircraft methods would work on that day. It is very important to have a good forecast before you go and fly a mission of this type. I am not sure who designed this flight and for what, but it does not work here for your purpose. Perhaps you can find another flight that works better.

Done. Please see discussion above.

Reference

Conley, S., I. Faloona, S. Mehrotra, M. Suard, D. H. Lenschow, C. Sweeney, S. Herndon, S. Schwietzke, G. Petron, J. Pifer, E. A. Kort, and R. Schnell: Application of Gauss's theorem to quantify localized surface emissions from airborne measurements of wind and trace gases, Atmos. Meas. Tech., 10, 3345-3358, <https://doi.org/10.5194/amt-10-3345-2017>, 2017.

Karion, A. et al.: Methane emissions estimate from airborne measurements over a western United States natural gas field, Geophys. Res. Lett., Vol. 40, 1-5, doi:10.1002/grl.50811, 2013.

Karion, A. et al.: Aircraft-Based Estimate of Total Methane Emissions from the Barnett Shale Region, Environ. Sci. Technol. 2015, 49, 8124-8131, DOI: 10.1021/acs.est.5b00217, 2015.

Turnbull, J. C., Karion, A., Fischer, M. L., Faloona, I., Guilderson, T., Lehman, S. J., Miller, B.R., Miller, J. B., Montzka, S., Sherwood, T., Saripalli, S., Sweeney, C., and Tan, P.P.: Assessment of fossil fuel carbon dioxide and other anthropogenic trace gas emissions from airborne measurements over Sacramento, California in spring 2009. Atmos. Chem. Phys., 11, 705–721, 2011, doi:10.5194/acp-11-705-2011, 2011.

Response letter to Review #2

Responses from the Authors are given in blue italicized text throughout: Thank you for your very helpful feedback. Specific items of language, font size, etc. which will be addressed in the revised manuscript are colored here with gray highlighting.

General Comments:

This manuscript includes emission estimates of CO₂ and CH₄ from the Sacramento, California, area from aircraft measurements on three different days. It presents some important and interesting investigations on the sensitivity of flux estimation toward the mass balance method used, the treatment of wind measurements, the choice of background, the inclusion of entrainment at the top of the boundary layer, and different interpolation and extrapolation methods. Still, I think the manuscript needs improvement in the structure, explanation of the methods used as well as the presentation of obtained data and results. The manuscript needs major revisions before it can be accepted for publication in AMT.

The structure of the manuscript could be improved with respect to the different sensitivity studies. I recommend choosing one “best-conduct” approach, explaining and using it for the flights first, and then doing the sensitivity studies and relating their results to this “best-conduct” approach to see each choices influence on the flux calculation individually. Thus there would be one section each on the mass balance method used (Gauss vs. downwind curtain), the treatment of wind measurements (raw winds vs. mass-balanced winds), the choice of background (minimum vs. average), the inclusion of entrainment at the top of the boundary layer, and different interpolation (kriging, vertical interpolation) and extrapolation methods (kriging, constant, exponential weighting function, Gaussian fit).

The structure of the manuscript will be completely reorganized based on your suggestion of a "best conduct" approach followed by variants. More calculations were performed to make our points clear in the revised version of manuscript.

The outline of the revised manuscript will be this:

1. Introduction

2. Data and Methods

2.1 Data collection

2.2 Data gridding

2.2.1 Extrapolation to the surface

2.2.2 Elliptical fit and measurement interpolation (Kriging method)

3. Flux calculations

3.1 Base case experiment

3.2 Sensitivity Tests

3.2.1 Sensitivity of calculated flux to wind treatment

3.2.2 Sensitivity of calculated flux to the choice of background concentrations

3.2.3 Sensitivity of calculated flux to vertical mass transfer

3.2.4 Sensitivity of calculated flux to the PBLH estimate

3.2.5 Sensitivity of calculated flux to the closed shape

3.3 Flux uncertainties

4. Conclusions

The presentation of measured data differs for the three flights and the two compounds CO₂ and CH₄. Please choose the same set of figures for each flight, making sure all important data used in the flux calculation (like wind speed) is shown for all flights.

We appreciate this comment. We will include the wind data in the revised manuscript (see above) and will revise our figures.

The results of using different treatment of input data are the different flux estimates. These numbers are often only named in the text. I think a tabular representation of results for each sensitivity study (or two combined studies, like in Table 1) would increase the readability of the manuscript. I really liked Table 1 and its discussion.

We are glad that Table 1 was clear and helpful. We will expand it in the revised manuscript, separate it into two tables [Table 1 (urban scale), Table 2 (local scale)], and also include a new Table 3 showing comparison with the Turnbull et al. study and bottom-up inventories.

Table 1. Urban scale fluxes over Sacramento on November 18, 2013.

Background	Wind		Urban Scale (large loop)			
			November 18, 2013			
			CO ₂ (Mt yr ⁻¹)	Difference from base case (percent)	CH ₄ (Gg yr ⁻¹)	Difference from base case (percent)
min	Mass-balance	100 m layer avg	25.6±2.6		87.1±8.7	
		Whole column avg	26.6±2.7	3.9%	88.7±8.9	1.8%
avg	Mass-balance	100m layer avg	25.6±2.6	<1%	87.4±8.7	<1%
		Whole column avg	26.6±2.7	3.9%	89.0±8.9	2.1%
min	Raw		3.7± 0.4	86%	13.0±1.3	85%
avg	Raw		25.5±2.6	<1%	91.1±9.1	4.6%

Table 2. Local scale fluxes over landfill and rice field over Sacramento on July 29, 2015.

Background	Wind		Local Scale (small loop): July 29, 2015							
			Landfill				Rice Field			
			CO ₂ (10 ⁻¹ Mt yr ⁻¹)	Difference from base case (percent)	CH ₄ (Gg yr ⁻¹)	Difference from base case (percent)	CO ₂ (10 ⁻¹ Mt yr ⁻¹)	Difference from base case (percent)	CH ₄ (Gg yr ⁻¹)	Difference from base case (percent)
min	Mass - balance	100 m layer avg	2.2±0.8		7.1±2.5		2.5±0.4		2.5±0.4	
		Whole column avg	2.2±0.8	<1%	6.9±2.4	2.8%	2.5±0.4	<1%	2.6±0.4	2%
avg	Mass- balance	100 m layer avg	2.2±0.8	<1%	7.1±2.5	<1%	2.5±0.4	<1%	2.5±0.4	<1%
		Whole column avg	2.2±0.8	<1%	6.9±2.4	2.8%	2.5±0.4	<1%	2.5±0.4	<1%
min	Raw		3.7±1.3	68%	8.9±3.1	25%	1.7±0.3	30%	1.8±0.3	28%
avg	Raw		2.2±0.8	<1%	7.1±2.5	<1%	2.6±0.4	2%	2.5±0.4	<1%

Table 3. Flux estimates for the Sacramento urban area from measurements made on November 18, 2013. The two "curtain" rows below used the same wind treatments as the "whole cylinder" rows (mass-balanced wind).

		CO ₂ (Mt yr ⁻¹)	CH ₄ (Gg yr ⁻¹)
Whole cylinder-AJAX	(bg = min, 100m layer avg)	25.6 ± 2.6	87.1 ± 8.7
	(bg = avg, 100m layer avg)	25.6 ± 2.6	87.4 ± 8.7
Curtain -AJAX	(bg = min)	17.3 ± 1.7	64.4 ± 6.4
	(bg = avg)	8.9 ± 0.9	24.1 ± 2.4
Turnbull et al. (2011)		13.4 (with uncertainty of ~ 100%)	
Vulcan estimates for Sacramento		11.5	
CEPAM estimate for Sacramento		10.0	

^a Turnbull et al. (2011) data was collected in 2009; the value given here was converted from the mean reported value of 3.5 Mt C yr⁻¹ with a 1.1% yr⁻¹ increase in CO₂ flux to adjust to 2013.

^b Bottom-up inventory estimates of the annual total emissions from Sacramento County from Vulcan (Gurney et al., 2009) and the California Air Resources Board CEPAM database (Turnbull et al, 2011) are included for comparison. The Vulcan inventory is available only for 2002, and the CEPAM database is available for 2004. We applied a 1.1% yr⁻¹ increase in CO₂ flux to adjust to 2013.

I am not sure if all of your flights are well suited for flux estimation. Generally, you would look for a well-mixed boundary layer in order to decrease the uncertainty of flux below the lowest flight height. On November 17, 2015, the winds are quite different from one flight level to another and very weak at the lowest level. Furthermore, detecting the highest CO₂ concentration in an upwind part of the flight path shows that this day is not suitable for flux estimation. Also the local flux estimates on July 29, 2015, show low wind speed with changing direction.

Based on the comments of both reviewers, we have decided to remove the November 2015 case due to the vertical variability in wind speeds. However, we still believe July 29, 2015 is appropriate for testing the "closed shape" approach for flux estimates and have retained these cases in the current analysis.

Your calculation of mass-balanced wind is interesting. It seems as if the mass-balanced wind in Fig. 5 is constant with height. Shouldn't it vary with height because you use the average wind for each level? What is your surface condition? Why is kriging used? Please explain in more detail how the "mass-balanced" wind field is generated? The difference in the flux estimate does not surprise me (1.359). You have very good wind measurements, and you definitely see a change in wind speed with height in Fig. 5b. Low wind speed with high concentrations and high wind speed with low concentration might result in the same flux. Thus, Fig. 5c looks quite logical to me. If you remove all your information on the vertical wind speed change, as you did in Fig. 5e, then, of course, the flux only represents the concentration measurement. Why do you neglect your information on the wind situation? Did you ever calculate the mass-imbalance of the raw winds? Is it significant?

Thank you for your insightful discussion. Yes, the mass-balanced wind should vary with height when we use the average wind for each level. We have tested a variety of thicknesses for the vertical levels, and the results are now reported in the modified Table 1 (above). The original Fig. 5e was showing the "whole column average" case, and we apologize for not specifying this clearly in the original text. For reference, we show here the wind field with all four treatments. Panel (d) here is the same as Figure 5e in the original manuscript. We intend to include panel (b) here in an extended version of Fig. 5 in the revised manuscript.

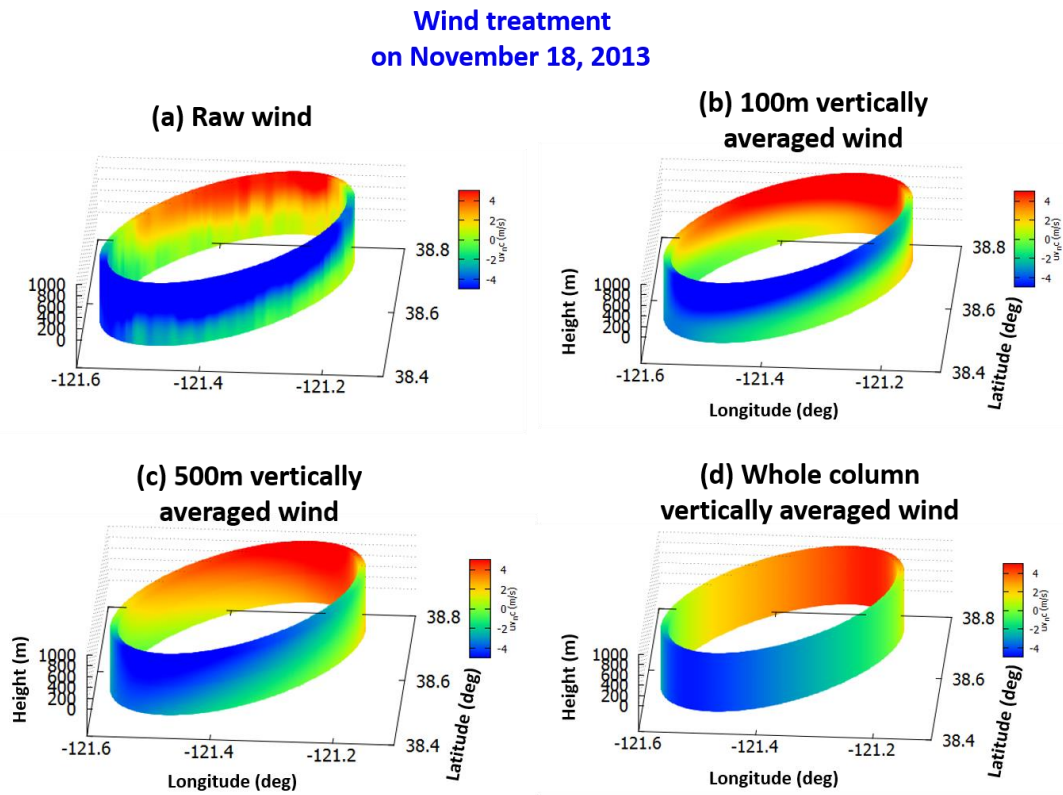


Figure: (a) the raw wind, (b) 100m vertically averaged wind, (c) 500m vertically averaged wind, and (d) whole column averaged wind on November 18, 2013. The blue color represents the inflow toward (and red outflow from) the cylinder so that it is defined as negative (positive) wind. (The similar plots are in Fig. 6 in the revised manuscript).

Your use and understanding of the divergence method seems flawed. Please review the Gauss theorem and describe it correctly in l. 257. I do not believe that background is necessary for this method. You simply calculate all fluxes through the surface of the cylinder (outflow – inflow) and thus receive the change of mass within the cylinder.

We do not need to know the background value for estimating flux when adopting the circular pattern of flight. This is clearly demonstrated in our experiments, showing that the flux estimates were not sensitive to the choice of background (minimum or averaged value). We will work harder on the language in the revised manuscript.

Please check the publication of Conley et al. (2017), which nicely explains the application of Gauss theorem on aircraft mass balance flights. For your second method (the curtain downwind of the sources) you definitely need a background, and here the influence of choice of the background value on the flux estimate is quite interesting.

Thank you for the suggestion. We referenced Conley et al. (2017), and looked at their approach. We carefully considered their method and compared them to our approach.

Your calculation of the flux through the top of the cylinder is useful, but I do not understand how you determine the surface flux. First, with the Gauss theorem you need to assume that all the mass change inside the cylinder (e.g. what leaves through the surface) comes from the sources on the ground, thus what you determine is the surface flux. Second, on the ground the vertical wind speed is zero. How can the surface flux calculated with your method then be different from zero?

Since the lowest flight altitude is about ~250 meters above the ground level, we can't directly measure the surface CO₂ or CH₄ concentration or wind. The vertical velocity near the surface was very small, but it was not zero ($W = -0.006$ m/s for November 18, 2013 case). So we could still calculate the surface flux part. But the surface flux was much smaller than the entrainment flux, and the entrainment flux itself was not much compared to the flux computed on the "cylindrical" (wall) surface. Although the contribution of surface flux uncertainty to the total flux estimate uncertainty could be improved, we decided not to focus on this in the current study since the contribution of vertical mass transfer to the total flux estimate is relatively small.

Finally, could you calculate an overall uncertainty of your flux estimates from the different calculation methods and treatment of input parameters?

We have determined the overall uncertainty of our flux estimates based on the kriged and mass balance wind methods. By assuming that the errors of each factor are Gaussian in nature, and each measurement (e.g., CO₂ and wind) is independent (no covariance), we estimate the overall uncertainties in the calculated flux by calculate the relative uncertainties from each point to the adding the fractional uncertainties of the kriged CO₂, CH₄, and winds in quadrature, as in Nathan et al. (2015). We also consider the uncertainty due to estimate of PBLH. We will add a brief discussion to the revised manuscript comparing the distribution of the calculated fluxes reported in the revised Tables to the calculated 10% uncertainty estimate.

Please improve the consistency of your terminology. For example, you defined the two ways of treating your wind measurements as “raw wind” and “mass-balanced wind”. In the following manuscript you then repeatedly use mean wind, measured wind, averaged wind, area-mean wind...

Very important points. Thank you for providing "fresh eyes" to notice this with. We should stick to using "raw wind" and "mass-balanced wind". We improved this in the revised manuscript.

I also recommend grammar checking by an English native speaker and thorough checking of references to Figures and Sections. Furthermore, please increase the size of the axis labels and color bars on most of your plots. They are not readable.

We improved the size and the quality of the plots in the revised manuscript.

Specific Comments and Technical Corrections:

I. 43: Which meteorological factors?

We meant the wind speed and measurement. We will rephrase it in the revised manuscript.

I. 46: “emissions fluxes” should become “emission fluxes”. Please check the whole manuscript.

Thanks. We double checked this in the revised manuscript.

II. 48-49: This should be reformulated due to the low winds on Nov. 17, 2015, and the high concentrations in the upwind part of the flight pattern.

We agree with you and have decided that this flight was not adequate for flux estimates. Hence, we will remove this flight from our analysis.

II. 49-50: The wind variability and seasonality has not been investigated in this study. Please reformulate.

We agree with you. In the revised manuscript, we removed those parts.

I. 51: Where do you show the influence of the distance to the emission sources?

We don't show this. We corrected the sentences in the revised manuscript.

I. 58: What is your “modeling strategy”? Do you do any modeling?

Here we meant the “statistical modeling”. Using one of the geostatistical methods, kriging, we filled the gaps between measured data.

I. 61: Why don't you mention your investigation of the background and wind treatment in the Abstract?

This is a good idea. In the revised manuscript, we mentioned our background and wind treatment in the abstract.

I. 65: Introduce abbreviations once and then use during the remainder of the manuscript (e.g., GHG).

Yes, we corrected that in the revised manuscript.

I. 66: Is air-quality important in this study?

No, but accurate emission estimates will affect “air quality” and its regulation, so this is why we mentioned this in the introduction.

I. 69: Check your use of “give rise to” ...

We changed the word to “causes”.

I. 72: What is the “role of human behavior in altering the emissions”? Do we need to know it for national emission estimates?

Good points, we don't need to do know, so we removed this part.

I. 76: What are indirect emissions?

"Indirect emission" was intended to describe information in emission databases which are inferred or extrapolated or given a time dependence that is not directly measured. We will find a more direct way to state this in the revised manuscript.

I. 78: Please give an example of a bottom-up inventory using proxy data to achieve fine spatial resolution.

Vulcan inventory CO₂ data. (Gurney et al., 2009)

II. 83-86: What about flux estimates of European cities?

This a great point. So we added studies for European cities in the revised manuscript: (Peylin et al, 2005; Kountouris et al., 2018).

I. 94: What do you mean with "those efforts reach general agreement on emission inventories across the cities"?

We rephrased It in the revised manuscript. "While those efforts reach general agreement on emission inventories across the cities" will be changed to "Since current emission inventories do not consider individual characteristics of each city, they have limitations..."

I. 106: Supplementary Material

We reworded it.

I. 108: Do you really mean "uniform vertical mixing", or maybe "uniform distribution of trace gases"?

We reworded it. "uniform vertical mixing" will be changed to "uniform distribution of trace gases with altitude within the PBL and with time".

I. 110: Does this sentence ("These studies...") apply to the first or second category, or maybe both??

These studies apply to the first category.

I. 112: Does the "single-screen multi-transect method" really depend on constant wind speed? *You could also use average wind at each transect or even raw wind at each measurement point.*

Correct. The original sentence was based on the implementation of the method and the assumptions used by Karion et al. (2015). We will clarify this in the revised manuscript and then draw the comparison to our data set which contains in situ wind measurements, allowing the calculation you suggest (which is now included in the new Table 3).

I. 119: The cylinder pattern should be "around" a source and not only "near".

You're right. We corrected it in the revised manuscript.

I. 126: Why are the additional point sources considered sources of uncertainty?

If there are not included inside the oval, any uncounted point sources could be considered additional "unknown" sources of GHGs that should have been included in our urban-scale study. "Uncertainty" was probably not the best word to use, and we will fix or omit this sentence in the revised manuscript.

I. 131: I think we all got the concept of three-dimensional space (delete the parentheses).

Yes, we deleted the parentheses.

I. 134: The PBLH is not hard to measure. It is relatively easily determined from a vertical profile of temperature and humidity as you have done in this study. You even stated that the different approaches you used led to similar results. So what is difficult with respect to the PBLH? It is certainly difficult to model correctly, as you stated that substantial differences exist between models and reanalysis data. Also consider the large diurnal variability of PBLH.

We removed "that is hard to measure".

I. 135: Please don't use "observed" in connection with models. This might confuse.

Yes, we corrected it into "exist in both models and reanalysis data".

I. 139: Do you really think the execution of flights is a goal of the study? Or is it merely necessary for the other goals?

One of the goals of this study is to test the flux estimate when using the cylindrical flight pattern. To reduce the confusion, we removed the word "execute" in the revised manuscript.

I. 145: Which "value"?

We changed it into "mixing ratios" in the revised manuscript.

I. 153: Describe the three flights here and mention figure 1. It is not mentioned at all in the text.

Yes, we did it.

I. 154: How many whole-air standards do you use for calibration?

The CO₂ and CH₄ instrument (Picarro Inc., model 2301-m) is calibrated before each flight using two whole-air standards from the National Oceanic and Atmospheric Administration's Earth System Research Laboratory (NOAA/ESRL; CO₂ = 416.267 and 393.319 ppmv; CH₄ = 1.98569 and 1.84362 ppmv). In addition, a set of secondary, synthetic standards was used to verify the linearity of the instrument across a wider range of concentrations. We included this information in the revised manuscript.

I. 159: Take off time is not sufficient. Please give the total flight times in UTC. Using Pacific Standard Time and Pacific Daylight Time here needs more explanation on why you give take-off times in different ways.

One flight was executed in the winter and one during Daylight Savings Time. We will re-write this section more clearly: Sampling occurred 21:10 – 22:00 UTC for the November flight (local standard time is UTC minus 8 h, 13:10 – 14:00 PST) and 20:55 – 21:45 UTC for the June flight. We included this in the revised manuscript.

Sect. 2.2: Review order of sections: I would first discuss the interpolation method and then the extrapolation.

We will consider this suggestion when constructing the revised manuscript. The significant restructuring we plan to do (shown above) may benefit from discussing the interpolation first, but we can't judge which is best until we invest the time in restructuring and re-ordering the figures.

I. 163: Reformulate: "Because the lowest flight level was typically between 250 m and 380 m above the surface ..."

We corrected it as suggested.

I. 165: Sentence needs restructuring: The "unmeasured values" lead to uncertainty whether or not a "well-mixed layer assumption" is made. Split sentence!

Yes, we worked on that.

I.168: Refer to Figure 2 here. There is no reference to it in the text.

We did that.

I. 169: What do you mean by "elevated" plume? Is it lifted of the ground or are there large enhancements of the concentration?

We mean the former: lifted off the ground.

I. 170: How exactly do you derive the background level? What is the “lowest flight measurement”? Has it got anything to do with the “lowest flight level” which you use in the formula? Is the background only determined from the lowest flight level? Why are you talking about background at this point? It is a section on extrapolation to the ground. Do you also extrapolate the background values? What do X and t stand for?

We apologize for the wording in the original manuscript at line 170. Our description of the “constant” method was unnecessarily confusing. The blue curves in Figure 2 show what we were trying to describe: at all altitudes below the yellow diamond (lowest flight level), the mixing ratio was presumed to be exactly equal to the value measured at the lowest flight level. Please also see the new figure below in supplementary materials. The bottom left panel shows more clearly how the values measured along the lowest flight level are assigned to all grid cells below the measurement altitude.

X is the given trace gas concentration, and t is the single parameter representing each point on the ellipse (eccentric anomaly)

I. 172: Do you mean that the details of the method are described in Gordon et al. (2015)?

Yes, that is what we mean.

I. 173: How is the Gaussian distribution of the plume dispersion calculated?

The Gaussian fit method is similar to the exponential fit method, except that the surface-sourced plume dispersion follows a Gaussian distribution function. For a given set of (x: height, f(x): GHG) pairs, we get the rate of change and the mixing ration at the surface ($C_{suf}(s)$) at each given s parameter from the gaussian function,

$$f(x) = C_{top}(s) + (C_{suf}(s) - C_{top}(s)) * \exp(-x^2 / 2s^2)$$

The detailed calculation method is based on Gordon et al. (2015), so we did not include this equation in the revised manuscript.

Sect. 2.3: Consider renaming the section to “Measurement interpolation”.

Thank you. That is a nice suggestion.

II.176-186: Should this be a separate section called: Projection of data to cylinder surface?

Yes, we wrestled with that. It is a bit too small to stand alone, but it might make sense to do that in the revised structure.

I. 182: What is Y?

(X(t), Y(t)) is the each point on the ellipse represented by a single parameter (t, eccentric anomaly). So X refers to the longitude and Y refers to the latitude.

I. 190: Refer to Fig. S4 as you show these differences there. Consider over plotting the measurements on the kriged and interpolated fields for better assessment of your result that kriging better captures individual plume features. What altitude range do the elliptical cylinder plots cover? Ground to PBLH? Please state in the figure caption.

Thank you for the good suggestion. To better explain the different interpolation methods, we will incorporate Fig. S4 with Fig. 2 in the revised manuscript. We plot up to the highest measurement altitude for the elliptical cylinder plots. However, for computing the actual fluxes, we only integrate the fluxes from the surface ($z=0$) to the top of the PBLH. We will state this clearly in the figure caption in the revised main and supplementary material.

II. 214-227: Consider a separate section on uncertainties.

This is a good idea. We will make this as a separate section. See our new outline for the revised manuscript (page 1-2).

I. 216: Not only downwind interpolated values induce uncertainty. Upwind values as well.

You're right. We removed "downwind" from the sentence.

I. 226: Add "observations" behind "direction".

Yes, we added this in the revised manuscript.

I. 229: Remove "to the choice of background value and" because this is not the topic of this section. You do not investigate the wind characteristics but the treatment of wind measurements.

We removed it in the revised manuscript.

I. 230: Remove "In one"

We corrected it.

I. 231: What is "measured points"? How did you measure them?

We meant the discrete measurement locations (lon, lat, height) at a given time obtained by aircraft. We will endeavor to find better wording in the revised version.

I. 233: Stick to one tense (averaged, equaled).

We were careful in using tense in the revised manuscript.

I. 233: "By assuming non-divergence, mass can be balanced." This is correct, but is this really what you need here?

This is important. Because this is not divergent, the inflow and outflow are the same, and we can apply the mass-balance idea to our flux calculation.

I. 242: Do you assume PBLH to be constant during your flights? At what time during the flight did you measure the profile?

Yes, we assume that PBLH is constant throughout our flights. Sampling profiles occurred 21:10 – 22:00 UTC for the November flight (local standard time is UTC minus 8 h, 13:10 – 14:00 PST) and 20:55 – 21:45 UTC for the June flight.

I. 243: Is the boundary layer "growing" during your flights? How do you know?

No, we assumed that there is not sufficient time for change in the PBLH during our flights (less than 1.5 hours) We think the confusion comes from the word that we used. We will change it from "boundary layer growth" to "boundary layer height" in the revised manuscript.

I. 248: How is $C(t,z)$ determined? How can one point surround the top of the cylinder? How is the background defined here?

We apologize for the grammar error. The sentence should have read " $C(t,z)$ is the CO_2 concentration ($g\ m^{-3}$) at each point around the top of the cylinder (where $z=h$), and $C_{bg}(h)$..."

We used this formulation for each method (sensitivity test) of defining the background.

I. 252: Is the entrainment calculated from the kriged data?

Yes.

I. 263: Flux is defined through a surface. Thus it cannot be “inside” the cylinder.

You are right. Flux is defined through a surface. We will fix the grammar in this section in the revised manuscript.

II. 265-280: See my comment in the General Comments section on the use of a background value with the Gaussian divergence theorem. If you consider inflow and outflow, you do not need a background. In your formula, the result should be invariant to the value of background mixing ratio chosen if you consider positive contributions as outflow and negative contributions as inflow.

Thank you for elaborating on this. This is also why we used the mass-balanced mean wind, so that influx mass and outflux mass are the same and the total flux estimate is not dependent on having an understanding of background mixing ratios. We will mention it in the revised manuscript.

I. 291: Use present tense.

We changed it in the revised manuscript.

I. 295: Remove “concentration”.

We removed it in the revised manuscript.

I. 299: How is the kriged estimate less arbitrary in an area far away from measured values? What assumptions is it based on? Is the state of the PBL (stable/unstable) taken into account?

We believe kriging is less arbitrary because we have more constraints for formulating a kriged estimate. When we calculate fluxes based only on the measured data, without filling in the gaps between flight levels, the total flux estimate will obviously be much smaller than when we account for the entire surface of the cylinder using interpolated data. With an urban-scale cylinder (with a circumference on the order of 100 km), it is impossible to map out the entire surface (~100 km²) with dense measurements. Although kriging cannot be better than actual observations, it can be a good alternative to “mimic” actual data. We disagree with the reviewer's opinion that we solely rely on the kriging without an understanding of the data. We carefully performed the variogram analysis, and carefully chose the kriging parameters (sill, range, and nugget) based on the experimental and theoretical variogram obtained from the actual data we measured.

In contrast, other methods are solely based on general assumptions without the actual inspection of the existing spatial dataset.

I. 300: You don not mention the Gaussian fit method depicted in Figure 2 at all.

We mentioned it in section 2.2 (Line 172) in the original manuscript. The Gaussian fit method is similar to the exponential fit method, except that the surface-sourced plume dispersion follows a Gaussian distribution. See the explanation above. We will mention it more clearly in the revised manuscript.

Sect. 3.1: What is the influence of the different choice of interpolation and extrapolation on the flux estimate? Here a table similar to Table one would be great.

Thank you for a good comment. However, what we focus in this study is the impact of treatment of wind measurement and background on the flux estimate, not comparing different interpolation methods

(although we mentioned these for completeness using Fig. 2). Furthermore, although we did show different GHG mixing ratio assumptions below the lowest flight level, we do not consider how to treat the wind below the lowest flight level. We may assume a constant wind speed and compute the flux for each of the extrapolation methods, but we are not sure how to interpret those values and we believe this will give us additional challenges, leading to additional uncertainty in total flux estimates without understanding the physical meaning of the calculated values. Furthermore, we already mentioned that the difference of CO₂ estimate below lowest flight level could lead to the change of GHG concentration up to 20%.

I. 304: Remove “gap of the”.

We removed it in the revised manuscript.

II. 314-320: Please mark all the locations mentioned in the text on a map so the reader can confirm your statement.

We marked it in the revised manuscript.

I. 325: Present tense.

Yes, we used consistent verb tense.

I. 327: Please check “a farther”.

We changed it to “far”.

I. 330: Maybe use the last sentence of this paragraph as its first. Good introduction.

This is a good advice, but we restructured the paragraph and changed sentences in the revised manuscript. We placed it in section 3.1.(~ Line 280 - 282) in the revised manuscript.

I. 350: The PBLH you determine from the vertical profile might have an uncertainty of <1%, but is this value representative for the whole measurement area with this accuracy? What about changes over time and with the location? How does a less defined PBLH influence the uncertainty?

We assumed that PBLH does not change during our 1.5 hour flight. The urban-scale area studied is approximately 20 km x 40 km with pretty uniform topography, thus we expect the PBLH to be the same throughout the sampled domain. However, we do acknowledge that a different estimate of PBLH can increase the uncertainty. Please see the response below.

Fig. S6: Looking at your method of estimating PBLH there seems to be a possible error of more than 1 % as well. In Fig. S6d it becomes clear, that you use the 50 m averaged values for checking the gradients. Then you place it at the top of the layer with the highest gradient. Here it is visible, that this point is easily 40 m above the layer where a 20 m averaged profile would see the gradient. Thus your uncertainty is around 50 m, which would be almost 10 % for a PBLH of 600 m.

That is a very good point. As you pointed out, the uncertainty of the PBLH can be up to 10% if we determine the PBLH based on the largest gradient of the vertical profile of the potential temperature. We will consider the uncertainty of the PBLH estimate and include it in the total uncertainty estimate in the revised manuscript. Based on our 3 measurements, the uncertainty due to PBLH estimate for urban scale is about ~10%, but the uncertainty due to PBLH estimate for the local-scale is about 1-5 % so that the change of PBLH does not affect the total flux estimate. As seen in Fig. S6, the vertical range of the largest gradient of potential temperature is very small, compared to the urban-scale. This leads us to another important message: the uncertainty gets larger when we deal with urban-scale flux estimate. We will include the uncertainty due to the estimate of PBLH in the total flux uncertainty estimate in the revised manuscript.

I. 355 ff: See my comment on the treatment of “mass-balanced wind” in the General Comments section.
We made new tables for the comparison as you suggested. Please see the tables (page 2-3).

Sect. 3.3: Please already refer to your Table 1 when naming the results.
Yes, we did so.

I.267: Where is an “actual” location of the rice field? Please show locations on a map rather than just giving coordinates. This is very hard to visualize for a reader.
The labels in Figure S8 are awfully hard to read, and for that we apologize. We will improve them in the revised version

I. 370: “the local emissions are attributed to these high flux estimates”. Did you mean: “The high flux estimates are attributed to the local emissions”?
Yes. Thank you for pointing this out. We will fix it in the revised manuscript.

I. 374: Formulation: “mean wind vector at the dominant wind direction (positive and one direction) and speed”. How is this calculated?
Many previous studies use the mean wind averaged over the PBLH. Karion et al. (2015) estimate the total CH₄ emission in the flight region (curtain flight) using a mass balance approach. According to their study, when the mean horizontal wind speed and direction are steady during the transit of an air mass across an area, the resulting calculated horizontal flux is equal to the surface emission between the background location and the downwind measurement. This calculation required the assumption of steady horizontal wind direction, a well-developed convective PBL, and measurements sufficiently downwind of the emission source such that the emissions are vertically distributed throughout the PBL.

I. 381: There is no Table 2.
We fixed this.

I. 387: Raw wind is displayed in the bottom two lines.
We fixed it in the revised manuscript.

II. 390-391: This sentence is incomplete and not logical.
We changed it in the revised manuscript.

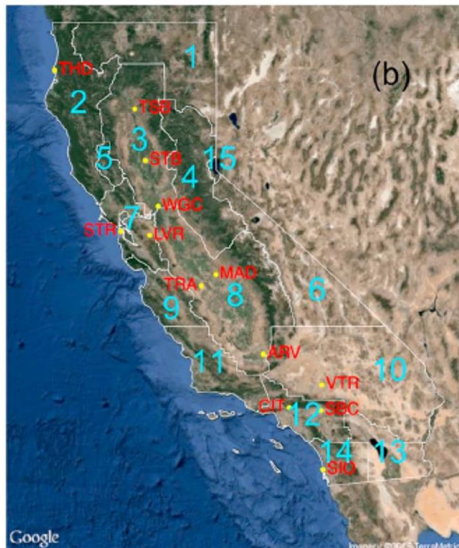
I. 394: Table 1 shows a range of 3.68 - 26.58 Mt CO₂ yr⁻¹ for the whole city.
Thank you for catching that. It must have been a hold-over from an earlier draft. We decided to use the emission estimate from the base case experiment, so we put the one estimate here.

I. 396 ff: Here you investigate the difference between using the complete ellipse and only the downwind part. This should be a separate section, and the results should be presented in another table.
Yes, we presented it in a new table (Table 3) in the revised manuscript.

I. 399: Change “From this study,...” to “According to these calculations...”
Thank you for catching that. It must have been a hold-over from an earlier draft.

I. 401: Table 1 gives a range of 13-92 Mt CO₂ yr⁻¹ for Nov. 18, 2015.
We corrected it in the revised manuscript. We decided to use the emission estimate from the base case experiment, so we put the one estimate here.

I. 402: Please indicate “Region-3” on a map.



These figures are from the study led by Jeung et al. (2016), and region 3 refers to the Sacramento valley. Each number represents the region classification based on California Air Basins (<https://www.arb.ca.gov/ei/maps/statemap/abmap.htm>). Thus, this covers much larger area than we actually measured for the flux calculation for this study. We will explain this better in the revised version.

I. 405: Is vi) the same as i)?

Yes, so we corrected that.

I. 405: Which of these does “This” refer to?

Good point. We changed this to “Consideration of these factors “ in the revised manuscript. (Line 397 in the revised manuscript)

II. 415-422: “Note ... Table 2.” All this is repetition to before and not about the topic of this section which is “vertical mass transfer”.

We agree with that. We removed this part in the revised manuscript.

I. 428: Remove “First,”

We removed this in the revised manuscript.

I. 431: Specify: “different flux calculation methods”

We removed it.

I. 453: There is a contradiction here “the final flux estimates become similar”, because the beginning of the sentence states that the background value is a major source of uncertainty.

As you pointed out, background concentration is not important for the cylindrical flight, and we actually showed that the total flux is insensitive to the choice of background concentration when we used the mass-balanced mean wind. We stated that background value is a major source of uncertainty when we do not use mass-balanced wind for cylindrical flights. We will rewrite this more clearly in the revised manuscript.

I. 459: Insert “that” after “suggesting”.

We removed that part in the revised manuscript.

II. 460-468: This section is a general overview of the flight results and should be placed earlier in the Conclusions.

We slightly changed the paragraph and moved them to the earlier in the conclusions.

I. 463: An overview of wind conditions should also be placed in the Results section.

This is a good point and we mentioned it in the earlier in the conclusion in the revised manuscript.

I. 464: This result (isolated high concentrations of CO₂) has not been shown in the Results section either. *We showed a high concentration of CO₂. This is shown in Fig. 4(c) and Fig. 5(a, d) in the original manuscript. We will more clearly discuss these plots in the revised manuscript.*

I.470: Why did you expect sources to be concentrated on the downwind side?

We didn't mean that we expect sources to be on the downwind side. What we tried to state is that horizontal flux is transported to the downwind side. We think this confusion comes from the unclear wording. We are sorry for the confusion and we will be more clear in the revised manuscript.

I. 471: “Furthermore” does not fit here.

We removed this in the revised manuscript.

I. 471: Wind variability definitely influences the flux estimates, not only during different times of the year. So this seems logical. It would be much more interesting how large the uncertainty due to this is assumed to be.

We agree with that. We were interested in the influence of the wind treatment on the final flux estimate. However, we only used the measured wind, not any other source of wind data. It would be interesting to understand the magnitude of the uncertainty of the total flux estimate depending on the source and treatment of the wind data (e.g. measured wind vs. modeled wind with different temporal and spatial resolutions), but this is beyond the scope of this study and will be a topic of the future study.

I. 475: The size of the ellipse is another factor that appears here for the first time in the manuscript. There is no data given on how large your ellipses were and what the influence is in the Results section.

We analyzed two flight data at different size – urban scale (~ 20 x ~40 km) and local scale (< 3km). We mentioned the scale in the introduction (Line 144 in the original manuscript), and it sounds like we should reiterate it in the new Section 2.1.

I. 480 and 481: Remove two of the three “further”.

We removed this in the revised manuscript.

I. 482: Do you really want to assess: “seasonality of sensitivity of emission estimates”? Just start with the seasonality of emissions first.

Good point. No, we changed it into “seasonality of emission estimates” in the revised manuscript.

I. 484: Where do you show the sensitivity of emission estimate uncertainty to temperature and potential temperature?

We removed the sentences.

II. 490-491: This sentence needs some revision and focus.

We worked on them in the revised manuscript.

Figures

Fig. 1: There is no shading visible in Fig. 1c.

By shading we meant “color fill” in Fig. 1c. The blue color represents inflow (airflow passing through the cylinder, negative sign) and red color represents outflow (airflow passing out from the cylinder, positive sign), respectively.

Fig. 2: What is the “altitude of the lowest flight data”? Please indicate the location of these measurements on a map, giving coordinates is not very helpful.

The altitude of the lowest flight can be shown in the time series plots (shown in the response to reviewer #1). We will include this in the revised manuscript. We will also indicate the location of the measurement in the map.

Fig. 3d: Is the ellipse shown from the ground to the highest flight level or which altitude range?

Yes, the ellipse is shown from the ground to the highest flight measurement level (~ 1000 m). This is the same as shown in the time series plots (shown in response to reviewer #1).

Fig. 4: Please provide headings with the date of the flight for the left and the right column.

We removed the Nov. 17, 2015 case, and the date was shown in the figure caption.

Fig. 5: Why is the mean wind kriged? This has not been mentioned in the text.

We first kriged the measured wind and then computed the mean wind (averaged the kriged wind) at each level. We tested levels of 100m, 200m, 500m, 1000m thickness, as well as the whole cylinder.

Fig. 7: Why is there this large space between the two sets of bars? What is “area-mean”?

This just means “mass-balanced wind (whole vertical layer)”. We were careful and consistent with our terminology in the revised manuscript.

Table 1: Tables normally have their description above not below them.

Thanks for reminding us of that. We modified them in the revised manuscript accordingly.

Supplementary Material:

There appear to be bits and pieces of text strewn throughout the Supplement. Please give them a heading and a number so it becomes clear where they belong, and you then may also refer to them from the main manuscript.

Fig. S1: Figure b color bar label is missing.

We will correct it.

I. 7: I am not sure if you can say that emissions are “accumulated” downwind. They are transported downwind, but accumulation would mean that there is very slow wind only.

We agree with you. We used the wording carefully in the revised manuscript.

II. 11-12: This is not true. With a certain flight it is also possible to detect emissions from more than one point source within the city, throughout the city and downwind. It gets problematic if there are sources further upwind of the city that gets mixed with the city plume and cannot be separated from it.

We will correct them in the revised manuscript.

II. 15: You mention three types of flight patterns in the main manuscript but only show two of them here. *We showed two flight in the revised manuscript.*

Fig S2: Reformulate “throughout the altitude”. Color bar labels are missing. *We removed the plot in the revised manuscript.*

I. 25: “accumulated” s.a. *We will work on them in the revised manuscript.*

I. 28: Why is air at lower wind speeds less dispersive? *We removed November 17, 2015 case, so we removed these parts.*

I. 28 ff: Reformulate sentence “Both flights ...” *We removed November 17, 2015 case, so we removed these parts.*

I. 30: Who uses continental scale wind for flux estimates? *We removed the wind rose plots.*

Fig. S3: This figure is not mentioned in the main manuscript. Please add flight dates to the left of the plots. *We mentioned this figure in the section 1 in the revised manuscript.*

I. 36: Consider “falling”. For methane the dashed line is blue. Remove “observation”. *We changed it into “corresponding”. And we removed “observation” in the revised manuscript.*

Fig. S4: Why are there “boxes” or vertical cuts visible in (d)? Does this have to do with gridding? What is the grid size? Could you plot the measurements on top of the interpolated fields? This way it is easier to assess your statement “kriging reflects the individual plume characteristics better”. Could you show the extrapolated fields to the ground as well? Which step is performed first: interpolation or extrapolation? Is this described in the text?

Also: Use the same color bar range for all plots.

Yes, the boxes (vertical columns) are related to the bin size for the interpolation and fit. Above the lowest flight level, we can use interpolation, but below the flight level, we need to do extrapolation. The white boxes represents no result due to the lack of the number of data used.

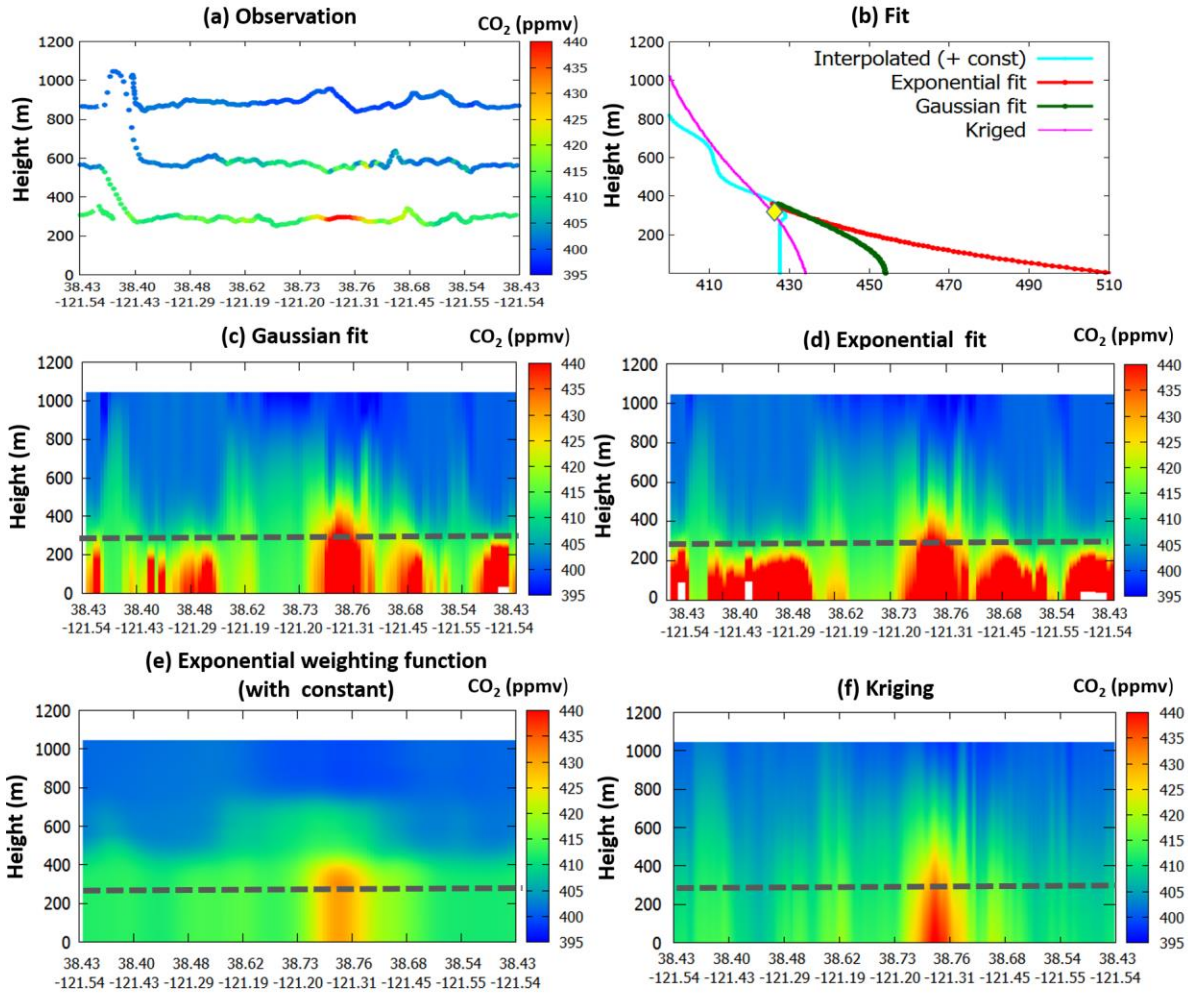


Figure: (a) Observed CO₂ over the Sacramento loop on November 18, 2013. (b) The vertical profiles of calculated CO₂ mixing ratios around 38.75° N, 121.27° W. The yellow diamond indicates the altitude of the lowest flight data. The kriged values (magenta), interpolated values with exponential weighting function and extrapolated values using constant (cyan), gaussian fit (green), and exponential fit (red) are compared. The CO₂ mixing ratio obtained from (c) the gaussian fit, (d) exponential fit, (e) exponential weighting function with constant, (f) kriging method. The empirical fits were generated based on the approach by Gordon et al. (2015). In panels (c) and (d), the white boxes result from no fit due to the lack of the data points. (Fig. 3 in the revised manuscript)

The figures above show the CO₂ field extrapolated to the ground. We do both interpolation and extrapolation in one process. We applied a formula for gaussian fit and exponential fit (Gordon et al., 2015) based on the lowest flight level data). For the interpolation, we used the exponential weighting function for the data above lowest flight level (for the interpolation), and then a constant value for the locations below the lowest flight level (for the extrapolation). Yes, we will use the same color bar range for all panels. The black dashed line represents an approximate lowest flight line. For more information, please see Fig. 3 in the revised manuscript.

I. 57: Don't (b) and (d) also show only the subset of the ellipse? Could you change the direction of these plots? Then this arrow would not be necessary.

The horizontal range is much larger than the vertical range. So, it is very hard to see the actual difference if you try to compare the whole ellipse. That is why we just try to show only a subset of the ellipse for comparison. But as you see in the plots above, there is still a noticeable difference between kriging and interpolation with an exponential weighting function. Yes, we changed the direction of this plot. The modified plot is below.

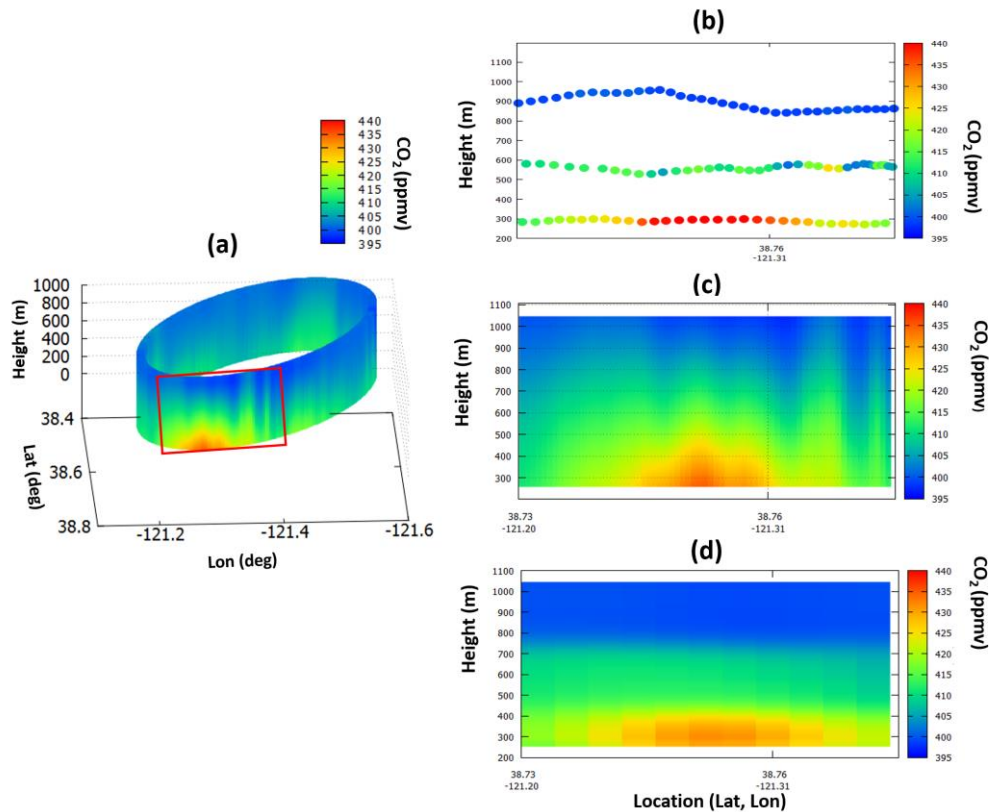


Figure: (a) Kriged CO₂ mixing ratio, (b) Measured CO₂ mixing ratio, (c) CO₂ mixing ratio using kriging interpolation method, (d) interpolated CO₂ mixing ratio using a conventional exponential weighting function along a subset of the ellipse around Sacramento on November 18, 2013. This portion of the perimeter corresponds to the red box of the elliptical cylinder shown in panel a. The vertical extent of the elliptical and 2-D plots is set to the highest measurement altitude. (Fig. S3 in the supplementary material).

I. 82: Remove the sentence: “The CH₄ enhancement was localized near the landfill.” This is obvious.

We removed it in the revised manuscript.

I. 83: Also remove “..., and we ... case.” This is also obvious.

We removed it in the revised manuscript.

Fig. S7: This figure is not mentioned in the main manuscript.

We incorporate the Fig. S7 into Fig. 7 in the revised manuscript and removed the rose plot.

Reference

Conley, S., I. Faloona, S. Mehrotra, M. Suard, D. H. Lenschow, C. Sweeney, S. Herndon, S. Schwietzke, G. Petron, J. Pifer, E. A. Kort, and R. Schnell: Application of Gauss's theorem to quantify localized surface emissions from airborne measurements of wind and trace gases, *Atmos. Meas. Tech.*, 10, 3345-3358, <https://doi.org/10.5194/amt-10-3345-2017>, 2017.

Gordon, M., Li, S.-M., Staebler, R., Darlington, A., Hayden, K., O'Brian, J., and Wolde, M.: Determining air pollutant emission rates based on mass balance using airborne measurement data over the Alberta oil sands operations, *Atmos. Meas. Tech.*, 8, 3745-3765, doi:10.5194/amt-8-3745-2015, 2015.

Jeong, S., et al.: Estimating methane emissions in California's urban and rural regions using multi-tower observations, *J. Geophys. Res. Atmos.*, 121, 13,031–13,049, doi:10.1002/2016JD025404, 2016.

Karion, A. et al.: Methane emissions estimate from airborne measurements over a western United States natural gas field, *Geophys. Res. Lett.*, Vol. 40, 1-5, doi:10.1002/grl.50811, 2013.

Karion, A. et al.: Aircraft-Based Estimate of Total Methane Emissions from the Barnett Shale Region, *Environ. Sci. Technol.* 2015, 49, 8124-8131, DOI: 10.1021/acs.est.5b00217, 2015.

Kountouris, P., Gerbig, C., Rodenbeck, C., Karstens, U., Koch, T. F., and Heimann, M., 2018: Atmospheric CO₂ inversions on the mesoscale using data-driven prior uncertainties: quantification of the European terrestrial CO₂ fluxes.

Nathan, B., Golston, L. M., O'Brien, A. S., Ross, K., Harrison W. A., Tao, L., Lary, D. J., Johnson, D. R., Covington, A. N., Clark, N. N., and Zondlo, M. A.: Near-Field Characterization of Methane Emission Variability from a Compressor Station Using a Model Aircraft, *Environ. Sci. Technol.*, 2015, 7896-7903, DOI: 10.1021/acs.est.5b00705, 2015.

Peylin, P., Rayner, P. J., Bousquet, P., Carouge, C., Hourdin, F., Heinrich, P., Ciais, P., and AEROCARB contributors, 2005; Daily CO₂ flux estimates over Europe from continuous atmospheric measurements: 1, inverse methodology, *Atmos. Chem. Phys.*, 5, 2173-3186, 2005.

Turnbull, J. C., Karion, A., Fischer, M. L., Faloona, I., Guilderson, T., Lehman, S. J., Miller, B.R., Miller, J. B., Montzka, S., Sherwood, T., Saripalli, S., Sweeney, C., and Tan, P.P.: Assessment of fossil fuel carbon dioxide and other anthropogenic trace gas emissions from airborne measurements over Sacramento, California in spring 2009. *Atmos. Chem. Phys.*, 11, 705–721, 2011, doi:10.5194/acp-11-705-2011, 2011.

Quantification of CO₂ and CH₄ emissions over Sacramento, California based on divergence theorem using aircraft measurements

5 Ju-Mee Ryoo^{1,2}, Laura T. Iraci¹, Tomoaki Tanaka^{1,8}, Josette E. Marrero^{1,9}, Emma L. Yates^{1,3},
Inez Fung^{4,5}, Anna M. Michalak⁶, Jovan Tadić^{6,7}, Warren Gore¹, T. Paul Bui¹, Jonathan M.
Dean-Day^{1,3}, Cecilia S. Chang^{1,3}

¹Atmospheric Science Branch, NASA Ames Research Center, Moffett Field, CA, 94035

10 ²Science and Technology Corporation (STC), Moffett Field, CA, 94035

³Bay Area Environmental Research Institute, Moffett Field, CA, 94035

⁴Department of Earth and Planetary Sciences, University of California, Berkeley, Berkeley, CA 94720

⁵Department of Environmental Sciences, Policy and Management, University of California, Berkeley, Berkeley, CA
94720

15 ⁶Department of Global Ecology, Carnegie Institution for Science, Stanford, CA 94305

⁷Now at Climate and Ecosystem Sciences Division, Lawrence Berkeley National Laboratory, Berkeley, CA 94720

⁸Now at Japan Weather Association, Tokyo, Japan

⁹Now at Sonoma Technology, Inc., Petaluma, CA, 94954

20

~~Submitted to~~ In revision for

25

Atmospheric Measurement Techniques

30

35

40 *Correspondence to:* Ju-Mee Ryoo (ju-mee.ryoo@nasa.gov)

Abstract

Emission estimates of carbon dioxide (CO₂) and methane (CH₄) and the meteorological factors affecting them are investigated over Sacramento, California, using an aircraft equipped with a cavity ring-down greenhouse gas sensor as part of the Alpha Jet Atmospheric eXperiment (AJAX) project. To better constrain the emissions fluxes, we designed flights in a cylindrical pattern and computed the emission fluxes from ~~three-two~~ flights using a kriging method and Gauss's divergence theorem.

~~The CO₂ and CH₄ mixing ratios at the downwind side of Sacramento show relatively consistent patterns across the three flights, but the fluxes vary as a function of different wind patterns on a given flight day. The wind variability, seasonality, and assumptions about background concentrations affect the emissions estimates, by a factor of 1.5 to 8. The uncertainty is also impacted by meteorological conditions and distance from the emissions sources. The largest CH₄ mixing ratio was found over a local landfill.~~

~~Differences in wind treatment and assumptions about background concentrations affect the emissions estimates by a factor of 1.5 to 7. The uncertainty is also impacted by meteorological conditions and distance from the emissions sources. The largest CH₄ mixing ratio was found over a local landfill. The vertical layer averaging affects the flux estimate, but the choice of raw wind or mass-balanced wind is more important than the thickness of the vertical averaging for mass-balanced wind for both urban- and local-scale.~~

The importance of vertical mass transfer for flux estimates is examined, ~~but-and~~ the difference in the total emission estimate with and without vertical mass transfer is found to be small, especially at the local scale. The total flux estimates accounting for the entire circumference are larger than those based solely on measurements made in the downwind region. This indicates that a closed-shape flight profile can better contain total emissions relative to a one-sided curtain flight because most cities have more than one point source and wind direction can change with time and altitude. To reduce the uncertainty of the emissions estimate, it is important that the sampling and modeling strategy account not only for known source locations but also possible unidentified sources around the city. Our results highlight that aircraft-based measurements using a closed-shape flight pattern are an efficient and useful strategy for identifying emission sources and estimating local and city-scale greenhouse gas emission fluxes.

Formatted: Font color: Auto

1. Introduction

70 The ability to obtain accurate emissions estimates of greenhouse gases (GHGs) has been highlighted as an important issue for many decades, not only for regulating local air quality but also for assessing national-scale air quality and greenhouse gas emissions. In particular, urban emissions need to be well-understood because approximately 70 % of anthropogenic greenhouse gas emissions originate from urban areas (International Energy Agency, 2008; Gurney et al., 2009, 2015). This often ~~gives rise to~~causes urban domes with higher ~~greenhouse gas~~ (GHG) mixing ratios than surrounding areas (Oke, 1982; Idso et al., 1998, 2002; Koerner and Klopatek, 2002; Grimmond et al., 2004; Pataki et al., 2007; Andrews, 2008; Kennedy et al., 2009; Strong et al., 2011). Therefore, estimating greenhouse gas emissions at regional ~~to national~~scales requires an improved understanding of urban GHG emissions ~~and the role of human behavior in altering these emissions~~ (Rosenzweig et al., 2010; Wofsy et al., 2010a, b).

80 The commonly used *bottom-up* inventories derive estimates of direct and indirect emissions of greenhouse gases based on an understanding of emission factors from the constituent sectors (Andres et al., 1999; Marland et al., 1985; Boden et al., 2010; California Air Resources Board, 2015; US EPA, 2016). These estimates rely on monthly or quarterly statistical averages of emission activities and often time-invariant emission factors, which mask behavioral patterns. ~~However,~~Recent *bottom-up* inventory data have improved from coarse estimates by using proxy data to produce fine spatial resolution estimates using specific activity data and emission factors corresponding to each emission source. In contrast, *top-down* methods (or inverse modeling), in which observed mixing ratios are partitioned into their sources, have also been used for constraining or cross-checking bottom-up emissions (Huo et al., 2009; Zhang et al., 2009; Cohen and Wang, 2014; Fischer et al., 2016; Miller and Michalak, 2017).

90 Efforts to understand urban-scale emissions using direct observation have been undertaken in several large ~~urban areas~~ cities including the ~~n~~Northeastern U.S. (Boston, Baltimore/Washington D.C., He et al., 2013; Dickerson et al., 2016), the U.S. Mountain West (Salt Lake City, Strong et al., 2011), Indianapolis (Mays et al. 2009; Turnbull et al., 2015; Lamb et al., 2016; Lauvaux et al., 2016), ~~and the~~sSouthwestern U.S., especially the Los Angeles basin (Duren et al., 2011; Kort et al., 2012) ~~and European cities~~ (Peylin et al. 2005; Kountouris et al., 2018). There are several methods to quantify emissions: in-situ measurements and flask collection through surface tower systems, space-based satellite retrievals, airborne in-situ measurements, mesoscale models, and Large Eddy Simulation (LES) modeling. As part of the Indianapolis Flux Experiment (INFLUX) project, airborne and tower measurements have been collected throughout Indianapolis to generate an extensive database. Over the western U.S., a legacy ~~dataset~~ network over Salt Lake City has collected measurements of CO₂ using surface tower systems for more than ~~one a~~ decade (Pataki et al., 2005, 2007; Strong et al., 2011). Results from this extensive dataset have included seasonal variability over years and source apportionment into anthropogenic and biogenic sources. ~~Since current emission inventories do not consider individual characteristics of each city~~ While those efforts reach general agreement on ~~emission inventories across the cities~~, they have limitations due to their geographical differences in topography,

Formatted: Font: 10 pt, Not Italic

105 climatology, different source attributions (such as types of industry and agriculture), as well as differences in the measurement and analysis methods.

110 One approach for estimating CO₂ and CH₄ fluxes over cities is the use of an aircraft-based mass balance method. Several studies have demonstrated the utility of this approach (Kalthoff et al., 2002; Mays et al., 2009; Turnbull et al., 2011; Karion et al., 2013, 2015; Cambaliza et al. 2014; Gordon et al., 2015; Tadić et al., 2017). Mass balance methods utilize many length scales and patterns. The flights target mostly local scales (< 3 km) and areas around the point sources (Nathan et al., 2015; Conley et al., 2017), but they also characterize urban-scales (e.g. 25 x 10 km for Gordon et al. (2015), 4 x 9 km for Tadić et al. (2017)) and ~~the large-scale~~larger-scales (40 km up to 175 km, especially for a downwind curtain flight (Mays et al., 2009; Turnbull et al., 2011; Karion et al., 2015)).

115 The flight patterns can be classified into three different categories: 1) single-height transect flight, 2) single screen ("curtain") flight with multiple transects, and 3) enclosed shapes (box, cylinder) (see Fig. S1 in Supplementary-Appendix Material). Commonly, there are assumptions made in these airborne sampling approaches. First, the single-height transect approach assumes a well-mixed boundary layer. Karion et al. (2013) measured CO₂ and CH₄ along a single-height transect with an assumption of uniform ~~vertical mixing~~distribution of trace gases with altitude within the PBL and with time. Turnbull et al. (2011) performed a flux estimate by incorporating detailed meteorological information and transecting an emission plume with an aircraft. These studies also assumed that emissions originate from point sources such as pipes and smokestacks, and travel downwind so that all pollution is reflected on the downwind "curtain" with constant wind speed. Second, the single-screen multi-transect method does not assume a uniformly mixed boundary layer condition but is dependent upon a constant wind speed. Without a well-mixed boundary layer assumption, Cambaliza et al. (2014) measured CH₄ along multiple height transects downwind of the city of Indianapolis (See Fig. S1a in Supplementary Material). However, they assumed that winds at the time of measurement were the same as at the time of emission (i.e., winds after the methane release were time-invariant). Third, the enclosed 3-D shape flights do not presuppose any of the assumptions described above. Gordon et al. (2015) measured various GHG with a stacked box flight pattern, to capture the vertical variation in mixing ratio both upwind and downwind. Tadić et al. (2017) and Conley et al. (2017) accomplished emission estimates by flying a cylinder pattern ~~near-around~~an emission source to measure GHG both upwind and downwind for analysis based on the divergence theorem. More recently, Baray et al. (2017) used both a screen flight and box flight approach around oil sands facilities and showed that each flight pattern could be preferred, depending on the types of emissions and spatial characteristics, ~~of a particular situation~~.

135 ~~While these assumptions may be valid in certain conditions, they do not always hold. Most cities include multiple sectors, including industry, agriculture, and residential areas, and can have daily variability in wind that influences flux patterns. For example, a local landfill, various highways and several airports around Sacramento are significant sources of emissions and of uncertainty. To minimize uncertainty in flux estimates, these sources must be taken into consideration.~~ The method of extrapolation to unsampled areas can also be a large source of uncertainty. For example, Gordon et al. (2015) demonstrated the significant impact of extrapolation methods over the unsampled, near-surface region on the final emission estimate, unlike Cambaliza et al. (2014) who assumed that the city plume is rarely observed in a transect between the surface and the lowest altitude flight measurement.

Assumptions can break down when wind direction and speed vary with time and three dimensional space (e.g. longitude, latitude and altitude; (see Fig. 2S); incorrect use of wind data can result in increased uncertainty and reduction of accuracy. Flux estimates also require an estimate of the planetary boundary layer height (PBLH), an important physical parameter that is hard to measure. State-of-the-art atmospheric models and reanalysis products often estimate the PBLH, but substantial differences have been observed in existing in both models and reanalysis data (Wang et al. 2014). In addition, entrainment from the free troposphere into the planetary boundary layer (PBL) and fluxes from the surface have been ignored in most previous studies. Thus, more careful consideration and understanding of these factors are required for determining emission estimates using any of the three mass balance flight patterns.

The primary goals of this study are: i) to design and execute the cylindrical flight patterns for greenhouse gas observations for an urban domains (Fig. S1b in Supplementary Material) and to assess the impact of different interpolation and extrapolation methods on the emission estimate, ii) to test the sensitivity of emission estimates to a variety of factors such as wind, background mixing ratios, and different flux estimation methods, and finally iii) to examine the importance of vertical mass transfer on the flux estimates. To address these goals, we collect present here CO₂ and CH₄ data during three-two research flights over Sacramento (See Fig. 1a, Fig. S23 in Supplementary Material) for urban (35–60 km) and local scales (< 3 km), and determine emission fluxes using various treatments of wind conditions, background mixing ratios, and vertical mass transfer. The data and methodology are presented in section 2. Kriging results for the CO₂ and CH₄ concentrations fluxes for all three flights are shown in section 3. The sensitivities of flux estimates to different use of the wind, background value, and vertical mass transfer are also investigated. The conclusions of this study are presented in section 4.

2. Data and Methods

2.1 Data Collection

In situ measurements of CO₂ and CH₄ were performed as part of the Alpha Jet Atmospheric eXperiment (AJAX) project. Sampling occurred 21:10 – 22:00 UTC on November 18, 2013 (local standard time is UTC minus 8 h, 13:10 – 14:00 PST) and 20:55 – 21:45 UTC on June 29, 2015. The CO₂ and CH₄ instrument (Picarro Inc., model 2301-m) is calibrated before each flight using two whole-air standards (high and low) from the National Oceanic and Atmospheric Administration's Earth System Research Laboratory (NOAA/ESRL). In addition, we used these whole air standards to put accurate numbers onto secondary, synthetic standards, of which we have 5 or more of varying ranges. Thus, they give us a good handle on the linearity of the instrument, across varying concentration ranges. Water vapor corrections using Chen et al. (2010) were applied to calculate the dry mixing ratios of CO₂ used during this study. The overall uncertainty was determined to be 0.16 ppm for CO₂ and 2.2 ppb for CH₄ (Tanaka et al., 2016; Tadić et al., 2014).

—The Meteorological Measurement System (MMS) measures high-resolution pressure, temperature, and 3-D (*u*, *v*, and *w*) winds (Hamill et al., 2016). Take-off time from Moffett Field was between 20:30 and 21:00 UTC for each flight day discussed here. For the November flights, local time was 13:30–14:00 Pacific Standard Time; for the July

flight, take off was at 12:37 Pacific Daylight Time. The CO₂ and CH₄ mixing ratios and horizontal wind speed are plotted in Fig. 2.

Formatted: Subscript

Formatted: Subscript

2.2 Data gGridding

2.2.1 Extrapolation to the sSurface

180 Because the lowest flight path-level was typically between 250 and 380 m above the surface and there were no ground-based measurements along the flight tracks, there is always a gap in measurement data between the surface and the lowest flight altitude. Many studies adopt a well-mixed layer assumption below the lowest flight altitude (Karion et al., 2013), but theseThe unmeasured values can also lead to a significant bias and large uncertainties in estimating GHG mixing ratios and fluxes, depending on interpolation and extrapolation schemes
185 (Gordon et al., 2015). Thus, we investigated four methods to extrapolate mixing ratio values to the surface, which are termed 1) constant, 2) exponential fit, 3) gGaussian fit, and 4) kriged fit (see Fig. 3). The constant method assumes an elevated plume with a constant-background level. The background-constant level level-here is derived from the lowest flight measurement: $X(t, z) = X(t, z_L)$ for $z_0 < z < z_L$, where z_L is the lowest flight level. The exponential-fit method assumes an exponential decay of $X(t, z)$ from z_L to z_0 . The detailed method is based on
190 Gordon et al. (2015). The Gaussian fit method is similar to exponential fit method, except that the surface-sourced plume dispersion follows a Gaussian distribution. The detailed method is based on Gordon et al. (2015). The kriged fit was applied down to the surface level, extended from the sampled area above.

Formatted: Font color: Auto

Formatted: Font: Bold

195 Figures 3a and 3b show observed and estimated CO₂ mixing ratios at several locations over Sacramento on November 18, 2013. These results demonstrate that a large source of uncertainty and difference comes from not only the interpolation between flight levels but also the extrapolation of the data between the lowest flight level and the surface. For example, uncertainty in estimated GHG mixing ratios below the lowest flight level (indicated by the yellow diamond) can be large (up to ~ 20 %). In the worst cases, CO₂ mixing ratios span more than 80 ppm at the surface among the methods (Fig. 3b); CH₄ ranges > 0.15 ppm. Note that the differences between interpolation schemes where data exists (above ~ 250–380 m) are smaller than the differences between various methods below the lowest flight data. Without ground-based data, a proper choice of extrapolation schemes requires knowledge or presumption of the mixing ratio behavior in this region. Gordon et al. (2015) proposed that the case of elevated sources beneath the lowest flight level is best suited to constant extrapolation of mixing ratio to the surface (blue curve), while a ground-source should be represented with an exponential-fit extrapolation (red).

200
205 The various fits rely on different assumptions; the ordinary kriging method (magenta trace in Figs. 3b and 3f) also requires some assumptions (e.g., constant mean, constant variance, second-order stationarity and isotropy, and validity of the theoretical model), but the method leverages spatial and statistical properties of the observations to derive estimates, and seems to be less arbitrary than alternative interpolation/extrapolation methods. We note the similarity between the kriged values and the constant extrapolation method for both CO₂ and CH₄ (not shown). The gaussian and the exponential extrapolations produce large values below the measurement level, increasing the
210 uncertainty. However, the values above the lowest measurement level are very similar among the different fit methods. This indicates how sensitive the final flux estimate can be depending on the given interpolation and

extrapolation method and how much care should be taken when selecting the extrapolation methods when no data is available.

Formatted: Indent: First line: 0"

215 2.2.2 Elliptical fit and measurement interpolation (Kriging method)

Because the aircraft flew in a cylindrical pattern around the city, the flight paths were transformed into a polar coordinate system. The path was projected to the surface first and fit into an ellipse using least squares method to minimize the difference between the measured data and the fitted data. Then, we computed each point using the major and minor axis of the ellipse and parameter t . Each point on the ellipse was represented by a single parameter (t , eccentric anomaly), according to the equations:

220

$$\begin{aligned} X(t) &= X_0 + a \cos t \cos \phi - b \sin t \sin \phi \\ Y(t) &= Y_0 + a \cos t \sin \phi + b \sin t \cos \phi \end{aligned} \quad (1)$$

Field Code Changed

225 where a and b is a radius of the major, minor axis of the ellipse, respectively, ϕ is the angle between the X-axis and the major axis of the ellipse, and the parameter t is obtained from Eqn. (1), varying from 0 to 2π . Then, the data was gridded into a two-dimensional plane [t , height].

In order to assess the strengths of a kriging approach to quantifying emissions, two interpolation methods were assessed: interpolation using kriging and that using an exponential weighting function (see Fig. S4). The exponential weighting function at a given point (P) was defined as the weighted average of all the other points where the weights decrease exponentially with distance to P . Both approaches captured the general plume pattern (regions with high and low concentrations of CO_2), but the kriging approach did better at capturing individual plume features such as the range and magnitude, while interpolation with the exponential weighting function could not resolve such details (see Fig. S4 in Supplementary Material). Another benefit of kriging is that it can estimate values at unsampled locations using a weighted average of neighboring samples, thus reproducing the characteristics of the observed values.

235

Interpolation was performed by the ordinary kriging method (Chilés and Delfiner, 2012), modified from the IDL v8.1 kriging tool to fit an elliptical pattern. We chose ordinary kriging because there is no obvious trend in the data we use. Before kriging, we modeled the variograms for all relevant variables. A variogram (or semivariogram) is a function describing the degree to which the data are correlated as a function of the separation distance between observations. The empirical semivariogram of the data was fit using an exponential variogram model, based upon visual inspection of the experimental variograms. Three parameters were used to fit the theoretical variogram, namely the sill (the expected value of the semivariance between two observations as the lag distance goes to infinity), the range (the distance at which the variogram reaches approximately 95% of the sill), and nugget (representative of measurement error and amount of microscale variability in the data). Variogram modeling was first performed to derive parameters required to obtain ordinary kriged estimates. Various other types of kriging

240

245

exist in the literature on quantifying greenhouse fluxes (Tadić et al., 2017), but examining their differences is beyond the scope of this study.

We kriged the CO₂, CH₄, wind, temperature, and pressure observations to obtain both the estimate and the uncertainty for each variable at each grid point. The individual semivariograms of the variables for each flight were produced, and we present them for one flight in Fig. S5 in Supplementary Material. For each flight, the sampled data were kriged to a grid of maximum height divided by 150 in the vertical dimension; the horizontal dimension was kriged from end to end of the flight transect, enclosing the circumference of the entire city, divided by 360 in the horizontal direction. The vertical dimension was interpolated from the ground to the top of the flight measurement, but only data up to the estimated planetary boundary layer height (PBLH) was used for computing the flux estimates.

The uncertainty in the kriged results was assessed using the variance (and the standard deviation) of the kriged estimate at each point, as in Mays et al. (2009) and Nathan et al. (2015). In a statistical sense, the interpolated downwind CO₂ and CH₄ concentration is one of the largest sources of uncertainty in flux error estimates because the downwind flux calculation requires interpolated values at unsampled locations. Another well-known significant source of uncertainty comes from the wind measurement (Mays et al., 2009; Karion et al., 2015; Tadić et al., 2017). The grid resolution can also be a source of uncertainty. Nathan et al. (2015) reported that changing the grid resolution by a factor of 2 in either direction resulted in a 4 % absolute change in the emission rate, and showed that the grid size does not significantly bias the interpolated emission rates for their study. However, emission estimates may depend on scales of variability in the measured quantities and the grid resolution, in that the grid resolution has to be sufficiently fine to capture the observed scales of variability. They also demonstrated that the selection of the variogram model they used, such as Gaussian cosine, linear, exponential, and exponential-bessel variogram, did not affect the final emission estimate substantially (the difference is less than 5 %) in their case study. Moreover, uncertainties in greenhouse gas mixing ratio measurements, as well as in wind speed and direction, directly propagate the emission rates uncertainties.

3. Flux calculations

Figure 1 shows a map of the AJAX flight tracks on November 18, 2013 and July 29, 2015 over Sacramento and the vertical structure of the CO₂ mixing ratio on November 18, 2013. A simple illustration of the air flow demonstrates the basic idea of this study, Gauss's divergence theorem, which relates the flow through the surface to the volume of the cylinder (Fig. 1c). Mass coming in and out of the cylinder should be conserved if there is no leak through the top or the bottom of the cylinder (i.e., the flow into the cylinder balances with the flow out of the cylinder). More precisely, the surface integral through a closed system is equal to the volume integral of the divergence over the region inside the surface. Since the atmosphere has no upper boundary, we assume that vertical mass transfer is accomplished through entrainment from the top of the PBL, and surface flux from the bottom of the cylinder near the surface. In this way, the oval cylinder we design over the city has a closed surface, and the flux inside the cylinder is equal to the sum of the emission flux at the bottom.

Formatted: Do not check spelling or grammar

Formatted: Do not check spelling or grammar

In Section 3.1 we will first describe the "base case" calculation of fluxes, and in Section 3.2 we report the sensitivity of the fluxes to variations in several aspects of the method.

3.1 Base case experiment

Our base case experiment used the entire gridded, enclosed elliptical data curtain using kriging as both the interpolation and extrapolation method. We averaged the measured wind in vertical layers 100 m thick so that air (mass) coming into the cylinder equaled air leaving the cylinder (which we refer to as "mass-balanced wind"). We assigned the background to be the minimum concentration found in each 100 m layer. PBLH was determined as the altitude of the maximum gradient from a vertical profile of potential temperature (Wang et al., 2008) obtained from the MMS measurements during each flight. We included entrainment from the top and surface flux from the surface. The results of this base case are displayed in the top rows of Tables 1 (urban scale) and 2 (local scale).

Here we define the entrainment (surface) flux as the turbulent flux of the scalar at the boundary layer height (surface) (Faloona et al., 2005). Then we compute the entrainment flux at the top of the cylinder by multiplying the area of the top of the cylinder with $E = \overline{(w'c)'}_h \cdot A$, where A is the area of the top of the cylinder.

$c' = (C(t, z) - C_{bg}(h)) - C(t, z)$ is the CO₂ (or CH₄) mass concentration (g m⁻³) converted from the CO₂ (or CH₄) mixing ratio (ppmv) at a given point, t , along the perimeter of the top of the cylinder at $z=h$, and $C_{bg}(h)$ is the background concentration of CO₂ (or CH₄) at the top of the boundary layer. The CO₂ (CH₄) mass is calculated from the CO₂ (CH₄) mixing ratio (ppmv). Using this, we could make direct observations of the entrainment flux by measuring vertical velocity together with the trace gas mixing ratio throughout the boundary layer. The surface flux is computed at the surface ($z = 0$) in a similar manner.

We determined kriged data for each field from the measured CO₂, CH₄, wind, temperature, and pressure, and then subtracted background values from the trace gas data at each grid point. To convert the volume mixing ratio [ppmv] to a mass concentration [g m⁻³], the number of CO₂ or CH₄ molecules were computed based on the ideal gas law using the kriged temperature and pressure. Then, the net mass flow [g m⁻² s⁻¹] was integrated in the horizontal and vertical directions from the surface up to the top of the cylinder.

$$F = \iint \bar{U}(\theta, z) \sin(\alpha) \cdot (C(\theta, z) - C_{bg}) L d\theta dz \quad (2)$$

where L is the difference between two points on the ellipse, $\bar{U}(\theta, z)$ is the wind speed, α is the angle of the wind velocity relative to the flux surface, C is the concentration (g m⁻³), and C_{bg} is the background concentration at each level z . The component of the wind perpendicular to the flux surface was used in the flux calculation.

Figure 4 shows the measured methane over Sacramento, CA, for November 18, 2013, the projection to the ground, and the computed "flux surface". The kriged CH₄ not only captures the measured CH₄ mixing ratio, but also

Formatted: Font color: Auto

Field Code Changed

Field Code Changed

Field Code Changed

Field Code Changed

fills the unsampled area based on the observed data characteristics. Maximum values were found at 38.73° N, 121.2° W to 38.68° N, 121.45° W at 300 m. The high CH₄ region corresponds with highways, landfills and dairy farms.

For the same flight, Fig. 5 shows the observed and kriged CO₂ mixing ratio, and kriging uncertainty at each grid point. The kriged CO₂ field captures the main features of the observed CO₂ plume well. The CO₂ mixing ratios were much larger (up to 25 ppm higher at most spots) on the downwind side than the upwind side. The observations in Figs. 5(b–e) suggests that the vast majority of the emission sampled by the flights originates in the region identified as traffic regions (Roseville), airports, metropolitan areas (Arden-Arcade, Roseville, North Highlands, Fair Oaks) (see the map in Fig. 5a). Uncertainties of CO₂ were large near the surface, small from 200–900 m, and grew larger near the top of the sampled domain.

The vertical stretching pattern of CO₂ mixing ratios in Fig. 5(d) appears to be due to the large scale difference between the horizontal length (> 120 km) and the vertical length (< 1 km). When we applied our method to the local scale (horizontal scale < 3 km, see Fig. 7), or took a small horizontal portion of the large oval (see Fig. S3 in Supplementary Material), the vertical stretching pattern disappeared.

As shown in the top row of Table 1, we determined urban-scale flux values of $25.6 \pm 2.6 \text{ Mt CO}_2 \text{ yr}^{-1}$ and $87.1 \pm 8.7 \text{ Gg CH}_4 \text{ yr}^{-1}$ for this base case experiment. Note that we do not consider the uptake of CO₂ by vegetation, but the biological impact on CO₂ flux will be important especially during summer.

3.1.1 Wind treatment

To test the sensitivity of fluxes to the choice of the background value and the wind characteristics, we applied the measured high resolution (1 Hz) in-situ wind data to the flux calculation in two different ways. In one we used the measured wind at specific measured points without any correction (hereafter we refer to it as “raw wind”). In this case, inflow and outflow are not balanced within a cylinder. Alternatively, we averaged horizontal wind at each vertical level, so that air (mass) coming into the cylinder equaled air leaving the cylinder. By assuming non-divergence, mass can be balanced (here we refer to it as “mass-balanced mean wind”).

3.1.2 Background mixing ratios

Figure 1a shows a map of the three AJAX flight tracks over Sacramento and the vertical structure of the CO₂ mixing ratio on November 18, 2013, July 29, 2015, and November 17, 2015. A simple illustration of the air flow (computed as the pressure divided by the magnitude of the wind vector normal to the cylindrical surface) demonstrates the basic idea of this study. Gauss’s divergence theorem, which relates the flow through the surface to the volume of the cylinder. Mass coming in and out of the cylinder should be conserved if there is no leak throughout the top and the bottom of the cylinder (i.e., the flow into the cylinder balances with the flow out of the cylinder). More precisely, the outward flux of a vector through a closed system is equal to the volume integral of the divergence over the region inside the surface. Since the atmosphere has no upper boundary, we assume that vertical mass transfer is accomplished through an entrainment from the top of the PBL, and surface flux from the bottom of the cylinder near the surface. In this way, the oval cylinder we design over the city has a closed surface, and the flux inside the cylinder is equal to the sum of the emission flux at the bottom.

Formatted: Font color: Auto

Background values are one of the most important factors in obtaining flux estimates. Here we used three distinct methods to determine background values and calculate emission fluxes for each gas. First, we used the *minimum* value at each vertical level of the data (i.e., from the surface to the top of the PBL). Second, we used the *average* value at each vertical level. Third, we used two different vertically invariant, constant values throughout the whole height from the surface to the top of the PBL.

3.1.3 Planetary Boundary Layer Height (PBLH) and Entrainment

The potential temperature profile, which indicates atmospheric static stability and which significantly affects pollutant diffusion, is the most common operational method to determine PBLH. We determined PBLH as the altitude of the maximum gradient from a vertical profile of potential temperature (Wang et al., 2008) obtained from the MMS measurements. No significant sensitivity was found using several different PBLH detection algorithms, such as the parcel method (the interaction between dry adiabatic lapse rate and temperature), rapid decrease in water vapor (Wang and Wang, 2014), or Richardson number method (Wang et al. 2008). A simple example is shown in Supplementary Material Fig. S6.

The boundary layer growth is determined by the sum of entrainment velocity (w_e) and large scale mean vertical velocity (Vila Gueru de Arellano et al. 2004, Faloona et al., 2005, Trousdell et al., 2016). Here we define the entrainment (surface) flux as the turbulent flux of the scalar at the boundary layer height (surface). Then we compute the entrainment flux at the top of the cylinder by multiplying the area of the top of the cylinder with $E = \overline{(w'c')}_h \cdot A$ where A is the area of the top of the cylinder, $c' = (C(t, z) - C_{bg}(h))$, $C(t, z)$ is the CO₂ mass (g m⁻³) at a given point surrounding the top of the cylinder at $z=h$, and $C_{bg}(h)$ is the background concentration of CO₂ at the top of the boundary layer. The CO₂ mass is calculated from the CO₂ mixing ratio (ppmv). Using this, we could make direct observations of the entrainment flux by measuring vertical velocity together with the trace gas mixing ratio throughout the boundary layer. The surface flux is computed at the surface ($z=0$) in a similar manner.

3.1.4 "Best conduct" calculated fluxes

We determined kriged data for each field from the measured CO₂, CH₄, wind, temperature, and pressure, and then estimated the local background concentrations for both trace gases following three different approaches described above. Then we subtracted these background values from the trace gas data at each grid point. To convert the volume mixing ratio [ppmv] to a mass concentration [g m⁻³], the number of CO₂ or CH₄ molecules were computed based on the ideal gas law using the kriged temperature and pressure. Then, the net mass flow [g m⁻²s⁻¹] was integrated in the horizontal and vertical directions from the surface up to the top of the cylinder.

$$F = \iint \bar{U}(\theta, z) \sin(\alpha) (C(\theta, z) - C_{bg}) L d\theta dz \quad (2)$$

Formatted: Font color: Auto

Field Code Changed

where L is the difference between two points on the ellipse, $\bar{U}(\theta, z)$ is the wind speed, α is the angle of the wind velocity relative to the flux surface, C is the concentration (g m^{-3}), and C_{bg} is the background concentration at each level z . The component of the wind perpendicular to the flux surface was used in the flux calculation.

Field Code Changed

Field Code Changed

Field Code Changed

Estimates of GHG mixing ratios along the cylindrical boundary of the flight pattern are sensitive to the choice of interpolation schemes and extrapolation fits, especially at lower altitudes where there are no aircraft data available. Figure 2 shows CO_2 and CH_4 mixing ratios for November 18, 2013 and November 17, 2015 at several locations over Sacramento. These results demonstrate that a large source of uncertainty and difference comes from not only the interpolation but also the extrapolation of the data between the lowest flight level and the surface. For example, uncertainty in estimated GHG mixing ratios below the lowest flight level (indicated by the yellow diamond) can be large (up to ~20%). In the worst cases, CO_2 mixing ratios span more than 60 ppm at the surface among the methods; CH_4 ranges > 0.15 ppm. Note that the differences between interpolation schemes where data exists (above ~250–380 m) were smaller than the differences between the values obtained from the various methods below the lowest flight data. Without ground-based data, a proper choice of extrapolation schemes requires knowledge or presumption of the mixing ratio behavior in this region. Gordon et al. (2015) proposed that the case of elevated sources beneath the lowest flight level is best suited to constant extrapolation of mixing ratio to the surface (blue curve), while a ground source concentration should be represented with an exponential fit extrapolation (red).

The various fits rely on different assumptions; the ordinary kriging method (magenta traces in Figure 2) also requires some assumptions (e.g., constant mean, constant variance, second order stationarity and isotropy, and validity of the theoretical model). Ordinary kriging leverages spatial and statistical properties of the observations to derive estimates, and seems to be less arbitrary than alternative interpolation/extrapolation methods. We note the similarity between the kriged values and the constant extrapolation method for both CO_2 and CH_4 .

Figure 3 shows the measured methane over Sacramento, CA, for November 18, 2013, and the projection to the ground (plan view), the grid in panel (d) shows how we fit the data to compute the “flux surface” using kriging. The kriged CH_4 not only captures the measured CH_4 mixing ratio, but also fills the gap of the unsampled area based on the observed data characteristics. Maximum values were found at 38.73° N, 121.2° W to 38.68° N, 121.45° W at 300 m. The high CH_4 region corresponds with highways, airports and dairy farms, especially near the surface. Compared to the conventional interpolation without considering the individual characteristics of data, kriging can capture the most important features of the data (see Fig. S4 in Supplementary Material).

Figure 4 shows the observed and kriged CO_2 mixing ratio, and kriging uncertainty at each grid point on November 18, 2013, and November 17, 2015. The kriged CO_2 fields capture the main features of the observed CO_2 plume well. The centers of the large CO_2 plumes differed somewhat in magnitude and width, reflecting the varied source characteristics for CO_2 . The CO_2 mixing ratios on November 18, 2013, were much larger (up to 25 ppm higher at most spots) than those on November 17, 2015.

Formatted: Do not check spelling or grammar

The observations in Figs. 4(a–f) suggest that the vast majority of the emission sampled by the flights originates in the region identified as traffic regions (Roseville), airports, metropolitan areas (Arden Arcade, Roseville, North Highlands), and dairy farms. On both days, the largest CO_2 mixing ratios were seen on the northeast side of the oval, which was the downwind side when sampled in 2013 and the upwind side in 2015 (see Fig. S2 in Supplementary

Formatted: Font color: Auto, Not Highlight

Formatted: Not Highlight

Material), indicating that all areas need to be taken into consideration to understand the emission characteristics, obtain the actual flux estimates, and reduce uncertainties. The detailed wind direction speed are shown in Fig. S2 in Supplementary Material.

Formatted: Font: Bold

The vertical stretching pattern of CO₂ mixing ratios in Figs. 4(g-j) appears to be due to the large scale difference between the horizontal length (> 120 km) and the vertical length (< 1 km). When we applied our method to the local scale (horizontal scale < 3 km, see Fig. 6), or took a small horizontal portion of the large loop (see Fig. S4 in Supplementary Material), the vertical stretch pattern disappeared.

Formatted: Indent: First line: 0"

Panels (i, j) show the uncertainty was largest near the ground, in particular over the unmeasured area (e.g., November 17, 2015, below ~200 m, 38.63° N, 121.11° W ~ 38.81° N, 121.18° W), and when the data were observed a farther from the elliptical path. The uncertainty in a narrow region at ~1 km for November 17, 2015, resulted from the lack of data when aircraft was entering and exiting the cylinder. Furthermore, there were no measurements on the ground, so the estimates below 200 m were dependent only on the data around 200 m, which was an additional source of the uncertainty. Uncertainties of CO₂ were large near the surface, small from 200–900 m, and grew larger near the top of the sampled domain.

Formatted: Font: Bold

By assuming that the errors of each factor are Gaussian in nature and each measurement (e.g. CO₂ and wind) is independent (no covariance), we estimate the overall uncertainties in the calculated flux by adding the fractional uncertainties of the kriged CO₂, CH₄, and winds in quadrature, as in Nathan et al. (2015). The overall uncertainties of the CO₂ and CH₄ mixing ratios (emission estimates) are similar: both of them are less than 2(1) %. When we only compute the fluxes for the lateral part of the cylinder using the errors from the CO₂ and CH₄ mixing ratios and the wind measurement (normal component of the flux surface), the overall uncertainty of the emission estimate over the urban scales is about 4%, and 14% for both CO₂ and CH₄ on November 18, 2013 and November 17, 2015. The uncertainties over the local scales over landfill and rice field for both CO₂ and CH₄ on July 29, 2015 are about 35% and 17%. When we include the entrainment flux at the top and the surface flux at the bottom of the cylinder in addition to the flux in the lateral part, the total uncertainty was increased by about less than 1% or remains the same for both CO₂ and CH₄. This appears to be because the contribution of the vertical mass transfer through entrainment and the surface flux to the total flux estimates is relatively small, as we will show in section 3.5.

Although we used much more accurate in-situ wind measurements than most past studies for flux calculation, the wind was still the most important variable for the uncertainty of flux estimates, consistent with previous studies. This probably partially stems from the uncertainty in the wind at interpolated locations or the sparsity of the measurements. Cambaliza et al. (2014) estimated the uncertainty of the emission rates from kriging analysis is about 50 %. Nathan et al. (2015) also estimated the overall statistical uncertainty of the emission rate over a compressor station in the Barnett Shale as ± 55 %. We did not consider the uncertainty of PBLH here because we used the PBLH based on our in-situ meteorological data and estimate its uncertainty to be < 1 %.

Formatted: Do not check spelling or grammar

Formatted: Do not check spelling or grammar

Formatted: Do not check spelling or grammar

3.2 Sensitivity Tests

Formatted: Font: Bold, Font color: Auto

3.2.1 Sensitivity of calculated flux to wind treatment

Wind variability and measurement assumptions can lead to errors in the CO₂ and CH₄ flux estimates (Mays et al., 2009; Cambaliza et al., 2014, 2015; Nathan et al., 2015; Karion et al., 2013, 2015), and the way in which winds are estimated and quantified especially matters. For November 18, 2013, the wind was southwesterly at the low altitude, but it changed its direction to southeasterly as height increased. Figure 5 demonstrates the clear difference in flux estimates when the 2-D raw wind and the mean for each level (mass-balanced) wind are used. Note that we captured high fluxes (panel f) along with high CO₂ and CH₄ mixing ratio when we used the mass-balanced wind (e), while we were less likely to obtain a strong emission signal when using the raw wind data (h), which might be attributed to an imbalance of inflow and outflow to the cylinder. The total flux was ~7 times different between wind cases: 3.68 Mt CO₂ yr⁻¹ and 13.00 Gg CH₄ yr⁻¹ calculated with raw wind, and 26.55 Mt CO₂ yr⁻¹ and 88.82 Gg CH₄ yr⁻¹ with mean wind using the minimum mixing ratio of each level as the background and including vertical mass transfer (see Table 1, rows 1 and 3). The difference was much less for the flight in November 2015.

The importance of wind data on the flux calculation is also seen in local scale emission calculations (see Fig. S8 in Supplementary Material). For the small cylinder over the landfill site on July 29, 2015, Fig. 6 shows the observed and kriged CH₄ mixing ratio and the flux estimation using either the raw wind (c) or the mass-balanced wind (d). As before, the kriged CH₄ is a good representation of the local characteristics of the CH₄ field. Reassuringly, the elevated CH₄ concentration was reconstructed over 121.19° W, 38.52° N, which was the actual location of the landfill (See also Fig. S8 in Supplementary Material). The CH₄ fluxes (7–10 Gg CH₄ yr⁻¹) estimated using measured wind (varying with time and space) reflect the strong enhancement of CH₄ mixing ratios at local scales. Considering light wind conditions (< 2.5 m s⁻¹) and high temperature during July, the local emissions are attributed to these high flux estimates. The choice of distinct wind treatments led to a 30% difference in the total CH₄ estimate and 70% in CO₂ for this particular case. The CH₄ concentration and its flux are low over the rice field on that day (See in Fig. S7–S8 in Supplementary Material).

Many previous studies estimated CO₂ and CH₄ fluxes based on the mean wind vector at the dominant wind direction (positive and one direction) and speed (Turnbull et al. 2011; Karion et al. 2015), often using simulated wind obtained from a coarse resolution model. The mass-balanced area-mean wind of the cylindrical loops in this study was based on actual measurements, not coarse resolution model data, which enhances the accuracy of our flux estimates. To test the sensitivity of fluxes to the treatment of wind, we applied the measured high-resolution (1 Hz) in-situ wind data to the flux calculation in two different ways. We averaged horizontal wind on each vertical level (100 m for the base case, 500 m (not shown), or the whole cylinder as one layer), so that air (mass) coming into the cylinder equaled air leaving the cylinder. We also evaluated the calculated fluxes when the measured wind was used without any averaging (hereafter we refer to it as “raw wind”). In this case, inflow and outflow are not required to be balanced.

For November 18, 2013, the wind was southwesterly at the low altitudes, but it changed its direction to southeasterly as height increased. Figure 6 demonstrates the clear difference in flux estimates when the 2-D raw wind or the mass-balanced wind is used. The right column in Fig. 6 shows that we captured high fluxes when we used the mass-balanced wind (middle and bottom rows), while we were less likely to obtain a strong emission signal

Formatted: Font color: Auto

Formatted: Tab stops: 5.17", Left

Formatted: Do not check spelling or grammar

when using the raw wind data (top), which might be attributed to an imbalance of inflow and outflow to the cylinder. The total flux was ~7 times different between wind cases: 3.7 Mt CO₂ yr⁻¹ and 13.0 Gg CH₄ yr⁻¹ calculated with raw wind, and 25.6 Mt CO₂ yr⁻¹ and 87.1 Gg CH₄ yr⁻¹ using mass-balanced wind with 100 m vertical average, leading to 86% and 85% difference compared to the base case (see Table 1).

The importance of wind data on the flux calculation is also seen in local-scale emission calculations, but not as dramatically as in those for the urban scale (see Table 2). For the small cylinder over the landfill site on July 29, 2015, Figure 7 shows the observed and kriged CH₄ mixing ratio and the flux estimation using the raw wind and mass-balanced wind over the landfill site. As before, the kriged CH₄ is a good representation of the local characteristics of the CH₄ field. Reassuringly, the elevated CH₄ concentration was reconstructed over 121.19° W, 38.52° N, which was close to the nearby landfill (See also Fig. 4, Fig. S6 in Supplementary Material). Considering light wind conditions (< 4 m s⁻¹) and high temperature during July, the high flux estimates are attributed to the local emissions. For local-scale, the difference in the flux estimate using raw wind and mass-balanced wind is relatively small. For example, even when using raw-wind over the landfill, the difference of the calculated flux from base case is ~25 % for CH₄, which is about 1/3 smaller than the difference of calculated flux from the base case for urban-scale (~ 85%) for CH₄. For CO₂, when using raw-wind the difference of calculated flux from base case gets larger, but it is still smaller than the difference for urban-scale (See Table 1).

Another interesting finding here is the importance of vertical averaging effect of wind, which is also shown in Figs. 6 and 7. Even when using the mass-balanced wind, the whole-column-averaged wind can underestimate or overestimate the final flux estimate depending on the situation. Certainly, care needs to be paid when treating wind as a mean in both the horizontal and the vertical. Many previous studies estimated CO₂ and CH₄ fluxes based on the mean wind vector at the dominant wind direction (positive and one direction) and speed (Turnbull et al. 2011; Karion et al. 2015), often using simulated wind obtained from a coarse resolution model. Even when using high resolution measured winds in place of coarse resolution model data, we can see the impact of averaging wind on the flux estimate. However, overall, the choice of raw wind or mass-balanced wind is more important than the thickness of the vertical averaging for mass-balanced wind for flux estimate for both urban- and local-scale. Furthermore, the flux estimates using raw wind are more sensitive to the choice of the background for both urban- and local scale. For example, when we use raw wind with average background concentration, the flux estimate is about the same as the base case flux estimate (See bottom rows in Table 1 and Table 2).

3.2.2 Sensitivity of calculated flux to the choice of background concentrations

Since both CO₂ and CH₄ mixing ratios vary with altitude, we employed a vertically variant background value for each trace gas. Tables 1 and 2 show the calculated CO₂ and CH₄ emission fluxes using two different wind methods and two different background treatments for different flight days. The rows labeled "min" were generated using the minimum kriged mixing ratio in each altitude band as the background for all data at that level. The rows in Table 1 identified by "Bg=avg" used the average mixing ratio on each of the 150 vertical levels as the background on that level.

Formatted: Tab stops: 5.17", Left

Formatted: Font color: Auto

530 The sensitivity of calculated flux to the choice of the background treatment was significant when we used raw wind (top two rows in Tables 1). This was true both with the vertical mass transfer (Table 1) and without (not shown). In contrast, when we use the mean wind, the emission estimates for both CO₂ and CH₄ are nearly identical for either choice of the background treatment.

535 Interestingly, emission rate estimates were similar for the case of raw wind with averaged CO₂ or CH₄ as the background values and both cases using mass-balanced (mean) wind. To satisfy mass conservation, we also computed the entrainment flux from the top ($z=h$) and the surface flux from the bottom of the cylinder ($z=0$). The data from Table 1 is also shown in Figure 7 as the non-hatched bars.

540 Our city-wide estimate of 15–28 Mt CO₂ yr⁻¹ is higher than the result by Turnbull et al. (2011), who reported 3.5 Mt CO₂ yr⁻¹ over Sacramento in February 2009. When we examine only the small portion of the ellipse which shows the highest CO₂ mixing ratio (e.g. 121.45–121.20° W and 38.65–38.76° N in 2013), CO₂ fluxes calculated using spatially varying wind with minimum values for the background were 4.2 Mt yr⁻¹ in 2013 and 5.5 Mt yr⁻¹ in 2015. When calculating fluxes using mean wind with average values for background, the "downwind side" emission rates were about 4.4 and 3.5 Mt yr⁻¹. From this study, the fluxes from the downwind portion of the cylinder were responsible for only ~15–23% of the total emissions.

545 Our city-wide estimate of 89–95 Gg CH₄ yr⁻¹ on November 18, 2013 corresponds to 53–57% of the 167 Gg CH₄ yr⁻¹ (about 140–220 Gg yr⁻¹), reported by Jeong et al. (2016) over Region 3 (San Joaquin Valley area including Sacramento). On November 17, 2015, we calculated a significantly smaller emission rate (8–11 Gg yr⁻¹). Direct comparison between different flux estimates is challenging due to various factors, such as i) differences in the areas covered, ii) differences between bottom-up inventory and top-down estimates, iii) the variance of measurement methods (tower, aircraft, and model), iv) underestimation of the emissions from known sources, v) seasonal and interannual variability, vi) different spatial coverages, and vii) lack of understanding of unidentified sources. This will be one of the most important areas for improvement for establishing better emission estimate databases in the future.

550 Background values are one of the most important factors in obtaining flux estimates, and theoretically, the background values should be cancelled out for the enclosed-shape mass-balance flight. Here we used several distinct methods to determine background values and calculate emission fluxes for each gas to assess if our method could remove some of the uncertainty due to assigning the background. As in the base case, we used the *minimum* concentration over the layer height (e.g., 100 m or whole column averaging). In comparison, we also calculated fluxes using the *average* concentration in each layer as the background. Third, we also tested two different, vertically invariant, constant values.

560 Tables 1 and 2 show the calculated CO₂ and CH₄ emission fluxes using two different wind methods and two different background treatments. The rows labeled "min" were generated using the minimum kriged mixing ratio in each altitude band as the background for all data at that level. The rows identified by "avg" used the average mixing ratio in each altitude band as the background on that level.

The bottom two rows of Tables 1 and 2 show the sensitivity of calculated flux to the choice of the background treatment was significant when we used raw wind; the estimate using average concentration for the background

Commented [RJ(SRA1): Should we use that LARGE range????

565 closely matched the base case, but using the minimum concentration for the background resulted in significantly
different calculated fluxes, as we mentioned earlier. This was true both with the vertical mass transfer (Table 1) and
without (not shown). In contrast, when we use the mass-balanced wind, the emission estimates for both CO₂ and
CH₄ are nearly identical for either choice of background treatment. Interestingly, when an average mixing ratio at a
570 given vertical level is used for the background concentration, emission estimates with raw wind are similar to
emission estimates with mass-balanced wind. To satisfy mass conservation, we also computed the entrainment flux
from the top ($z=h$) and the surface flux from the bottom of the cylinder ($z=0$). The data from Table 1 is also shown
in Fig. 8 as the non-hatched bars.

3.2.3 Sensitivity of calculated flux to vertical mass transfer

575 Many previous studies assume that vertical mass transfer can be neglected (Cambaliza et al., 2014; Conley et
al., 2017). To quantify the validity of this assumption, we compare the flux determined when including or neglecting
the entrainment and surface fluxes. Figure 87 shows the urban-scale emission rate estimates over Sacramento, CA
using spatially and temporally varying ("raw") wind and the mean ("mass balanced") wind. We chose the
background values as i) average value of each vertical level, ii) the minimum value of each level, or iii) one of two
580 fixed values at all altitudes. The fixed values were chosen in the range between the minimum and median mixing
ratios. Note that the total fluxes using the mean wind were not sensitive to the choice of the background value (< 3
%), whether background value was minimum, average, or constant values). However, as discussed in Section 3.4, the
total fluxes using spatially varying wind (u, v) were sensitive to the choice of the background value on both flight
days for both gases. Like the urban scale analysis, the flux estimates over the landfill and rice field local scale
585 cylinders using raw wind with average background were similar to those using mass-balanced mean wind at each
level with either minimum or average values as background (shown in Table 2). The differences in CO₂ and CH₄
fluxes with and without (hatched bars in Figure 7) vertical mass transfer were determined to be only 16-17% on the
urban scale and less important for the local emission estimates (<10%). The differences in CO₂ and CH₄ fluxes
with and without (hatched bars in Fig. 8) vertical mass transfer were determined to be about 11% for CO₂ and 21%
590 for CH₄ on the urban scale and much less important for the local emission estimates (< 8%).

3.2.4 Sensitivity of calculated flux to ~~the~~ PBLH estimate

595 — We also consider sensitivity of calculated flux to the PBLH. We determine the PBLH based on the largest
gradient of the vertical profile of the potential temperature. Based on this definition, the uncertainty of our three
measurements due to PBLH estimate for urban scale is about ~10%, and that for the local scale is about 1-5% so
that the change of PBLH does not affect the total flux estimate. As seen in Fig. S6, the vertical range of the largest
gradient of potential temperature is very small, compared to the urban scale. This leads us to another important
message: the uncertainty gets larger when we deal with urban scale flux estimate. We also considered the sensitivity
of the calculated flux to the PBLH. The potential temperature profile, which indicates atmospheric static stability
and which significantly affects pollutant diffusion, is one of the most common operational methods to determine
600

Formatted: Font color: Auto

Formatted: Font: Bold

Formatted: Font color: Auto

Formatted: Font: Bold

Formatted: Font color: Auto

Formatted: Indent: First line: 0"

Formatted: Font: Bold

Formatted: Font: Bold, Do not check spelling or grammar

PBLH. No significant sensitivity was found using several different PBLH detection algorithms, such as the parcel method (the interaction between dry adiabatic lapse rate and temperature), rapid decrease in water vapor (Wang and Wang, 2014), or Richardson number method (Wang et al. 2008). A simple example is shown in Supplementary Material Fig. S5. When we determined the PBLH based on the largest gradient of the vertical profile of the potential temperature, the uncertainty due to PBLH estimate for urban scale is about ~10 %, and that for the local-scale is about 1-5 %, thus the change of PBLH does not affect the total flux estimate, especially for the local-scale. As seen in Fig. S5, the vertical range of the largest gradient of potential temperature is very small for the local-scale, compared to the urban-scale. This leads us to another important message: the uncertainty can increase when we consider urban-scale flux estimates.

3.2.5 Sensitivity of calculated flux to the closed shape

Our city-wide estimate of about 25.6 ± 2.6 Mt CO₂ yr⁻¹ (e.g., using the base case of mass-balanced wind with minimum background concentration) is higher than the result by Turnbull et al. (2011), who reported 13.6 Mt CO₂ yr⁻¹ (3.5 MtC yr⁻¹) over Sacramento in February 2009 (See Table 3). When we examine only the small downwind portion of the ellipse which shows the highest CO₂ mixing ratio (e.g. 121.45–121.20° W and 38.65–38.76° N in 2013, See Figs. 5(b, d)), CO₂ fluxes calculated using mass-balanced wind with *minimum* concentration for the background were about 17.3 ± 1.7 Mt yr⁻¹ in 2013. When calculating fluxes using mass-balanced wind with *average* concentration for background, the "downwind side" emission estimates were 8.9 ± 0.9 Mt CO₂ yr⁻¹. According to these calculations, the fluxes from the downwind portion of the cylinder were responsible for only ~35–68 % of the total emissions. The Turnbull et al. (2011) data were collected in 2009; the value given here was converted from the mean reported value of 3.5 Mt C yr⁻¹ with a 1.1% yr⁻¹ increase in CO₂ flux to adjust to 2013. Bottom-up inventory estimates of the annual total emissions from Sacramento County from Vulcan (Gurney et al., 2009) and the California Air Resources Board CEPAM database (Turnbull et al., 2011) are included for comparison in Table 3. The Vulcan inventory is available only for 2002, and the CEPAM database is available for 2004. We applied a 1.1% yr⁻¹ increase in CO₂ flux to adjust to 2013.

Our city-wide estimate of 87.1 Gg CH₄ yr⁻¹ (e.g., flux estimate using mass-balanced wind, 100 m vertically averaged wind) on November 18, 2013 corresponds to 52 % of the 167 Gg CH₄ yr⁻¹ (~ 140–220 Gg yr⁻¹) reported by Jeong et al. (2016) over Region-3 (San Joaquin Valley area including Sacramento). Direct comparison between different flux estimates is challenging due to various factors, such as i) differences in the areas covered, ii) differences between bottom-up inventory and top-down estimates, iii) the variance of measurement methods (tower, aircraft, and model), iv) underestimation of the emissions from known sources, v) seasonal and interannual variability, and vi) lack of understanding of unidentified sources. Consideration of these factors will be one of the most important areas for improvement for establishing better emission estimate databases in the future.

3.1.5 Flux uncertainties

Formatted: No underline, Underline color: Auto

640 The uncertainty in the kriged results was assessed using the variance (and the standard deviation) of the kriged estimate at each point, as in Mays et al. (2009) and Nathan et al. (2015). In a statistical sense, the interpolated CO₂ and CH₄ concentration is one of the largest sources of uncertainty in flux error estimates because the flux calculation requires interpolated values at unsampled locations. Another well-known significant source of uncertainty comes from wind measurement (Mays et al., 2009; Karion et al., 2015; Tadić et al., 2017). The grid resolution can also be a source of uncertainty. Nathan et al. (2015) reported that changing the grid resolution by a factor of 2 in either direction resulted in a 4 % absolute change in the emission rate, and showed that the grid size does not significantly bias the interpolated emission rates for their study. However, emission estimates may depend on scales of variability in the measured quantities and the grid resolution, in that the grid resolution has to be sufficiently fine to capture the observed scales of variability. They also demonstrated that the selection of the variogram model they used, such as gaussian-cosine, linear, exponential, and exponential-bessel variogram, did not affect the final emission estimate substantially (the difference is less than 5 %) in their case study. Moreover, uncertainties in greenhouse gas mixing ratio measurements, as well as in wind speed and direction observations, directly propagate the emission rates uncertainties.

650 Uncertainties in the individual kriged CO₂ values are large near the surface, small from 200–900 m, and grow larger near the top of the sampled domain. Figure 5e shows the uncertainty is largest near the ground, in particular over the unmeasured area (e.g., November 18, 2013, below ~ 200 m), and when the data were observed far from the elliptical path. Furthermore, there were no measurements on the ground, so the estimates below 200 m were dependent only on the data around 200 m, which was an additional source of the uncertainty.

655 By assuming that the errors of each factor are gaussian in nature, each measurement (e.g., CO₂ and wind) is independent, we estimate the total uncertainties in the calculated flux by adding the fractional uncertainties of the individual kriged CO₂, CH₄, and winds in quadrature (Nathan et al., 2015). We also added the fractional uncertainty of the PBLH estimates in quadrature to the uncertainty of the flux; they are about 10% for the urban scale and 1-5% for the local scales, so that the change of PBLH does not affect the total flux estimate, especially for the local scale. Furthermore, when we include the entrainment flux at the top and the surface flux at the bottom of the cylinder in addition to the flux in the lateral part, the total uncertainty was increased by about <1% or remained the same for both CO₂ and CH₄. This appears to be because the contribution of the vertical mass transfer through entrainment and the surface flux to the total flux estimates is relatively small. By including all these factors, the overall uncertainty of the emission flux estimate over the urban scales is about 10% for both CO₂ and CH₄. The overall uncertainties over the local scales over landfill and rice field for both CO₂ and CH₄ are about 35% and 17%.

660 Although we used much more accurate in-situ wind measurements than most past studies for flux calculation, the wind was still the most important variable for the uncertainty of flux estimates, consistent with previous studies. This partially stems from the uncertainty in the wind at interpolated locations or the sparsity of the measurements. Cambaliza et al. (2014) estimated the uncertainty of the emission rates from kriging analysis is about 50%. Nathan et al. (2015) also estimated the overall statistical uncertainty of the emission rate over a compressor station in the Barnett Shale as ± 55%.

Formatted: Indent: First line: 0"

4. Conclusions

675 We have estimated CO₂ and CH₄ fluxes over Sacramento, California, on three days using an airborne in-situ
dataset from the Alpha Jet Atmospheric eXperiment (AJAX) project and have tested the sensitivity of emission
estimates to a variety of factors. ~~First, we deployed cylindrical flight patterns of two sizes that differ from common
curtain flights to estimate the total flux at urban and local scales. We also applied a kriging interpolation method to
the data, capturing the characteristics of the data at both observed and unsampled locations. Second, we tested the~~
680 ~~sensitivity of flux estimates to the wind, background concentrations, and different flux calculation methods. We
found that the way in which winds are estimated and how background values were chosen were the dominant factors
in determining the total flux estimate. Third, we took into account not only the inflow and the outflow through the
cylinder around the city, but also the vertical mass transport (e.g., entrainment and surface flux) and tested the~~
~~sensitivity of the total flux estimate to the vertical mass transfer for both urban and local scales. We deployed~~
685 ~~cylindrical flight patterns of two sizes that differ from common curtain flights to estimate the total flux at urban and
local scales. We also applied a kriging interpolation method to the data, capturing the characteristics of the data at
both observed and unsampled locations. Then, we tested the sensitivity of flux estimates to the wind treatments
(either raw wind or mass-balanced wind) and background concentrations and found these two factors were the
dominant factors in determining the total flux uncertainty. When we used the mass-balanced wind for flux
calculation, the sensitivity of the emission estimate to the choice of background was minimal (Table 1). Raw wind~~
690 ~~produced similar flux estimates when the background mixing ratio was set to the average value on each vertical
layer. In contrast, choosing the background as the minimum value observed on each level led to calculated fluxes
that were substantially different.~~

~~Additionally, we took into account not only the inflow and the outflow through the cylinder around the city,
but also the vertical mass transport (e.g., entrainment and surface flux) and tested the sensitivity of the total flux
estimate to the vertical mass transfer for both urban and local scales. The winds observed on November 18, 2013
came from the southeast, showing high concentrations of CO₂ downwind of industrial facilities. CH₄ over a rice
field showed lower emission rates than those over the landfill, and this may be due to the relatively high wind, no
particular point source, and reduced CH₄ emissions as a result of low humidity. Considering the wind speed was
much lower in July (especially over the landfill), this indicates that most of the emission was produced from local
sources for the July 29, 2015 case.~~

~~When we used the area mean wind for flux calculation, the sensitivity of the emission estimate to the choice of
background was minimal (Table 1). Urban scale CO₂ flux was similar in both years sampled (20–27 Mt CO₂ yr⁻¹),
but the calculated CH₄ flux was different by ~9x (~90 Gg CH₄ yr⁻¹ in 2013 and ~10 Gg CH₄ yr⁻¹ for the flight in
2015). Using measured winds, not averaged, produced similar flux estimates when the background mixing ratio was
set to the average value on each vertical layer. In contrast, choosing the background as the minimum value observed
on each level led to calculated fluxes that were substantially lower for the flight in 2013.~~

~~The Planetary Boundary Layer Height (PBLH) was calculated using the vertical profiles of potential
temperature and was used together with the vertical fluxes for computing the entrainment from the top and the~~

710 ~~surface flux from the bottom of the cylinder. Neglecting vertical mass transfer can increase the uncertainty of the total flux estimate by up to 17% in our cases.~~

The advantage of the closed shape (i.e., elliptical in this study) approach over the curtain flight is to make a more precise “total” emissions estimate possible by taking into account all unknown sources of emissions.

Regarding the balanced incoming and outgoing fluxes within a closed volume, we suggest that emission estimates

715 using mean measured wind computed over a closed shape can be beneficial for several reasons. First, the flux estimates calculated using mass-balanced ~~mean~~ wind reduce the sensitivity to the choice of background. From Fig.

6 and Table 1 we found that the background value is one of the major sources of uncertainty in both CO₂ and CH₄ emission estimates ~~when using raw wind~~, but ~~when we use as the background value either the minimum value~~

720 ~~(which is often similar to the air away from the source) or the mean value at each vertical level, the final flux estimates become similar~~not mass-balanced wind. Second, ~~when we analyze only a small portion of the large loop~~

~~(e.g., downtown hot spot region) to mimic the curtain flight style, the final flux estimates are highly sensitive to the background choice no matter how the measured wind data are treated. These also indicate that the flux estimates for the closed elliptical loops over the city would reduce sensitivity to the choice of background values.~~

725 ~~Vertical averaging of wind also affects the flux estimate, but the choice of raw wind or mass-balanced wind is more important than the thickness of the vertical averaging for mass-balanced wind on both urban and local scales.~~

~~Second, when we analyze only a small portion of the large loop (e.g., downtown hot spot region) to mimic the curtain flight style, the final flux estimates are highly sensitive to the background choice no matter how the measured wind data are treated. Thus, we propose that the flux estimates for the closed elliptical loops have a reduced sensitivity to the choice of background values in comparison to the curtain geometry.~~

730 The spatial variation of CO₂ and CH₄ observed in the cylindrical flight pattern measured over Sacramento reveals that there were several local sources throughout the entire city, not only concentrated on the downwind side.

Furthermore, ~~the variability of wind may contribute to different flux estimates at a similar time of year (e.g., November).~~ Our sensitivity study reveals that the unbalanced wind varying with time and space may be a source of methodological uncertainty.

735 ~~Thus, use of constant wind speed or unrepresentative coarse resolution of wind (e.g., model output) by focusing only on the downwind side may lead to significant uncertainty in the estimation of the greenhouse gas emission fluxes. The size of the ellipse measuring urban emission appeared to be another factor affecting flux estimates. In general, the vertical mass transfer does not significantly contribute to the total emission estimate (especially at local scales), but it can modify total emission estimates by up to 11% for CO₂ and 21% for CH₄ urban scales in our cases. For the local scale (~ 3 km), the vertical mass transfer was not important due to the small turbulent fluxes. The Planetary Boundary Layer Height (PBLH) was calculated using the vertical profiles of potential temperature and was used together with the vertical fluxes for computing the entrainment from the top and the surface flux from the bottom of the cylinder.~~

740 ~~Thus, use of constant wind speed or unrepresentative coarse resolution of wind (e.g., model output with coarse resolution) by focusing only on the downwind side may lead to significant uncertainty in the estimation of the greenhouse gas emission fluxes. The size of the ellipse measuring urban emission appeared to be another factor affecting flux estimates. In general, the vertical mass transfer does not significantly contribute to the total emission~~

745 ~~estimate.~~

Formatted: Do not check spelling or grammar

estimate (especially at local scales), but it can modify total emission estimates by up to 17 % for urban scales in our cases. For the local scale (~ 3 km), the vertical mass transfer was not important due to the small turbulent fluxes.

750 There are still several issues to be addressed ~~further in future studies~~. First, ~~further~~ sector-specific emissions and their uncertainties for CO₂ and CH₄ need to be further identified (Miller and Michalak, 2017). Second, the seasonality of ~~sensitivity of~~ emission estimates to various factors needs to be examined. ~~We expect that the biological impact on CO₂ flux by the CO₂ uptake by vegetation will be important especially during summer~~. Finally, understanding the sources of uncertainties in emission estimates, and how different they can be under various ~~meteorological~~ conditions (~~such as temperature, atmospheric stability~~) need to be investigated further. ~~We found that the uncertainty of the emission estimates can be also sensitive to temperature, and potential temperature (to determine PBLH)~~. In this sense, the changing climate over California makes it harder to predict future emission patterns. The use of aircraft measurements presented here provides the tremendous opportunity to measure the entire urban plume.

760 This effort is not limited to one particular city. There has been increasing interest in performing inter-city comparisons to validate datasets in a more efficient and adequate manner, to create a uniform database that is useful for emission controls (Urban greenhouse gas measurements workshop, 2016). Given that data are available over several cities which have different conditions, we can test how to obtain emission estimates from several cities. Differences in the socio-economic, geologic, and industrial characteristics of cities lead to a need to compare emission estimates between them, as together they can contribute significantly to the total GHG emission at national and global scales. Thorough comparison among datasets and a customized sharing system between different
765 research groups will lead to reducing the uncertainty of emission estimates.

Formatted: Do not check spelling or grammar

Author contribution

Ju-Mee Ryoo, Laura T. Iraci, Tomoaki Tanaka, Josette E. Marrero, Emma L. Yates, Warren Gore designed the experiments, and they carried them out. T. Paul Bui and Cecilia S. Chang prepared MMS instruments on Alpha jet and Jonathan. M. Dean-Day processed the data. Anna M. Michalak and Jovan Tadić participated in experiment design and supported the interpretation of the statistical analysis. Inez Fung gave insightful comments, and Laura T. Iraci gave helpful guidance in formulating the structure of this study. Ju-Mee Ryoo developed the statistical model code and performed the analysis as well as prepared the manuscript with contributions from all co-authors.

770

775

Competing interests

The authors declare that they have no conflict of interest.

780 **Acknowledgements**

The authors appreciate the support and partnership of H211 L.L.C, with particular thanks to K. Ambrose, R. Simone, T. Grundherr, B. Quiambao, and R. Fisher. Technical contributions from Z. Young, R. Vogler, E. Quigley, and A. Trias made this project possible. Funding was provided by the NASA Postdoctoral Program, Bay Area Environmental Research Institute, and Science and Technology Corporation. Funding for instrumentation and aircraft integration is gratefully acknowledged by Ames Research Center Director's funds. Resources supporting this work were provided by the NASA High-End Computing (HEC) Program through the NASA Advanced Supercomputing (NAS) Division at NASA Ames Research Center.

785

References

- 790 Andres, R.J., Fielding, D.J., Marland, G., Boden, T.A., Kumar, N. and Kearney, A.T.: Carbon dioxide emissions
from fossil-fuel use, 1751-1950, *Tellus*, 51B, 759-765, 1999.
- Andres, C.: Greenhouse gas emissions along the rural to urban gradient, *J. Environ. Plann. Manage*, 51, 847–870,
2008.
- Baray, S., Darlington, A., Gordon, M., Hayden, K. L., Leithead, A., Li, S.-M., Liu, P. S. K., Mittermeier, R. L.,
795 Moussa, S. G., O'Brien, J., Staebler, R., Wolde, M., Worthy, D., and McLaren, R.: Quantification of Methane
Sources in the Athabasca Oil Sands Region of Alberta by aircraft mass-balance, *Atmos. Chem. Phys. Discuss.*,
<https://doi.org/10.5194/acp-2017-925>, 2017.
- Boden, T.A., Marland, G., and Andres, R.J.: Global, Regional, and National Fossil-Fuel CO₂ Emissions, Carbon
Dioxide Information Analysis Center, Oak Ridge National Laboratory, U.S. Department of Energy, Oak Ridge,
800 Tenn., U.S.A. doi 10.3334/CDIAC/00001_V2010, 2010.
- California Air Resources Board: California greenhouse gas emission inventory – 2015 edition, available at:
<http://www.arb.ca.gov/cc/inventory/data/data.htm>, 2015.
- Cambaliza, M. O. L., Shepson, P. B., Caulton, D. R., Stirm, B., Samarov, D., Gurney, K. R., Turnbull, J., Davis, J.
J., Possolo, A., Karion, A., Sweeney, C., Moser, B., Hendricks, A., Lauvaux, T., Mays, K., Whetstonr, J.,
805 Huang, J., Razlivanov, I., Miles, N. L., and Richardson, S. J.: Assessment of uncertainties of an aircraft-based
mass balance approach for quantifying urban greenhouse gas emissions, *Atmos. Chem. Phys.*, 14, 9029-9050,
2014, doi:10.5194/acp-14-9029-2014, 2014.
- Cambaliza, M. O. L., Shepson, P. B., Bogner, J., Caulton, D. R., Stirm, B., Sweeney, C., Montzka, S. A., Gurney, K.
R., Spokea, K., Salmon, O. E., Lavoie, T. N., Hendricks, A., Mays, K., Turnbull, J., Miller, B. R., Lauvaux, T.,
810 Davis, K., Karion, A., Moser, B., Miller, C., Obermeyer, C., Whetstone, J., Prasad, K., Miles, N., and
Richardson, S.: Quantification and source apportionment of the methane emission flux from the city of
Indianapolis, *Sci. Anthropol.*, 3: 000037, doi: 10.12952/journal.elementa.000037, 2015.
- Chen, H., Winderlich, J., Gerbig, C., Hofer, A., Rella, C. W., Crosson, E. R., Van Pelt, A. D., Steinbach, J., Kolle,
O., Beck, V., Daube, B. C., Gottlieb, E. W., Chow, V. Y., Santoni, G. W., and Wofsy, S. C.: High-accuracy
815 continuous airborne measurements of greenhouse gases (CO₂ and CH₄) using the cavity ring-down
spectroscopy (CRDS) technique, *Atmos. Meas. Tech.*, 3, 375-386, 2010.
- Chilés, J. P. and Delfiner, P.: *Geostatistics: Modeling Spatial Uncertainty*, 2nd ed., John Wiley & Sons, Inc.:
Hoboken, NJ. DOI: 10.1002/9781118136188.ch3, 2012.
- Cohen, J. B., and Wang, C.: Estimating global black carbon emissions using a top-down Kalman Filter approach, *J.*
820 *Geophys. Res. Atmos.*, 119, 307–323, doi:10.1002/2013JD019912, 2014.
- Conley, S., I. Faloon, S. Mehrotra, M. Suard, D. H. Lenschow, C. Sweeney, S. Herndon, S. Schwietzke, G. Petron,
J. Pifer, E. A. Kort, and R. Schnell: Application of Gauss's theorem to quantify localized surface emissions
from airborne measurements of wind and trace gases, *Atmos. Meas. Tech.*, 10, 3345-3358,
<https://doi.org/10.5194/amt-10-3345-2017>, 2017.

- 825 Dickerson, R.R., Ren, X., Shepson, P.B., Salmon, O.E., Brown, S.S., Thornton, J.A., Whetstone, J.R., Salawitch, R.J., Sahu, S., Hall, D., Grimes, C., Wong, T.M.: Fluxes of Greenhouse Gases from the Baltimore-Washington Area: Results from WINTER 2015 Aircraft Observations, AGU fall meeting abstract #A14F-04, 2016.
- Duren, R.M., and Miller, C.E.: Towards robust global greenhouse gas monitoring, *J. Greenhouse Gas Meas and Manag.* 1:2, 80-84. doi:10.1080/20430779.2011.579356, 2011.
- 830 Falona, I., Lenschow, D. H., Campos, T., Stevens, B., Zanten, M. V., Blomquist, B., Thornton, D., Bandy, A., and Gerber, H.: Observations of entrainment in eastern Pacific marine stratocumulus using three conserved scalars, *J. Atmos. Sci.*, 62, 3268-3285, 2005.
- Fischer, M. L.: Atmospheric Measurement and Inverse modeling to improve GHG emission estimates, Air Resource Board project 11-306, ARB report, 2016.
- 835 Gordon, M., Li, S.-M., Staebler, R., Darlington, A., Hayden, K., O'Brien, J., and Wolde, M.: Determining air pollutant emission rates based on mass balance using airborne measurement data over the Alberta oil sands operations, *Atmos. Meas. Tech.*, 8, 3745-3765, doi:10.5194/amt-8-3745-2015, 2015.
- Grimmond, C. S. B., J. A. Salmond, T. R. Oke, B. Offerle, and A. Lemonsu: Flux and turbulence measurements at a densely built-up site in Marseille: Heat, mass (water and carbon dioxide), and momentum, *J. Geophys. Res.*, 109, D24101, doi:10.1029/2004JD004936, 2004.
- 840 Gurney, K. R., Mendoza, D. L., Zhou, Y., Fischer, M. L., Miller, C. C., S. Geethakumar, and de la Rue Ca, S.: High resolution fossil fuel combustion CO₂ emission fluxes for the United States, *Environ. Sci. Technol.*, 43, 5535–5541, 2009.
- Gurney, K.R., Romero-Lankao, P., Seto, K.C., Hutyra, L.R., Duren, R., Kennedy, C., Grimm, N.B., Ehleringer, J.R., Marcotullio, P., Hughes, S., Pincetl, S., Chester, M.V., Runfola, D.M., Feddema, J.J., and Sperling, J.: Tracking urban emissions on a human scale, *Nature* 525:179-181, 2015.
- Hamill, P., Iraci, L. T., Yates, E. L., Gore, W., Bui, T. P., Tanaka, T., and Loewenstein, M.: A New instrumented Airborne Platform For Atmospheric Research. *Bulletin of the American Meteorological Society*, DOI: <http://dx.doi.org/10.1175/BAMS-D-14-00241.1>, 2016.
- 850 He, H., Stehr, J.W., Hains, J.C., Krask, D.J., Doddridge, B. G., Vinnikov, K.Y., Canty, T.P., Hosley, K.M., Salawitch, R.J., Worden, H.M., and Dickerson, R.R.: Trends in emissions and concentrations of air pollutants in the lower troposphere in the Baltimore/Washington airshed from 1997 to 2011. *Atmos. Chem. Phys.* 13, 1-16, doi:10.5194/acp-13-1-2013, 2013.
- Huo, H., Zhang, Q., He, K., Wang, Q., Yao, Z., and Streets, D. G.: High-resolution vehicular emission inventory using a link-based method: A case study of light-duty vehicles in Beijing, *Environ.Sci. Technol.*, 43, 2394–2399, 2009.
- 855 Idso, C.D., S.B. Idso, R. C. Balling Jr.: The urban CO₂ dome of Phoenix, Arizona. *Physical Geography*, 19, 95–108, 1998.
- Idso, S. B., C. D. Idso, and J. R. C. Balling: Seasonal and diurnal variations of near-surface atmospheric CO₂ concentration within a residential sector of the urban CO₂ dome of Phoenix, AZ, USA, *Atmos. Environ.*, 36, 1655–1660, 2002.
- 860

- International Energy Agency: World Energy Outlook 2008, Paris; New Milford, Conn.: International Energy Agency; Turpin Distribution, 2008.
- 865 Jeong, S., et al.: Estimating methane emissions in California's urban and rural regions using multi-tower observations, *J. Geophys. Res. Atmos.*, 121, 13,031–13,049, doi:10.1002/2016JD025404, 2016.
- Kalthoff, N., Corsmeier, U., Schmidt, K., Kottmeier, Ch., Fiedler, F., Habram, M., Slemr, F.: Emissions of the city of Augsburg determined using the mass balance method., *Atmos. Environ.*, 36, Supplement No. 1, S19-S31, 2002.
- 870 Karion, A. et al.: Methane emissions estimate from airborne measurements over a western United States natural gas field, *Geophys. Res. Lett.*, Vol. 40, 1-5, doi:10.1002/grl.50811, 2013.
- Karion, A. et al.: Aircraft-Based Estimate of Total Methane Emissions from the Barnett Shale Region, *Environ. Sci. Technol.* 2015, 49, 8124-8131, DOI: 10.1021/acs.est.5b00217, 2015.
- Kennedy, C. A., et al.: Greenhouse gas emissions from global cities, *Environ. Sci. Technol.*, 43, 7297–7302, 2009.
- 875 Koerner, B., and J. Klopatek: Anthropogenic and natural CO₂ emission sources in an arid urban environment, *Environ. Pollut.*, 116, S45–S51, 2002.
- Kort, E.A., Frankenberger, C., Miller, C.E.: Space-based Observations of Megacity Carbon Dioxide, *Geophys Res Let* 39, doi:10.1029/2012GL052738, 2012.
- 880 Kountouris, P., Gerbig, C., Rodenbeck, C., Karstens, U., Koch, T. F., and Heimann, M., 2018: Atmospheric CO₂ inversions on the mesoscale using data-driven prior uncertainties: quantification of the European terrestrial CO₂ fluxes.
- Lamb, B. K., Cambaliza, M.O., Davis, K., Edburg, S., Ferrara, T., Floerchinger, C., Heimbürger, A., Herndon, S., Lavoie, T., Lauvaux, T., Lyon, D., Miles, N., Prasad, K., Richardson, S., Roscioli, J., Salmon, O., Shepson, P., Stirm, B., Whetstone, J.: Direct and indirect measurements and modeling of methane emissions in Indianapolis, IN, *Environ. Sci. Technol.*, 50(16), 8910–8917, doi:10.1021/acs.est.6b01198, 2016.
- 885 Lauvaux, T., Miles, N.L., Deng, A., Richardson, S.J., Cambaliza, M.O., Davis, K.J., Gaudet, B., Gurney, K.R., Huang, J., O'Keefe, D., Song, Y., Karion, A., Oda, T., Patarasuk, R., Sarmiento, D., Shepson, P., Sweeney, C., Turnbull, J., and Wu, K.: High resolution atmospheric inversion of urban CO₂ emissions during the dormant season of the Indianapolis Flux Experiment (INFLUX), *J. Geophys. Res.*, 121, doi:10.1002/2015JD024473, 2016.
- 890 Marland, G., Rotty, R.M., and Treat, N.L.: CO₂ from fossil fuel burning: global distribution of emissions, *Tellus*, 37B, 243-258, 1985.
- Mays, K. L., Shepson, P. B., Stirm, B. H., Karion, A., Sweeney, C., and Gurney, K. R.: Aircraft-based Measurements of the Carbon Footprint of Indianapolis, *Environ. Sci. Technol.*, 43, 7816–7823, 2009.
- 895 Miller, S. M. and Michalak, A. M.: Constraining sector-specific CO₂ and CH₄ emissions in the US, *Atmos. Chem. Phys.*, 17, 3963-3985, doi: 10.5194/acp-17-3963-2017, 2017.
- Nathan, B., Golston, L. M., O'Brien, A. S., Ross, K., Harrison W. A., Tao, L., Lary, D. J., Johnson, D. R. Covington, A. N., Clark, N. N., and Zondlo, M. A.: Near-Field Characterization of Methane Emission

Formatted: Font color: Auto

- Variability from a Compressor Station Using a Model Aircraft, *Environ. Sci. Technol.*, 2015, 7896-7903, DOI: 10.1021/acs.est.5b00705, 2015.
- 900 Oke, T.R.: The energetic basis of the urban heat island. *Q. J. R. Meteorol. Soc.* 108, 1–24, 1982.
- Pataki, D. E., Tyler, B. J., Peterson, R. E., Nair, A. P., Steenburgh, W. J., and Pardyjak, E. R.: Can carbon dioxide be used as a tracer of urban atmospheric transport?, *J. Geophys. Res.*, 110, D15102, doi:10.1029/2004JD005723, 2005.
- Pataki, D. E., Xu, T. Luo, Y. Q., and Ehleringer, J. R.: Inferring biogenic and anthropogenic carbon dioxide sources across an urban to rural gradient, *Oecologia*, 152, 307–322, 2007.
- 905 [Peylin, P., Rayner, P. J., Bousquet, P., Carouge, C., Hourdin, F., Heinrich, P., Ciais, P., and AEROCARB contributors, 2005; Daily CO2 flux estimates over Europe from continuous atmospheric measurements: 1. inverse methodology, *Atmos. Chem. Phys.*, 5, 2173-3186, 2005.](#)
- Rosenzweig, C., Solecki, W., Hammer, A. A., and Mehrotra, S.: Cities lead the way in climate- change action, *Nature*, 467, 909–911, 2010.
- 910 Strong, C., Stwertka, C., Bowling, D. R., Stephens, B. B., and Ehleringer, J. R.: Urban carbon dioxide cycles within the Salt Lake Valley: A multiple- box model validated by observations, *J. Geophys. Res.*, 116, D15307, doi:10.1029/2011JD015693, 2011.
- Tadić, J.M., Loewenstein, M., Frankenberg, C., Butz, A., Roby, M., Iraci, L.T., Yates, E.L., Gore, W., Kuze, A.: A comparison of in-situ aircraft measurements of carbon dioxide and methane to GOSAT data measured over Railroad Valley playa, Nevada, USA. *IEEE Trans. Geosci. Remote Sens.*, 52 (12), <http://dx.doi.org/10.1109/TGRS.2014.2318201>, 2014.
- 915 Tadić, J., Michalak, A., Iraci, L., Ilić, V., Biraud, S., Feldman, D., Thaopaul, B., Johnson, M. S., Loewenstein, M., Jeong, S., Fischer, M., Yates, E., Ryoo, J.-M.: Elliptic cylinder airborne sampling and geostatistical mass balance approach for quantifying local greenhouse gas emissions, *Environ. Sci. Tech*, doi: 10.1021/acs.est.7b03100, 2017.
- 920 Tanaka, T., Yates, E. L., Iraci, L. T. Johnson, M. S., Gore, W. Tadic, J. M., Loewenstein, M., Kuze, A., Frankenberg, C., Butz, A., and Yoshida, Y: Two-Year Comparison of Airborne Measurements of CO2 and CH4 with GOSAT at Railroad Valley, Nevada, *IEEE Trans. Geosci. Remote Sens.*, 54 (8), 4367-4375, 2016.
- 925 [Trousdel, J.F., S. A. Conley, A. Post, I. C. Faloona, 2016. Observing entrainment mixing, photochemical ozone production, and regional methane emissions by aircraft using a simple mixed layer model. *Atmos. Chem. Phys. Discuss.*, doi:10.5194/acp-2016-635, 2016.](#)
- Turnbull, J. C., Karion, A., Fischer, M. L., Faloona, I., Guilderson, T., Lehman, S. J., Miller, B.R., Miller, J. B., Montzka, S., Sherwood, T., Saripalli, S., Sweeney, C., and Tan, P.P.: Assessment of fossil fuel carbon dioxide and other anthropogenic trace gas emissions from airborne measurements over Sacramento, California in spring 2009. *Atmos. Chem. Phys.*, 11, 705–721, 2011, doi:10.5194/acp-11-705-2011, 2011.
- 930 Turnbull, J. C., Sweeney, C., Karion, A., Newberger, T., Lehman, S. J., Tans, P. P., Davis, K. J., Lauvaux, T., Miles, N. L., Richardson, S. J., Cambaliza, M. O., Shepson, P. B., Gurney, K., Patarasuk, R., Razlivanov, I.: Toward

- 935 quantification and source sector identification of fossil fuel CO₂ emissions from an urban area: Results from the influx experiment, *J. Geophys. Res. Atmos.*, 120, 292–312, doi:10.1002/2014JD022555, 2015.
- Urban greenhouse gas measurements workshop: National Institute of Standards and Technology (NIST), Gaithersburg, MD, April 05 – 06, 2016.
- US EPA: Inventory of US greenhouse gas emissions and sinks: 1990-2014, available at: <https://www3.epa.gov/climatechange/ghgemissions/usinventoryreport.html>, 2016.
- 940 ~~Vilà Gueru de Arellano, J., B. Gioli, F. Miglietta, H. J.J. Jonker, H. K. Baltink, R. W. A. Hutjes, and A. A. M. Holtslag, 2004. Entrainment process of carbon dioxide in the atmospheric boundary layer., *J. Geophys. Res.* 109, D18110, doi:10.1029/2004JD004725, 2004.~~
- Wang, S., Golaz, J.-C., and Wang, Q.: Effect of intense wind shear across the inversion on stratocumulus clouds, *Geophys. Res. Lett.*, 35, L15814, doi:10.1029/2008GL033865, 2008.
- 945 Wang, X., and C. Wang: Estimation of atmospheric mixing layer height from radiosonde data, *Atmos. Meas. Tech.*, 7, 1701-1709, doi:10.5194/amt-7-1701-2014, 2014.
- Wofsy, S. C., et al.: Measurement requirements for greenhouse gas concentrations in support of treaty monitoring and verification, *Eos Trans. AGU, Fall Meet. Suppl.*, Abstract GC41G- 04, 2010a.
- Wofsy, S. C., McKain, K., Eluszkiewicz, J., Nehr Korn, T., Pataki, D. E., and Ehleringer, J. R.: An observational method for verifying trends in urban CO₂ emissions using continuous measurements and high resolution meteorology, *Eos Trans. AGU, Fall Meet. Suppl.*, Abstract A13F- 0280, 2010b.
- 950 Zhang, Q., Streets, D. G., Carmichael, G. R., et al.: Asian emissions in 2006 for the NASA INTEX-B mission, *Atmos. Chem. Phys.*, 9, 5131–5153, 2009.

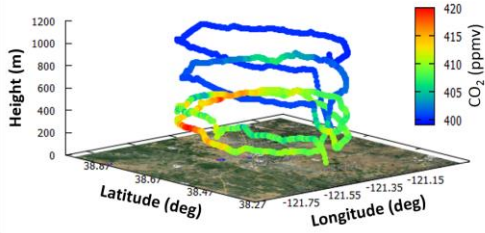
Formatted: Font: 10 pt

Formatted: Normal, Line spacing: single

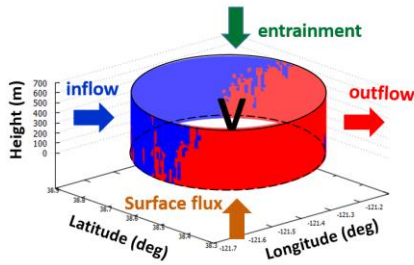
(a)



(b)



(c)



955

(a)



(b)

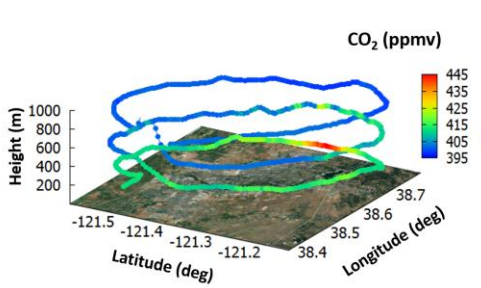


Figure 1: (a) Map of AJAX flight tracks on November 18, 2013 (orange) and July 29, 2015 (cyan) plotted in Google™ Earth. (b) Vertical measurements of CO₂ mixing ratio on November 17, 2015, and (c) simple illustration of airflow [$\text{kg m}^{-2} \text{s}^{-1}$] passing through cylinder (over Sacramento). The color represents the air mass flux (density [kg m^{-3}] multiplied by wind vector [m s^{-1}]) normal to the cylinder. The blue and red represent inflow and outflow, respectively. The vertical mass transfer through the top and bottom are referred to as the entrainment and surface flux, respectively.

Figure 1: (a) Map of AJAX flight tracks on November 18, 2013 (orange) and July 29, 2015 (cyan) plotted in Google™ Earth. (b) Vertical measurements of CO₂ mixing ratio on November 18, 2013, and (c) simple illustration of airflow [$\text{kg m}^{-2} \text{s}^{-1}$] passing through cylinder (over Sacramento). The color represents the air mass flux (density [kg m^{-3}] multiplied by wind vector [m s^{-1}]) normal to the cylinder. The blue and red represent inflow and outflow, respectively. The vertical mass transfer through the top and bottom are referred to as the entrainment and surface flux, respectively.

Formatted: Font color: Auto

November 18, 2013

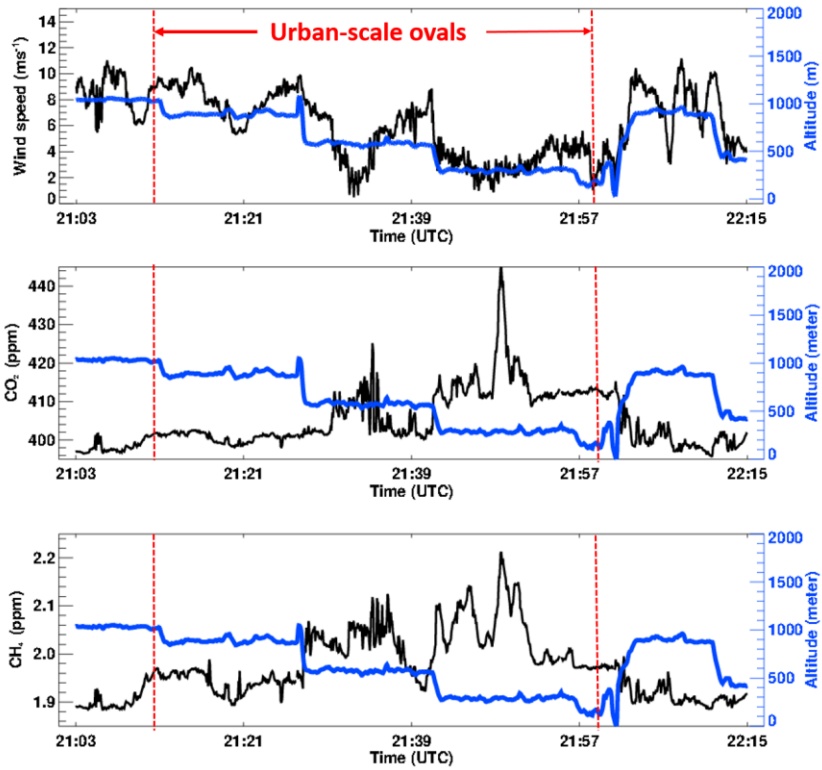
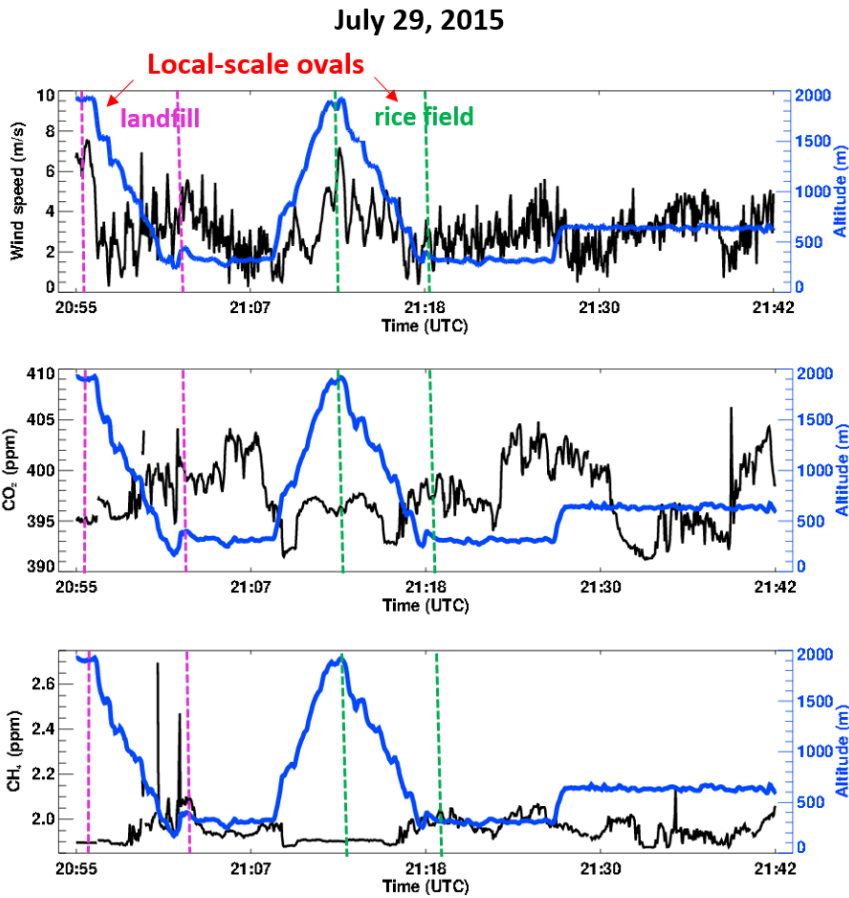


Figure 2a. A time series of (black line) CO₂, CH₄, wind, and (blue line) altitude of the aircraft flight track for November 18, 2103 observed over the Sacramento, CA. The red dashed lines represent the time duration during the flight over the whole Sacramento.

960

- Formatted: Font: Not Bold
- Formatted: Font: Not Italic, Font color: Auto
- Formatted: Font color: Auto
- Formatted: Font: Not Italic, Font color: Auto
- Formatted: Font color: Auto
- Formatted: Font: Not Italic, Font color: Auto
- Formatted: Font color: Auto
- Formatted: Font: Not Italic, Font color: Auto
- Formatted: Font color: Auto
- Formatted: Font: Not Italic, Font color: Auto
- Formatted: Justified



965 **Figure 2b:** The same as Fig. 2a except for July 29, 2015. The magenta dashed lines indicate the portion of the flight over the landfill, and the green dashed lines mark the start and end times of the rice field measurements.

Formatted: Justified

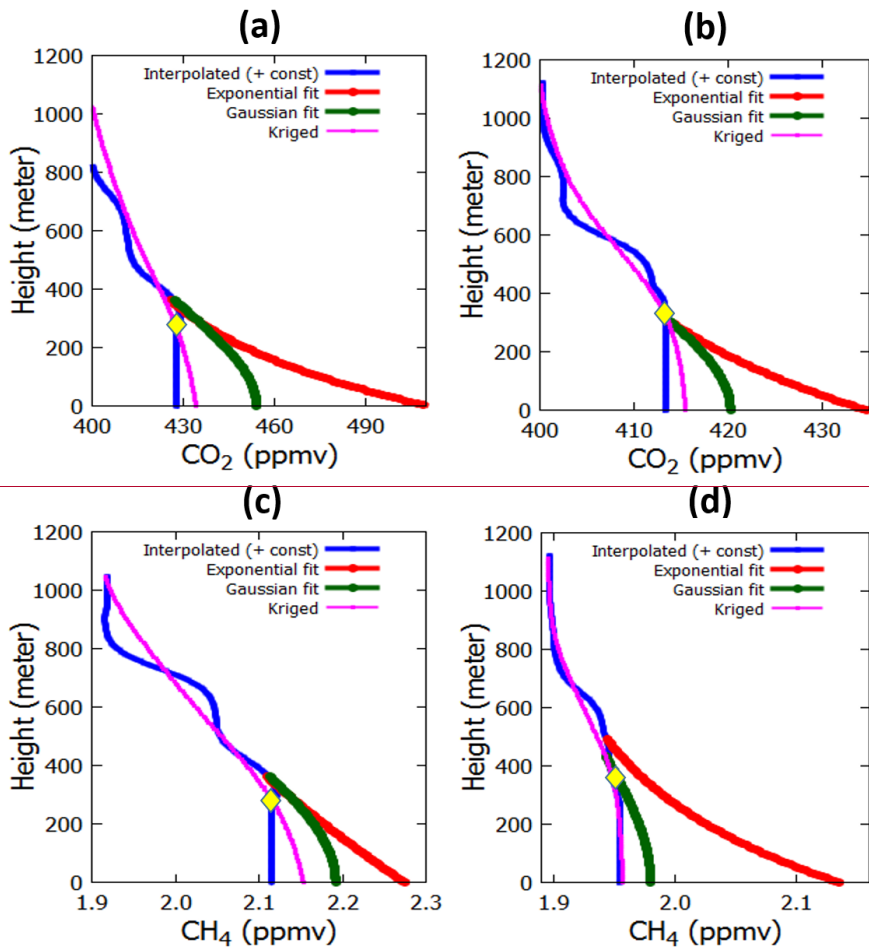


Figure 2: The CO₂ and CH₄ mixing ratios for (a, c) November 18, 2013, around 38.75° N, 121.27° W and for (b, d) November 17, 2015, around 38.84° N 121.27° W for CO₂ and 38.58° N, 121.13° W for CH₄. The yellow diamond indicates the altitude of the lowest flight data. The kriged values (magenta), interpolated values with exponential weighting function (blue), and extrapolated values using constant (blue line below diamond), gaussian fit (green), and exponential fit (red) are compared. The empirical fits were generated based on the approach by Gordon et al. (2015).

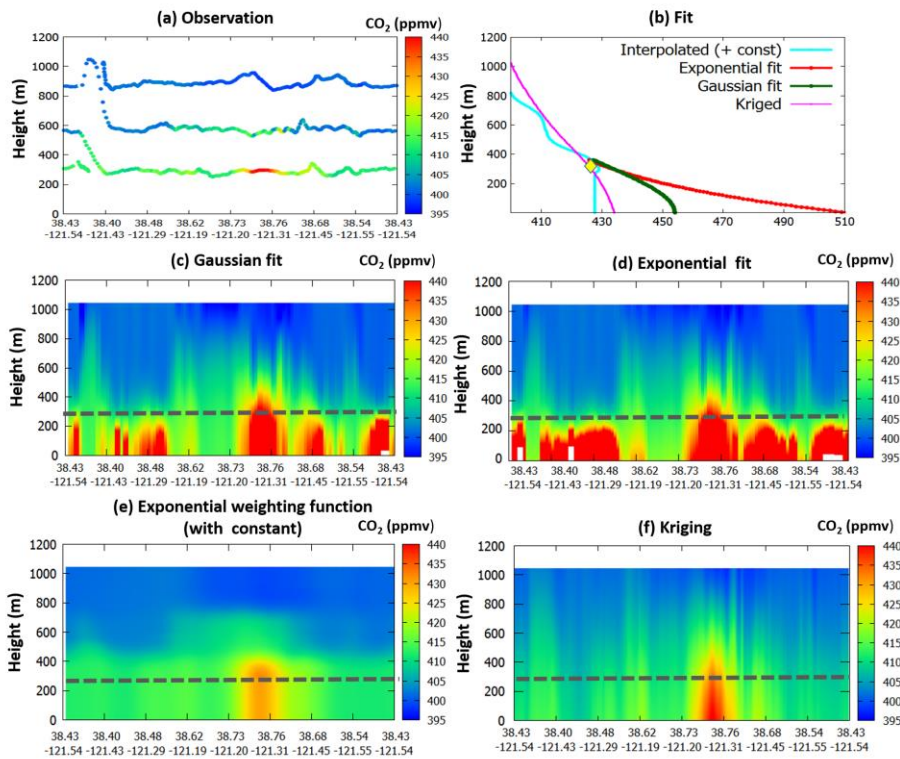


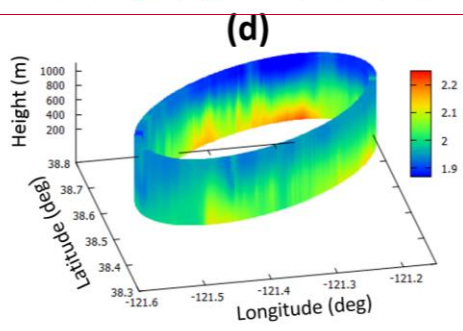
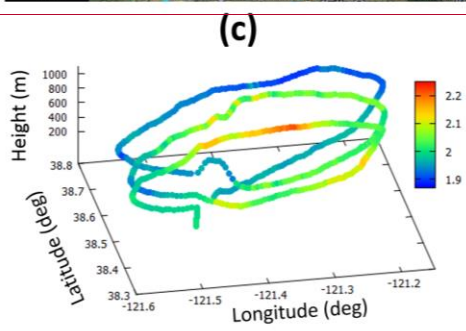
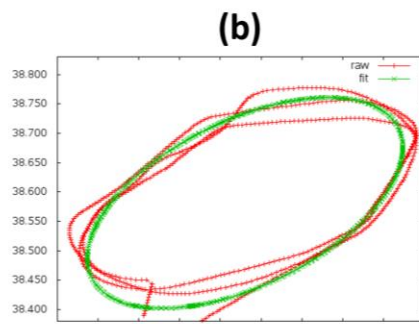
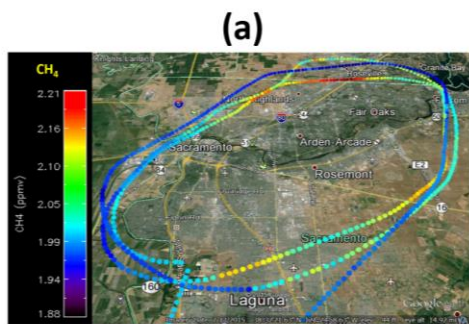
Figure 32: (a) Observed CO₂ over the Sacramento loop (b) The CO₂ and CH₄ mixing ratios for (a, c) November 18, 2013, around 38.75° N, 121.27° W and for (b, d) November 17, 2015, around 38.84° N 121.27° W for CO₂ and 38.58° N, 121.13° W for CH₄. The yellow diamond indicates the altitude of the lowest flight data. The kriged values (magenta), interpolated values with exponential weighting function (blue), and extrapolated values using constant (blue line below diamond), gaussian fit (green), and exponential fit (red) are compared. (c) The CO₂ mixing ratio obtained from (c) the Gaussian fit, (d) Exponential fit, (e) Exponential weighting function with constant, (f) kriging method for November 18, 2013. The yellow diamond indicates the altitude of the lowest flight data. The kriged values (magenta), interpolated values with exponential weighting function (blue), and extrapolated values using constant (blue line below diamond), gaussian fit (green), and exponential fit (red) are compared. The empirical fits were generated based on the approach by Gordon et al. (2015). In panels (c) and (d), the white boxes result from no fit due to the lack of the data points.

Formatted: Justified, Indent: First line: 0"

Formatted: Not Highlight

Formatted: Not Highlight

Formatted: Not Highlight



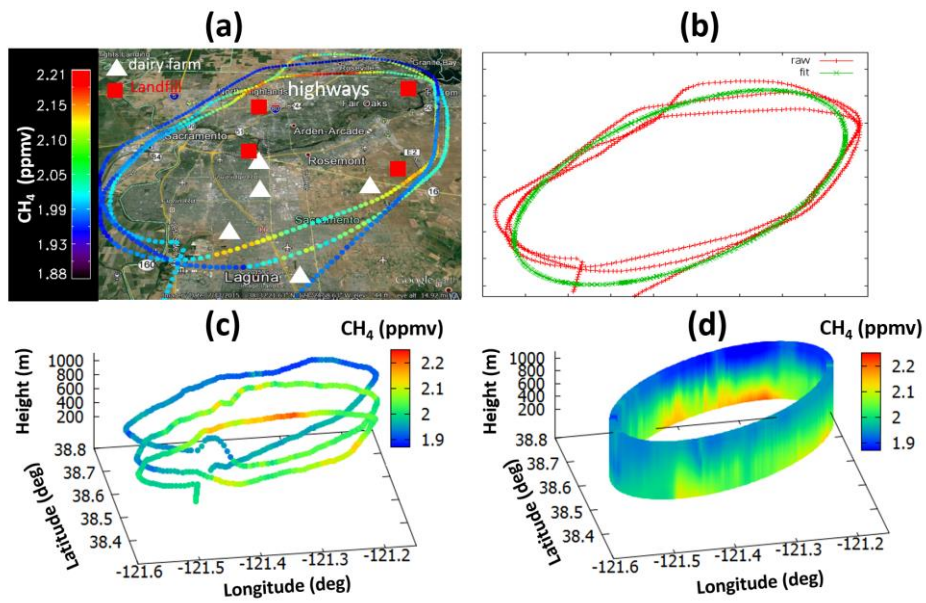
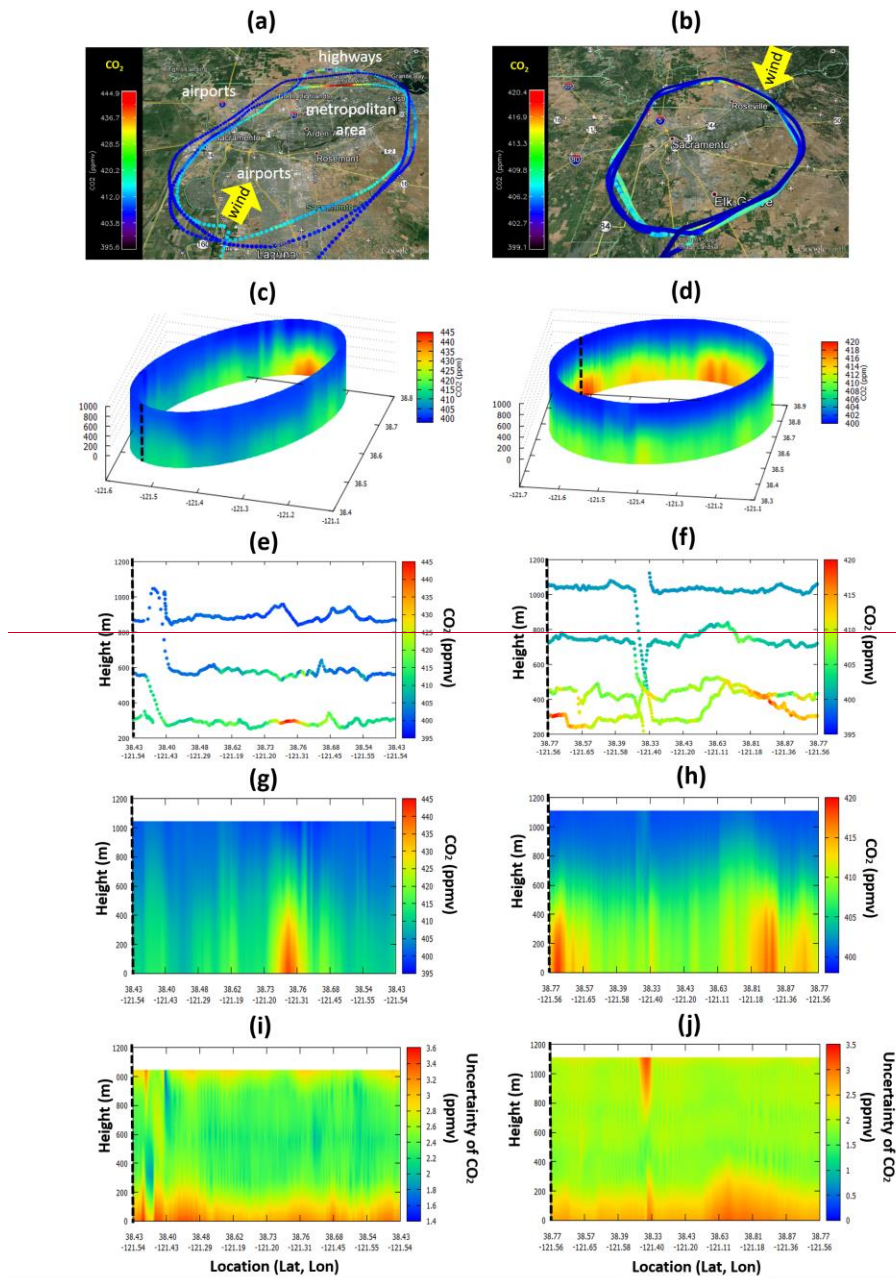


Figure 43: (a) Map of AJAX flight tracks colored by CH₄ mixing ratio for November 18, 2013, plotted in Google™ Earth. (b) The data (red) fitted to an oval (green). The observed CH₄ mixing ratios (c) are kriged to generate the cylindrical surface (d). The axes of the oval are approximately 50 and 40 km.

Formatted: Centered



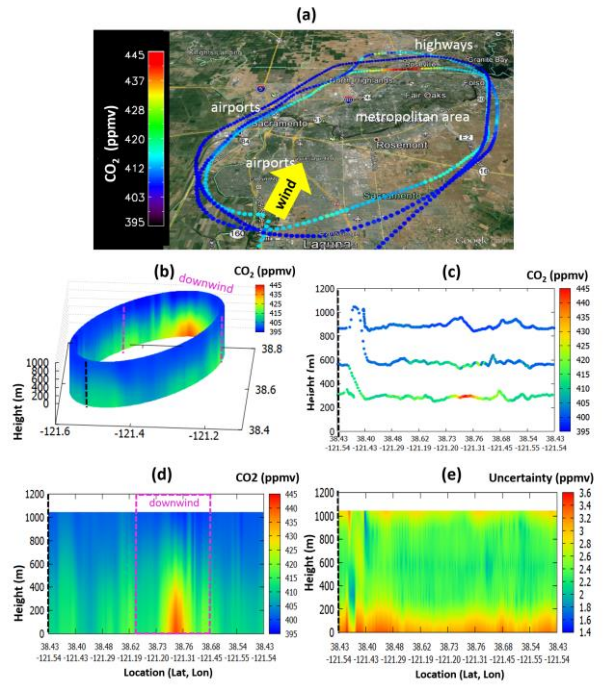


Figure 5.4: (a, b, c, f) Measured CO₂ mixing ratio, (c, d, g, h) the kriged CO₂ mixing ratio, and (i, j) the kriging uncertainty at each grid point on (left) November 18, 2013 and (right) November 17, 2015. The yellow arrows represent the dominant wind directions and the black dashed lines indicate where the surface is split open.

: (a) A map of AJAX flight track overlaid by the CO₂ mixing ratio, plotted in Google™ Earth, (b) the kriged CO₂ mixing ratio, (c) Measured CO₂ mixing ratio, (d) the same as (b) except plotted in two dimensions, and (e) the kriging uncertainty at each grid point on November 18, 2013. The yellow arrow represents the dominant wind direction, and the black dashed lines indicate where the surface is split open. The area enclosed by the magenta dashed lines represents the area we used as a downwind portion.

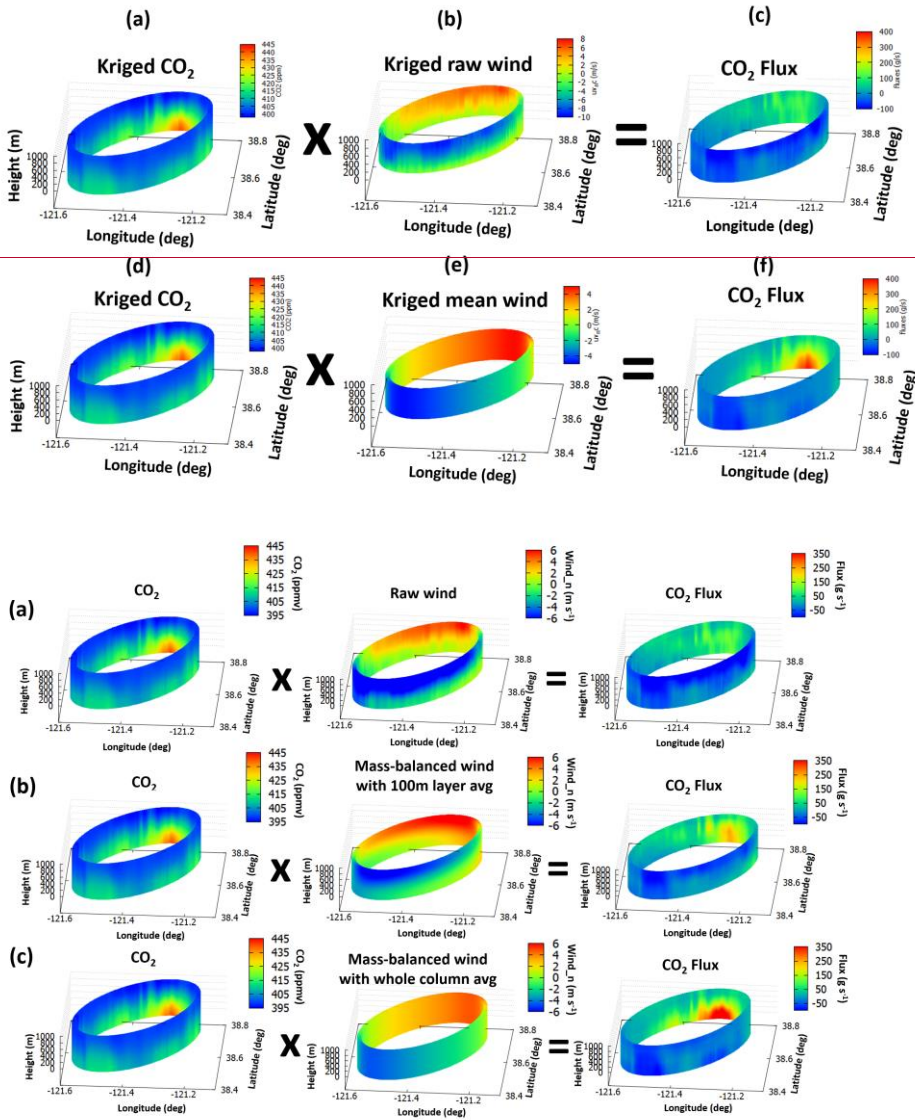
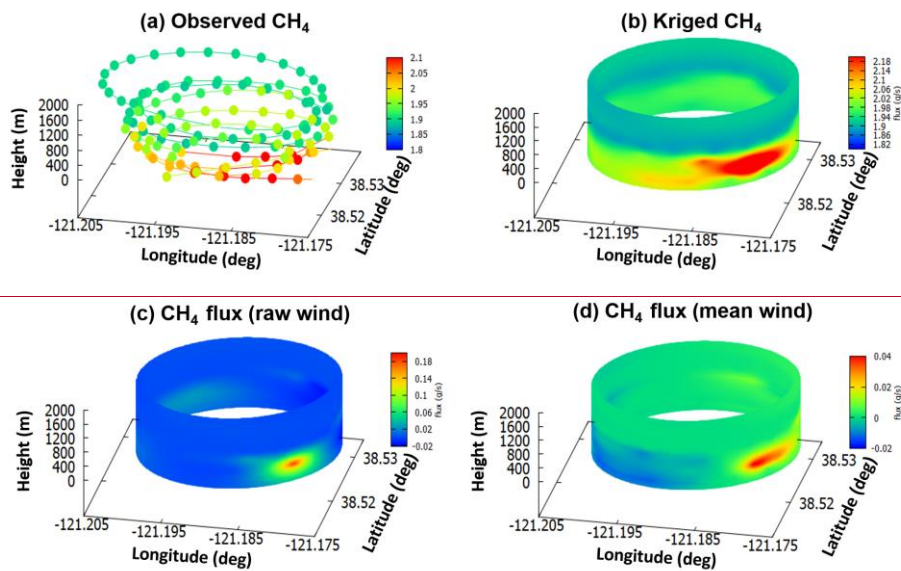


Figure 5: (a, d) Kriged CO₂ mixing ratio, (b) spatially-varying raw measured wind, (e) mass-balanced measured wind, (c) CO₂ flux using raw measured wind, (f) CO₂ flux using mass-balanced wind on November 18, 2013. In panels (b, e), the blue color represents the inflow toward (and red outflow from) the cylinder so that it is defined as negative (positive) wind. The background CO₂ was chosen as the minimum mixing ratio at each vertical level.

Figure 6: (a) Kriged CO₂ mixing ratio, the raw wind, and CO₂ flux using the raw wind, (b) Kriged CO₂ mixing ratio, 100m vertically averaged mass-balanced wind, and CO₂ flux using the mass-balanced wind, and (c) Kriged CO₂ mixing ratio, whole column averaged mass-balanced wind, and CO₂ flux using the mass-balanced wind on November 18, 2013. In the middle columns, the blue color represents the inflow toward (and red outflow from) the cylinder so that it is defined as negative (positive) wind. The background CO₂ was chosen as the minimum mixing ratio at each vertical layer.



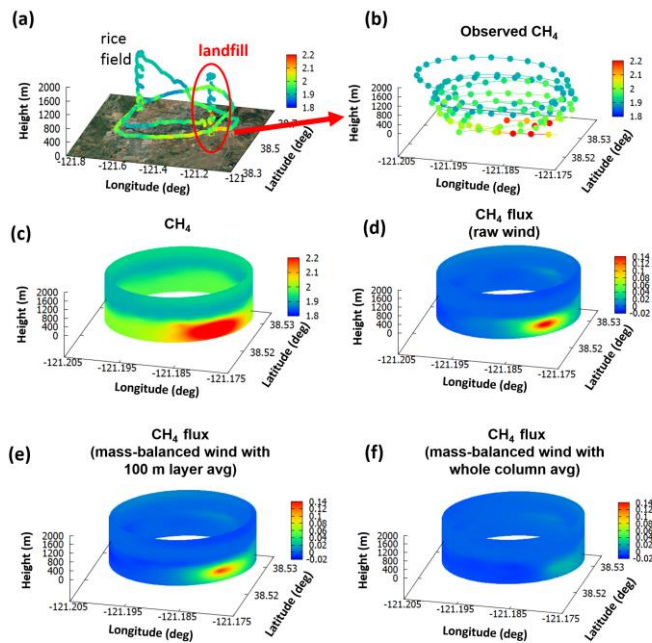
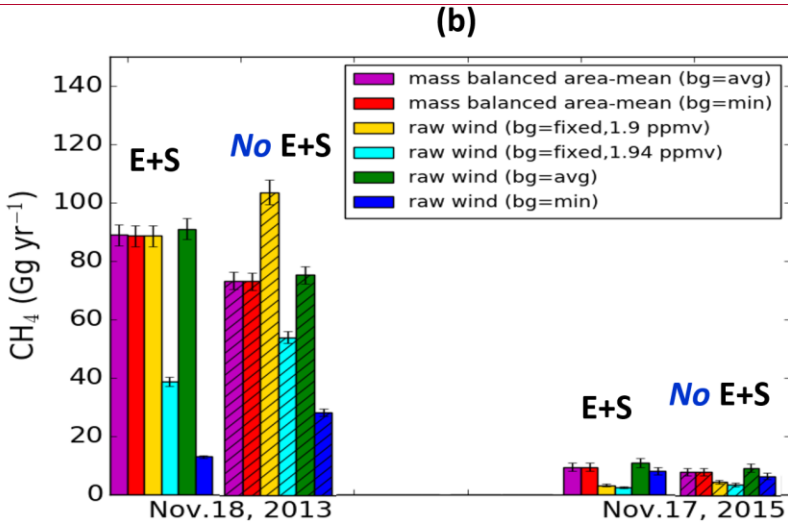
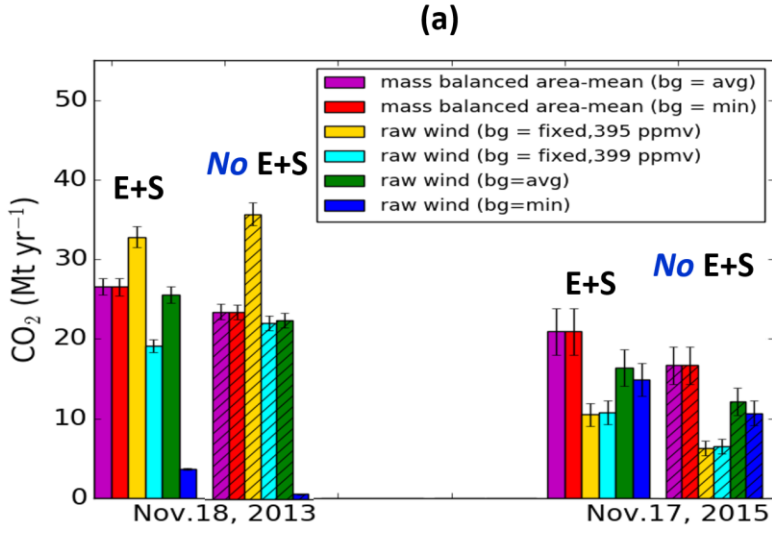


Figure 6: (a) The observed CH₄ mixing ratio, (b) the kriged CH₄ mixing ratio, (c) the CH₄ flux using raw measured wind, (d) the CH₄ flux using mass-balanced mean wind (for each layer) over the landfill location on July 29, 2015. The fluxes in (e, d) are computed based on equation (2). The background value was chosen as the minimum value at each vertical level. The approximate diameter of the cylinder is 3 km.

Figure 7: (a) The map of AJAX flight track with the observed CH₄ mixing ratio, (b) the observed CH₄ mixing ratio, (c) kriged CH₄ mixing ratio, (d) CH₄ flux using raw wind, (e) CH₄ flux the mass-balanced wind with vertically 100m averaged wind, and (f) CH₄ flux using mass-balanced wind (vertically averaged every 100m) over the landfill location on July 29, 2015. The fluxes are computed based on equation (2). The background value was chosen as the minimum value at each vertical layer. The approximate diameter of the cylinder is 3 km, and the color scale is capped at 2.2 ppmv in panels (b) and (c).



Formatted: Justified, Indent: First line: 0"

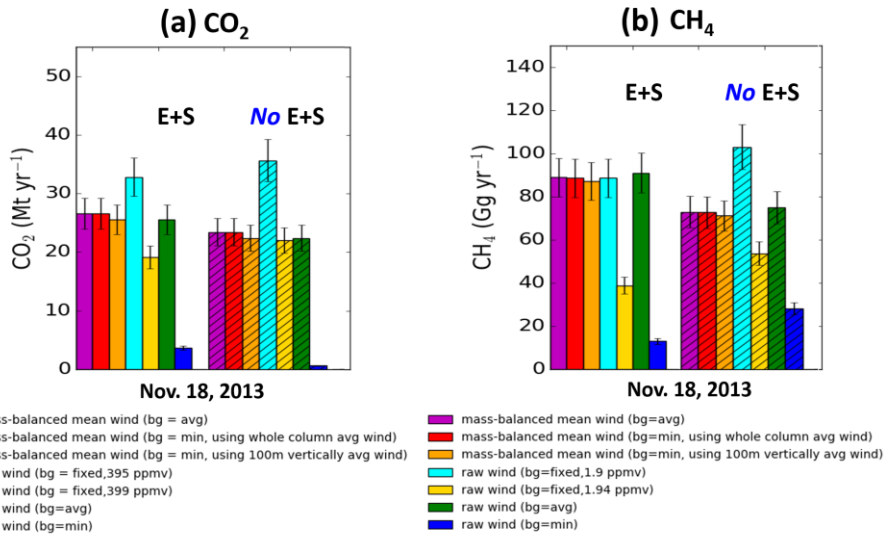


Figure 87: Urban-scale (a) CO₂ [Mt yr⁻¹] and (b) CH₄ [Gg yr⁻¹] emission rate estimates using raw wind and mass balanced area-mean wind, with different treatments of background values. Solid bars represent emission estimates with entrainment and surface flux (E+S), and hatched bars represent the corresponding emission estimates without consideration of entrainment and surface flux (No E+S). Error bars represent the uncertainty of the total emission fluxes. The average and minimum values for background are computed at each vertical level (about 7 meter interval), and the fixed value alternatives are 395 or 399 ppm for CO₂ and 1.90 or 1.94 ppm for CH₄ for all altitudes.

(a)

AJAX flight date		Urban Scale (large loop)			
		November 18, 2013		November 17, 2015	
		CO ₂ (Mt yr ⁻¹)	CH ₄ (Gg yr ⁻¹)	CO ₂ (Mt yr ⁻¹)	CH ₄ (Gg yr ⁻¹)
Mean wind	Bg = min	26.55±1.06	88.82±3.55	20.93±2.93	9.48±1.33
Mean wind	Bg = avg	26.58±1.06	88.99±3.56	20.92±2.93	9.51±1.33
Raw wind	Bg = min	3.68±0.15	13.00±0.52	14.92±2.10	8.16±1.14
Raw wind	Bg = avg	25.47±1.02	91.52±3.66	16.36±2.29	10.90±1.53

(b)

AJAX flight date		Local Scale (small loop): July 29, 2015			
		Landfill		Rice Field	
		CO ₂ (Mt yr ⁻¹)	CH ₄ (Gg yr ⁻¹)	CO ₂ (Mt yr ⁻¹)	CH ₄ (Gg yr ⁻¹)
Mean wind	Bg = min	0.22±0.08	7.83±2.74	0.25±0.04	2.63±0.45
Mean wind	Bg = avg	0.22±0.08	7.67±2.68	0.25±0.04	2.60±0.44
Raw wind	Bg = min	0.37±0.13	10.26±3.59	0.16±0.03	1.59±0.27
Raw wind	Bg = avg	0.22±0.08	8.13±2.85	0.25±0.04	2.66±0.45

Table 1

Figure 1: The calculated CO₂ and CH₄ emission fluxes using different wind methodology (raw or mean wind) and different background values (minimum or average values at each level) for (a) urban scale on two different flight (November 18, 2013 and November 17, 2015) and (b) local scale on July 29, 2015. The vertical mass transfer (entrainment and surface flux) is taken into account.

Table 1. Urban scale CO₂ and CH₄ fluxes over Sacramento using different wind treatment (raw wind: "raw", or mass-balanced wind: "mass-balance") and different background values (minimum or average values) on

- Formatted: Justified, Indent: First line: 0.3", Don't hyphenate
- Formatted: Justified, Line spacing: 1.5 lines, Don't hyphenate
- Formatted: Indent: First line: 0.3", Line spacing: 1.5 lines, Don't hyphenate
- Formatted: Indent: First line: 0.3", Line spacing: 1.5 lines, Don't hyphenate
- Formatted: Justified, Indent: First line: 0.3", Don't hyphenate
- Formatted: Justified, Indent: First line: 0.3", Line spacing: 1.5 lines, Don't hyphenate
- Formatted: Indent: First line: 0.3", Don't hyphenate
- Formatted: Justified, Indent: First line: 0.3", Don't hyphenate
- Formatted: Indent: First line: 0.3", Don't hyphenate
- Formatted: Justified, Indent: First line: 0.3", Don't hyphenate
- Formatted: Indent: First line: 0.3"
- Formatted: Indent: First line: 0.3", Don't hyphenate
- Formatted: Justified, Indent: First line: 0.3", Don't hyphenate
- Formatted: Indent: First line: 0.3", Don't hyphenate
- Formatted: Justified, Indent: First line: 0.3", Don't hyphenate
- Formatted: Justified, Indent: First line: 0.3", Don't hyphenate
- Formatted: Justified, Indent: First line: 0.3", Don't hyphenate, Tab stops: Not at 1.36"
- Formatted: Don't hyphenate
- Formatted: Justified, Indent: First line: 0.3", Don't hyphenate
- Formatted: Indent: First line: 0.3"
- Formatted: Justified, Don't hyphenate
- Formatted: Indent: First line: 0.3", Don't hyphenate
- Formatted: Justified, Indent: First line: 0.3", Don't hyphenate
- Formatted: Indent: First line: 0.3", Don't hyphenate
- Formatted
- Formatted: Indent: First line: 0.3", Don't hyphenate
- Formatted
- Formatted: Indent: First line: 0.3", Don't hyphenate
- Formatted

November 18, 2013. The vertical mass transfer (entrainment and surface flux) is included in these calculations.

Background	Wind		Urban Scale (large loop)			
			November 18, 2013			
			CO ₂ (Mt yr ⁻¹)	Difference from base case (percent)	CH ₄ (Gg yr ⁻¹)	Difference from base case (percent)
min	Mass-balance	100 m layer avg	25.6±2.6		87.1±8.7	
		Whole column avg	26.6±2.7	3.9%	88.7±8.9	1.8%
avg	Mass-balance	100m layer avg	25.6±2.6	<1%	87.4±8.7	<1%
		Whole column avg	26.6±2.7	3.9%	89.0±8.9	2.1%
min	Raw		3.7± 0.4	86%	13.0±1.3	85%
avg	Raw		25.5±2.6	<1%	91.1±9.1	4.6%

Table 2. Local scale CO₂ and CH₄ fluxes over landfill and rice field over Sacramento using different wind treatment (raw wind: “raw”, or mass-balanced wind: “mass-balance”) and different background values (minimum or average values at each level) on July 29, 2015. The vertical mass transfer (entrainment and surface flux) is taken into account.

Background	Wind		Local Scale (small loop): July 29, 2015							
			Landfill				Rice Field			
			CO ₂ (10 ³ Mt yr ⁻¹)	Difference from base case (percent)	CH ₄ (Gg yr ⁻¹)	Difference from base case (percent)	CO ₂ (10 ³ Mt yr ⁻¹)	Difference from base case (percent)	CH ₄ (Gg yr ⁻¹)	Difference from base case (percent)
min	Mass - balance	100 m layer avg	2.2±0.8		7.1±2.5		2.5±0.4		2.5±0.4	
		Whole column avg	2.2±0.8	<1%	6.9±2.4	2.8%	2.5±0.4	<1%	2.6±0.4	2%
avg	Mass- balance	100 m layer avg	2.2±0.8	<1%	7.1±2.5	<1%	2.5±0.4	<1%	2.5±0.4	<1%
		Whole column avg	2.2±0.8	<1%	6.9±2.4	2.8 %	2.5±0.4	<1%	2.5±0.4	<1%
min	Raw		3.7±1.3	68%	8.9±3.1	25 %	1.7±0.3	30%	1.8±0.3	28%
avg	Raw		2.2±0.8	<1%	7.1±2.5	<1 %	2.6±0.4	2%	2.5±0.4	<1%

Table 3. Flux estimates for the Sacramento urban area from measurements made on November 18, 2013. The two "curtain" rows below used the same wind treatments as the "whole cylinder" rows (mass-balanced wind).

^a Turnbull et al. (2011) data was collected in 2009; the value given here was converted from the mean reported value of 3.5 Mt C yr⁻¹ with a 1.1% yr⁻¹ increase in CO₂ flux to adjust to 2013.

^b Bottom-up inventory estimates of the annual total emissions from Sacramento County from Vulcan (Gurney et al., 2009) and the California Air Resources Board CEPAM database (Turnbull et al, 2011) are included for comparison. The Vulcan inventory is available only for 2002, and the CEPAM database is available for 2004. We applied a 1.1% yr⁻¹ increase in CO₂ flux to adjust to 2013.

		CO ₂ (Mt yr ⁻¹)	CH ₄ (Gg yr ⁻¹)
Whole cylinder-AJAX	(bg = min, 100m layer avg)	25.6 ± 2.6	87.1 ± 8.7
	(bg = avg, 100m layer avg)	25.6 ± 2.6	87.4 ± 8.7
Curtain -AJAX	(bg = min)	17.3 ± 1.7	64.4 ± 6.4
	(bg = avg)	8.9 ± 0.9	24.1 ± 2.4
Turnbull et al. (2011)		13.4 (with uncertainty of ~ 100%)	
Vulcan estimates for Sacramento		11.5	
CEPAM estimate for Sacramento		10.0	